

Real-time resource model updating in continuous mining environment utilizing online sensor data

Yüksel, Cansin

DOI

[10.4233/uuid:1572a346-95c9-43a5-bf81-81d1fbfde2e9](https://doi.org/10.4233/uuid:1572a346-95c9-43a5-bf81-81d1fbfde2e9)

Publication date

2017

Document Version

Final published version

Citation (APA)

Yüksel, C. (2017). *Real-time resource model updating in continuous mining environment utilizing online sensor data*. [Dissertation (TU Delft), Delft University of Technology]. <https://doi.org/10.4233/uuid:1572a346-95c9-43a5-bf81-81d1fbfde2e9>

Important note

To cite this publication, please use the final published version (if applicable). Please check the document version above.

Copyright

Other than for strictly personal use, it is not permitted to download, forward or distribute the text or part of it, without the consent of the author(s) and/or copyright holder(s), unless the work is under an open content license such as Creative Commons.

Takedown policy

Please contact us and provide details if you believe this document breaches copyrights. We will remove access to the work immediately and investigate your claim.

REAL-TIME RESOURCE MODEL UPDATING IN CONTINUOUS MINING ENVIRONMENT UTILIZING ONLINE SENSOR DATA

CANSIN YÜKSEL

Department of Geoscience and Engineering

Faculty of Civil Engineering and Geosciences

Delft University of Technology

Real-Time Resource Model Updating In Continuous Mining Environment Utilizing Online Sensor Data

Proefschrift

ter verkrijging van de graad van doctor
aan de Technische Universiteit Delft,
op gezag van de Rector Magnificus prof.ir K.C.A.M. Luyben;
voorzitter van het College voor Promoties,
in het openbaar te verdedigen op
woensdag 13 december 2017 om 10:00 uur

door

Cansın YÜKSEL

Master of Science in Mining Engineering, Hacettepe University, Turkey

Geboren te Ankara, Turkey

This dissertation has been approved by the:

promotors: Prof. dr. ir. J. D. Jansen and Prof. dr. -ing. J. Benndorf

copromotor: Dr. M.W.N. Buxton

Composition of the doctoral committee:

Rector Magnificus	chairman
Prof. dr. ir. J. D. Jansen	Delft University of Technology, <i>promotor</i>
Prof. dr. -ing. J. Benndorf	University of Technology Bergakademie Freiberg, <i>second promotor</i>
Dr. - M.W.N. Buxton	Delft University of Technology, <i>copromotor</i>

Independent members:

Prof. dr. ir. H. Wackernagel	MINES ParisTech, France
Prof. dr. A. E. Tercan	Hacettepe University, Turkey
Prof.dr.ir. AW Heemink	Delft University of Technology
Assoc. Prof. dr. K. Wolf	Delft University of Technology
Prof.dr. M.A. Hicks	Delft University of Technology, <i>reserved</i>

This research project is carried out within the Real-Time Reconciliation and Optimization in large open pit coal mines (RTRO-Coal) project and it is supported by Research Fund for Coal and Steel of European Union. RTRO Coal, Grant agreement no. RFCR-CT-2013-00003.

ISBN: 978-94-6233-803-6

Cover designed by Argun Çençen.

Printed in The Netherlands by Gildeprint.

Copyright © 2017 by Cansın Yüksel. All rights reserved.

An electronic version of this dissertation is available at: <http://repository.tudelft.nl>

To all who fight for their dreams...

SUMMARY

In mining, modelling of the deposit geology is the basis for many actions to be taken in the future, such as predictions of quality attributes, mineral resources and ore reserves, as well as mine design and long-term production planning. The essential knowledge about the raw material product is based on this model-based prediction, which comes with a certain degree of uncertainty. This uncertainty causes one of the most common problems in the mining industry, predictions on a small scale such as a train load or daily production are exhibiting strong deviations from reality. Some of the most important challenges faced by the lignite mining industry are impurities located in the lignite deposit. Most of the times, these high ash values cannot be captured completely by exploration data and in the predicted deposit models. This lack of information affects the operational process.

The current way of predicting coal quality attributes is using geostatistical interpolation or simulation methods to create resource models based on exploration data, which are very precise but separated by large distances and represent extremely small volumes. Mining companies have lately started to benefit from the recent developments in information technology, including online-sensor technologies for the characterization of materials, measuring the equipment efficiencies or defining the location of the equipment. KOLA (an abbreviation for Kohle OnLine Analytics) and RGI (radiometric measuring system) online-sensor measurements provide two different measurement systems that have recently been introduced to assess the components of the produced lignite. The precision of the data is lower than exploration data, which are analyzed in laboratories. However, these data are much more dense than exploration data and provide additional information about the coal attributes.

To benefit from this available dense data, a closed-loop concept for mining has recently been introduced. To enable fast online interpretation of online sensor data combined with an automated near-real time updating of the resource model, a new algorithmic approach was developed. This extends current practice in lignite mining, where data are analyzed off-line in a laboratory. Reconciliation exercises to integrate these data are done regularly, however the current practice is still intermittent involving time laps often exceeding weeks or months.

The proposed new concept offers to continuously fuse the online-sensor data measured from the production line into the resource or grade/quality control model and continuously provides locally more accurate estimates. The concept has been applied in two industrial coal mines with the aim of identifying local impurities in a coal seam and to improve the prediction of coal quality attributes in neighbouring blocks. This dissertation focuses on the development, validation and

application of the real-time resource model updating framework in a real mining environment.

In Chapter 2, a detailed problem specification is provided for each case study, which will be presented in the following chapters in order to prove the developed concept. The problem specification provided in this chapter includes the following information: case description (problems in coal quality control, mining operations overview etc.), geological formation of the lignite seams and the available sensor data.

In Chapter 3, the theory behind the real-time resource model updating framework is presented. The framework is derived from the Ensemble Kalman Filter approach for applications in coal production.

In Chapter 4, a 2D case study is performed in a fully controllable environment for validation purposes. Further, the approach is benchmarked against a proven alternative approach.

In Chapter 5, a demonstration in lignite production is given in order to identify the impurities (marine and fluvial sands) in the coal seams which should lead to better coal quality management. In this dissertation, this is done by mainly focusing on the ash content in the deposit. High ash values in coal seams, which are caused by the impurities, are greatly affecting the operational process. In this chapter, the application in coal mining is limited to a case where online measurements were unambiguously trackable due to a single extraction face being the point of origin for the produced material. A significant improvement is demonstrated which leads to better coal quality management. Furthermore, the sensitivity of the real-time resource model updating framework's performance with respect to different parameters for optimal application is investigated. Main parameters include the ensemble size, localization and neighbourhood strategies and the sensor precision.

In Chapter 6, another demonstration in lignite production, this time in a different mine, is presented. The challenge tackled in this chapter is the updating of local coal quality estimates in different production benches, based on measurements of a blended material stream. Moreover, for a practical application of the updating framework, a simple method for generating prior ensemble members, based on block geometries defined in the short-term model and the variogram, is presented. This method allows for a fast, semi-automated and rather simple generation of prior models instead of generating a fully simulated deposit model using conditional simulation in geostatistics. Finally, in order to prove that the developed framework continuously improves the future predictions with any kind of prior model, one last validation case study is illustrated in this mine by applying hypothesis testing.

In Chapter 7, the added value of the real-time resource model updating concept is demonstrated by using a value of information (VOI) analysis. The expected economical and environmental benefits of additional information (due to the

integration of the online-sensor measurements into the resource model) are compared to a case where there is no additional information integrated into the process.

In Chapter 8, the technological readiness level and industrial applicability of the real-time resource model updating framework is discussed.

Finally, in Chapter 9, main concluding remarks are provided, as well as recommendations for future research.

Cansın YÜKSEL

SAMENVATTING

In mijnbouw is het modelleren van de afzettingsgeologie de basis voor vele handelingen die in de toekomst plaats zullen vinden, zoals het voorspellen van kwaliteitskenmerken, minerale grondstofvoorkomens en ertsreserves, alsook het creëren van een mijn-ontwerp en lange-termijn productieplanning. De essentiële kennis van het grondstoffenproduct is gebaseerd op deze modelgebaseerde voorspelling, die een zekere mate van onzekerheid kent. Deze onzekerheid veroorzaakt een van de meest voorkomende problemen in de mijnbouwindustrie: voorspellingen op kleine schaal zoals een treinlading of dagelijkse productie vertonen sterke afwijkingen van de realiteit. Een van de meest belangrijke uitdagingen waarmee de bruinkool-mijnbouwindustrie wordt geconfronteerd zijn onzuiverheden die aanwezig zijn in de bruinkoolafzetting. Meestal kunnen deze hoge as-waarden niet volledig gevat worden door exploratiedata en in de voorspelde afzettingsmodellen. Dit gemis aan informatie heeft belangrijke weerslag op de operationele processen.

De huidige wijze van het voorspellen van kwaliteitskenmerken van bruinkool is het gebruiken van geostatistische interpolatie- of simulatiemethoden om modellen van de afzetting te creëren die gebaseerd zijn op exploratiedata, welke heel nauwkeurig zijn, maar gescheiden door grote afstanden, en welke extreem kleine volumes representeren. Mijnbouwmaatschappijen zijn pas geleden gaan profiteren van de recente ontwikkelingen in informatietechnologie, met inbegrip van online-sensor technologieën voor de karakterisatie van materialen, welke de instrumentariumefficiëntie meten of de locatie van de instrumenten definiëren. KOLA (een afkorting van Kohle OnLine Analytics) en RGI (een radiometrisch meetsysteem) online sensor metingen voorzien in twee verschillende meetsystemen, die recentelijk geïntroduceerd zijn om de componenten van de geproduceerde bruinkool te beoordelen. De nauwkeurigheid van de data is lager dan de exploratiedata, welke zijn geanalyseerd in laboratoria. Daarentegen hebben deze data een veel grotere dichtheid dan exploratiedata en leveren deze additionele informatie over de kolenkenmerken. Om voordeel te halen uit deze beschikbare dichte data, is onlangs een gesloten-kringloop concept voor mijnbouw geïntroduceerd. Om snelle online interpretatie van online-sensordata mogelijk te maken in combinatie met een geautomatiseerde near-real time bijwerking van het model van de bruinkoolafzetting, is er een nieuwe algoritmische aanpak ontwikkeld. Dit breidt de huidige praktijk in bruinkoolmijnbouw, waar data offline geanalyseerd worden in een laboratorium, uit. Harmonisatie-exercities om deze data te integreren worden regelmatig uitgevoerd. Echter, in de huidige praktijk gebeurt dit nog altijd met tussenpozen, in tijdspannes welke vaak langer zijn dan weken of maanden.

Het voorgestelde nieuwe concept biedt continue samensmelting van de online-sensordata, gemeten in de productie, en het grondstoffen- of gehalte-/kwaliteitscontrole-model en voorziet continue in lokaal nauwkeurigere schattingen. Het concept is toegepast in twee industriële kolenmijnen met als doel plaatselijke onzuiverheden in de koollaag te identificeren, evenals het verbeteren van de voorspelling van de kwaliteitskenmerken van de bruinkool in naburige blokken. Deze dissertatie focust op de ontwikkeling, validering en toepassing van het real-time actualisatiekader van het grondstoffenmodel van de bruinkoolafzetting in een werkelijke mijnbouwomgeving.

In Hoofdstuk 2 wordt een gedetailleerde specificatie gegeven voor elke case study, welke gepresenteerd zal worden in de volgende hoofdstukken, ten einde het ontwikkelde concept te bewijzen. De probleembeschrijving, welke wordt gegeven in dit hoofdstuk, bevat de volgende informatie: vraagstukbeschrijving (problemen in de kwaliteitscontrole van bruinkool, overzicht van de mijnbouwactiviteiten enz.), geologische informatie van de bruinkoollagen en de beschikbare sensordata.

In Hoofdstuk 3 wordt de theorie van een real-time actualisatiekader van een grondstoffenmodel gepresenteerd. Het kader is afgeleid van de Ensemble Kalman Filter-benadering voor toepassingen in de kolenproductie.

In Hoofdstuk 4 wordt omwille van validering een 2D case study uitgevoerd in een volledig controleerbare omgeving. Verder wordt de aanpak geijkt tegen een bewezen alternatieve aanpak.

In Hoofdstuk 5 wordt een demonstratie in bruinkoolproductie gegeven om de onzuiverheden (mariene en fluviatiele zanden) in de koollagen te identificeren, hetgeen zou moeten leiden naar verbeterde koolkwaliteitsbeheersing. In deze dissertatie wordt dit gedaan door in hoofdzaak te focussen op het as-gehalte in de afzetting. Hoge as-waarden in kolenlagen, welke worden veroorzaakt door onzuiverheden, zijn van grote invloed op het operationele proces. In dit hoofdstuk is de toepassing in kolenmijnbouw beperkt tot één geval waarbij online metingen ondubbelzinnig traceerbaar waren, vanwege één enkel productiefront dat de oorsprong was van het geproduceerde materiaal. Een belangrijke verbetering wordt getoond, welke leidt naar betere kwaliteitsbeheersing van de kool. Voorts wordt de gevoeligheid van de prestatie van het real-time actualiseringskader van het grondstoffenmodel onderzocht met betrekking tot de verschillende parameters voor optimale toepassing. De belangrijkste parameters zijn de ensemblegrootte, lokalisatie en 'neighbourhood strategies' (omgevingsstrategieën) en de sensor precisie.

In Hoofdstuk 6, wordt weer een andere demonstratie in de bruinkoolproductie gepresenteerd, ditmaal in een andere mijn. De uitdaging die in dit hoofdstuk wordt aangegaan is de actualisering van lokale kwaliteitsschattingen van kool in verschillende 'production benches' (productiebanken), gebaseerd op metingen aan een gemengde materiaalstroom. Bovendien wordt een eenvoudige

methode gepresenteerd voor een praktische toepassing van het actualiseringskader, voor het genereren van vorige ensemble-members, gebaseerd op blokgeometrieën welke zijn gedefinieerd in het korte- termijn model en het variogram. Deze methode staat een snelle, semiautomatische en tamelijk eenvoudige generering toe van vorige modellen, in plaats van de generering van een volledig gesimuleerd afzettingsmodel met gebruikmaking van voorwaardelijke simulatie in geostatistiek. Uiteindelijk, om te bewijzen dat het ontwikkelde kader continue de toekomstige voorspellingen verbeterd met wat dan ook voor een voorafgaand model, wordt in deze mijn een laatste validatie-case study geïllustreerd door het testen van de hypothese.

In Hoofdstuk 7, wordt de toegevoegde waarde van het real-time grondstoffenmodel-actualisatieconcept gedemonstreerd door het gebruiken van “value of information” (VOI) analyse. De verwachte economische en milieukundige voordelen van additionele informatie (als gevolg van de integratie van de online-sensor metingen in het grondstoffenmodel) worden vergeleken met een geval waar er geen additionele, in het proces geïntegreerde, informatie is.

In hoofdstuk 8 wordt het ‘technological readiness level’ (niveau van technologische praatheid) en de industriële toepassing van het real-time actualisatiekader van het grondstoffenmodel besproken.

Ten slotte worden in Hoofdstuk 9 de belangrijkste conclusies gepresenteerd, evenals aanbevelingen voor toekomstig werk.

Contents

List of Figures.....	xviii
List of Tables.....	xxi
1. INTRODUCTION.....	1
1.1. Background Information	2
1.2. Motivation and Scope	4
1.3. Outline	6
2. PROBLEM SPECIFICATION.....	7
2.1. Introduction	8
2.2. Case Study - 1: Garzweiler Mine.....	9
2.2.1. Case Description	9
2.2.2. Development of Impurities in Garzweiler Mine.....	9
2.2.3. Available Sensor Data	11
2.3. Case Study - 2: Profen Mine	13
2.3.1. Case Description	13
2.3.2. Development of Impurities in Profen Mine.....	14
2.3.3. Available Sensor Data	16
3. METHODOLOGICAL APPROACH	19
3.1. Introduction	20
3.2. A Formal Description of the Updating Algorithm.....	23
3.3. A Simplified Prior Model	28
4. METHOD VALIDATION IN A 2D CASE STUDY	31
4.1. Experimental Set-Up	32
4.2. Results and Discussion	34
4.3. Validation of the Developed Framework	37
5. DEMONSTRATION AND PROOF OF CONCEPT IN AN INDUSTRIAL ENVIRONMENT - CASE 1.....	41
5.1. Experimental Setup	42
5.2. Results And Discussions.....	44
5.3. Sensitivity analysis	47
5.3.1. Identification of Main Parameters	47
5.3.2. Experimental Set-Up	48
5.3.3. Experiments with Respect to Main Parameters	49
5.3.4. Results and Discussion.....	51
5.4. Conclusions	58
6. DEMONSTRATION AND PROOF OF CONCEPT IN AN INDUSTRIAL ENVIRONMENT - CASE 2.....	59
6.1. Data Preparation.....	60
6.1.1. Prior Model: Based on Drill Hole Data.....	60

6.1.2. Prior Model: Based on Short-Term Model	60
6.2. Experimental Set-Up	62
6.3. Results And Discussion	63
6.3.1. Results	63
6.3.2. Discussion.....	69
6.4. Hypothesis Testing.....	72
6.4.1. Results	74
6.4.2. Discussion.....	77
6.5. Conclusions	78
7. VALUE OF INFORMATION	79
7.1. Introduction	79
7.2. Economical and Environmental Aspects in Lignite Mining.....	82
7.3. A Stochastic Based Mine Process Optimizer	83
7.4. Value of Information.....	85
7.5. Case Study	86
7.5.1. Experimental Set-Up	86
7.5.2. Results	90
7.5.3. Discussion.....	97
7.6. Conclusions	102
8. TECHNOLOGICAL READINESS LEVEL & INDUSTRIAL APPLICABILITY	105
8.1. Technological Readiness Level & Industrial Applicability	106
9. CONCLUDING REMARKS.....	109
9.1. Conclusions	110
9.2. Recommendations for Future Research.....	112
REFERENCES.....	113
CURRICULUM VITAE	124

List of Figures

Figure 2.1: The ‘trappy’ sand of seam Frimmersdorf (Source: RWE)	11
Figure 2.2: Radiometric sensor measurement from excavator 285 (Source: RWE)	12
Figure 2.3: Complicated geology in the lignite mine	13
Figure 2.4: Production benches, belt system and drill holes on the study area	14
Figure 2.5: Profen open-cast mine standard section, Schwerzau field (Source: MIBRAG)	15
Figure 2.6: Radiometric sensor measurement device, installed on the conveyor belt, measuring blend of coal resulting from multiple excavators, just before the stock Pile (Source: MIBRAG)	17
Figure 3.1: Reservoir management represented as a model based closed-loop controlled process [37]	20
Figure 3.2: An overview of the EnKF based resource model updating concept	21
Figure 3.3: An overview of the KF based resource model updating concept	24
Figure 3.4: Real-time updating algorithm based on NS-EnKF approach, modified from [60]	26
Figure 3.5: Configuration of the real-time resource model updating concept, modified from [62]	27
Figure 3.6: Planned block geometries in the production benches	28
Figure 3.7: Flow chart of prior model generation	29
Figure 4.1: Mining sequence	33
Figure 4.2: Difference map between the real data and updated model on 50th simulation.	35
Figure 4.3: Validation experiment scheme	38
Figure 4.4: Average mean (left) and variance (right) maps of 290 posterior realizations accepted according to rejection sampling method	39
Figure 4.5: Average mean (left) and variance (right) maps of 1000 posterior realizations updated with real-time update framework	39
Figure 4.6: Difference map between the accepted posterior realizations from rejection sampling and updated posterior realizations from real-time update framework	40
Figure 5.1: Geological model	42
Figure 5.2: Production blocks	43
Figure 5.3: Experiment 1 - Updating: 2 nd slice of the 1 st block	45
Figure 5.4: Experiment 2 - Updating: 2 nd slice of the 2 nd block	45

Figure 5.5: Experiment 4 - Updating: 2 nd slice of the 4 th block.....	45
Figure 5.6: Experiment 7 - Updating: 2 nd slice of the 9 th block.....	46
Figure 5.7: MSE Graph for performed experiments.....	46
Figure 5.8: Prior model and measurement data (before updating).....	49
Figure 5.9: Experiment 2 – Ensemble size: 48	51
Figure 5.10: Experiment 5 – Ensemble size: 384	51
Figure 5.11: Comparison graph for different ensemble sized experiments	52
Figure 5.12: Experiment 6 – Localization option off, Neighborhood size: 225,225,6 m	52
Figure 5.13: Experiment 7 – Localization option on (225,225,3 m), Neighborhood size: 450,450,6 m.....	52
Figure 5.14: Experiment 8 – Localization option off, Neighborhood size: 450,450,6 m	53
Figure 5.15: Experiment 11 – Localization option on (450,450,6 m), Neighborhood size: 900,900,6 m.....	53
Figure 5.16: Comparison graph for different localization and neighborhood strategies experiments	53
Figure 5.17: Experiment 12 – Relative sensor error: 4%.....	54
Figure 5.18: Experiment 14 – Relative sensor error: 20%.....	54
Figure 5.19: Experiment 15 – Relative sensor error: 40%.....	54
Figure 5.20: Localization function illustrations	56
Figure 6.1: Results based on conditional simulation: Updating every 2 hours for 4 days. The green area represents the prediction period. The white area represents the learning period.....	64
Figure 6.2: Results based on conditional simulation: Updating every 2 hours for 4 days, 1 excavator producing. The green area represents the prediction period. The white area represents the learning period.....	64
Figure 6.3: Results based on conditional simulation: Updating every 2 hours for 4 days, 2 excavators producing. The green area represents the prediction period. The white area represents the learning period.....	65
Figure 6.4: Absolute error predictions (for the next 2 days) of after updating every 2 hours for 4 days	66
Figure 6.5: Results based on short-term model: Updating every 2 hours for 4 days. The green area represents the prediction period. The white area represents the learning period.....	67
Figure 6.6: Results based on short-term model: Updating every 2 hours for 4 days, 1 excavator producing. The green area represents the prediction period. The white area represents the learning period.....	67
Figure 6.7: Results based on short-term model: Updating every 2 hours for 4 days, 2 excavators producing. The green area represents the prediction period. The white area represents the learning period.....	68
Figure 6.8: Absolute error predictions (for the next 2 days) after updating every 2 hours for 4 days	69

Figure 7.1: Aim of the resource model updating framework	81
Figure 7.2: Visual representation of a series of schedules, with the 10 simulation days and the shift for each day in the first two rows. A red block means the excavator is not schedules, a green block means the excavator is scheduled to work. [92]	83
Figure 7.3: Resource models that are used in the experiments.....	86
Figure 7.4: VOI - Experimental scheme	88
Figure 7.5: Cost calculations of deviating from the target quality (ash %) - Case 1	91
Figure 7.6: VOI - Case 1	91
Figure 7.7: Cost calculations of deviating from the target quality (ash %) - Case 2	92
Figure 7.8: VOI - Case 2	92
Figure 7.9: Cost calculations of deviating from the target quality (ash %) - Case 3	93
Figure 7.10: VOI - Case 3	93
Figure 7.11: Cost calculations of deviating from the target quality (ash %) - Case 4	94
Figure 7.12: VOI - Case 4	94
Figure 7.13: Cost calculations of deviating from the target quality (ash %) - Case 5	95
Figure 7.14: VOI - Case 5	95
Figure 7.15: Cost calculations of deviating from the target quality (ash %) - Case 6	96
Figure 7.16: VOI - Case 6	96
Figure 8.1: Technology readiness levels	106

List of Tables

Table 4.1: MSE and BV plots for 1 excavator case – 2D Case study	34
Table 4.2: MSE and BV plots for 2 excavators case – 2D Case study	36
Table 4.3: MSE and BV plots – Rejection sampling.....	40
Table 5.1: Experimental scheme	50
Table 6.1: Calculated absolute errors for predictions- Prior model is based on drill hole data	66
Table 6.2: Calculated absolute errors for predictions - Prior model is based on short-term model	68
Table 6.3: Calculated absolute errors for predictions (for 23 days) - Prior model is based on drill hole data.....	74
Table 6.4: Calculated absolute errors for predictions (for 23 days) - Prior model is based on short-term model.....	75
Table 6.5: Test statistics calculation - Prior model is based on drill hole data	76
Table 6.6: Test statistics calculation - Prior model is based on short-term model	76
Table 7.1: Activity factors for excavators [92].....	84
Table 7.2: Case summarization for VOI experiments	90

1. INTRODUCTION

1.1. BACKGROUND INFORMATION

In mining, modelling of the deposit geology is the basis for many actions to be taken in the future, such as predictions of quality attributes (e.g. in coal or iron ore), mineral resources and ore reserves, as well as mine design and long-term production planning. The essential knowledge about the raw material product is based on this model based prediction, which comes with some degree of uncertainty. This uncertainty causes one of the most common problems in the mining industry, predictions on a small scale such as a train load or daily production exhibit strong deviations from reality.

Some of the most important challenges faced by the lignite mining industry are impurities (such as marine and fluvial sand intrusions) located in the lignite deposit. These impurities are indicated in the coal seams as high ash¹ values (e.g. more than 15% wet ash). Most of the times, these high ash values cannot be captured completely by exploration data and in the predicted deposit models. This lack of information affects the operational process significantly.

The current method of predicting coal quality attributes is using geostatistical interpolation or simulation methods to create resource models based on exploration data. These are very precise but separated by large distances and represent extremely small volumes. Mining companies have recently started to benefit from the recent developments in information technology, including online-sensor technologies for the characterization of materials, measuring the equipment efficiencies or defining the location of the equipment. KOLA (an abbreviation for Kohle OnLine Analytics) and RGI (radiometric measuring system) online-sensor measurements [1] provide two different measurement systems that have recently been introduced to assess the components of the produced lignite. The precision of the data are lower than exploration data, which are analyzed in laboratories. However, these data are much more dense than exploration data and provide additional information about the coal attributes.

To benefit from this available dense data, a closed-loop concept for mining has recently been introduced [2]. To enable fast online interpretation of online sensor data combined with an automated near-real time updating of the resource model, a new algorithmic approach was developed. This extends current practice in lignite mining, where data are analyzed off-line in a laboratory. Reconciliation exercises to integrate these data are done regularly, however the current practice is still intermittent involving time laps often exceeding weeks or months. The proposed new concept offers to continuously fuse the measured sensor data with

¹ The ash content of coal is one of the quality parameters of coal along with calorific value, moisture, sulphur content and etc. The ash content directly affects the heating value of the coal therefore coal with higher ash percentages is of lower quality than coal with lower ash percentages.

the resource model by using sequential resource model updating methods that originate from data assimilation.

A simple geostatistical re-modelling may not be sufficient for sensor-based updating for several reasons. The first reason is that the online sensors might measure blended material originating from different benches/blocks. To unambiguously track back and update, a filter solution is required. The second reason is that the quality of the online sensor data differs from exploration data and may require co-simulation procedures including models of co-regionalization, which adds complexity. The third reason is the change of support, which has to be taken into account due to the different reference volumes of resource blocks and sensor measurements. The fourth and most important reason is that linking the measurement with the resource block location to be updated is not straightforward. Sensors are installed at several locations along the extraction chain. To link measurements with blocks, a forward predictor is needed. This can be, for example, a material tracking system. The reasons mentioned above provide the motivation to explore alternative approaches instead of simple re-estimation.

Data assimilation methods offer the tools for fast incorporation of observations in order to improve predictions. The definition of data assimilation translates in mining as the process of combining the sensor measurement data with a prior estimate of the resource model, in order to produce a more accurate posterior estimate. Methods of data assimilation have found many successful applications in various fields. [3-8] examined and applied different data assimilation methods on dynamic atmospheric models with the aim of improved numerical weather forecasting. Applications to oceanographic problems, such as estimation and prediction of ocean eddy fields, wave propagation etc., [9-16] deepened and broadened the understanding of ocean circulation on regional, basin and global scales. Similar to this research, [17] successfully combined geostatistics and data assimilation methods and applied it in an estuarine system. More recently in reservoir engineering [18-21] applied a similar framework of resource model updating approach. The mentioned applications are all performed on nonstationary, dynamical models due to the nature of their research fields. The initial difference in application of the resource model updating concept among others comes from the requirement of the stationary, non-dynamic models.

The first investigation [22] proved that the approach works well within a synthetic case study under a variation of several control parameters (number of excavators, precision of the sensor, update interval, measurement interval, extraction mode/production rate). Wambeke and Benndorf [23] extended the framework for practical application, including the handling of attributes and measurements showing a non-Gaussian distribution, dealing with localization and inbreeding issues, avoiding spurious correlations and increasing the computational efficiency. Yet, so far, the amount of literature is small, particularly when considering the industrial application of the developed concept.

1.2. MOTIVATION AND SCOPE

One of the initial aims of this dissertation is to provide a tailored method. This tailored method is adapted to update coal quality attributes in a continuous mining environment and should improve the resource model accuracy. Providing more accurate deposit models will lead to an improvement in the detection of impurities (high ash contents) in future production areas. As a result, this approach will allow quicker reactions to gained knowledge, which in turn allows for quick changes in mine planning and operational decisions.

Moreover, further studies are required to understand the effects of the used parameters during the full scale application, to identify the sensitivity of the results and to explore the performance in depth. For this reason, an investigation on the performance of the resource model updating framework with respect to the main parameters, which are the ensemble size, localization and neighborhood strategies and the sensor precision is required. Findings of this research are expected to assist in future applications of the resource model updating concept by making it easier to achieve optimum performance.

In many mining operations material quality control measurements are taken at central locations in the downstream process, such as, on a central conveyor belt or from the trains that are loaded after the coal blending yard. In this case the measurements represent a blend or a combination of material originating from multiple extraction faces. The measurement of one sample cannot be tracked back to the origin of the material. However, a collection of multiple measurements over time would have the potential solve this unambiguity. In this contribution the updating framework is applied while multiple excavators are producing at different benches. This is done in order to understand the updating performance when feeding the blended coal observations back to multiple excavator locations from where the production originates.

A fourth aspect discussed in this dissertation is an implementation of the resource model updating framework in an operational environment with a focus on practicality. The resource model updating concept is based on EnKF, which requires ensemble members (realizations). These can be obtained by conditional simulation [24-27], which can be a time consuming effort, requiring expert knowledge. For operational implementations, the process should be rather simple and robust. Therefore, the aim is to investigate whether realizations of a prior model can be obtained rather simple and without loss of updating performance.

Thus, this dissertation aims to present a new application of the framework in a full scale lignite production, where the initial resource model generation is automated based on a short-term model. This would immediately increase the production efficiency in a real mining environment, by simply giving the opportunity to react on the changes of the resource model with newly gained information. Moreover, using the real-time resource model updating framework would also decrease the frequency of material misallocation. An improved

resource model reduces the amount of actual lignite being incorrectly allocated to the waste dump and similarly, a smaller amount of actual waste send to the stockpile.

This dissertation uses two case studies from actual lignite mining environments in order to achieve this aim.

In summary this research has the following objectives:

1. Providing a tailored method, which was adapted to update coal quality attributes in a continuous mining environment, in order to improve the resource model accuracy.
2. Applying the real-time resource model updating framework for a full scale lignite production environment.
3. Investigating the resource model updating framework performance with respect to main parameters.
4. Applying the real-time resource model updating framework while the sensor is observing a blend of coal resulting from multiple excavators.
5. Simplifying and semi-automating the updating framework for easier application in a real mining environment.
6. Evaluation of the added value by application of the real-time resource model updating framework.

This dissertation presents different applications of the real-time resource model updating framework during coal mining operations. However, the developed methodology could have a much wider scope of application. The entire mining industry could benefit from the application of the real-time resource model updating framework in other commodities and ore body styles, since the use of the framework leads to a direct increase in cost reductions.

1.3. OUTLINE

This dissertation is divided into 9 chapters and is organized in the following way:

Chapter 2 provides a detailed problem specification for each case study, which will be presented in the following chapters in order to prove the developed concept. The problem specification provided in this chapter includes the following information; case description (problems in coal quality control, mining operations overview etc.), geological formation of the lignite seams and the available sensor data.

Chapter 3 presents the principles behind the resource model updating framework, which is developed for a specific application in continuous mining and the mathematical formulation.

Chapter 4 illustrates a 2D validation case study in a fully controllable environment. Findings of the study are then presented.

Chapter 5 demonstrates an industrial application in Garzweiler mine, Germany. The application in continuous mining test case is illustrated and sensitivity analysis experiments are performed. Findings of the study are then presented. Key findings of the study are discussed and summarized.

Chapter 6 demonstrates an industrial application in Profen mine, Germany. This chapter discusses three different topics. First, it tests the performance of the resource model updating framework while the sensor is observing a blend of coal resulting from multiple excavators. The second topic is about simplifying and semi-automating the framework for an easier application in a real mining environment. The final topic is about applying hypothesis testing on the real case to prove that the developed framework continuously improves the future predictions.

Chapter 7 answers the following question: 'What is the value of integrating real-time production measurements into the resource model and executing an optimized mine plan, considering economical and environmental aspects?', by performing a case study.

Chapter 8 provides a discussion on the technological readiness level and industrial applicability of the real-time resource model updating framework.

Finally, in Chapter 9, an overview of the main conclusions, as well as recommendations and future research possibilities are described.

2. PROBLEM SPECIFICATION

This chapter provides a detailed problem specification for each case study, which will be presented in the following chapters in order to prove the developed concept. The problem specification provided in this chapter includes the following information; case description (problems in coal quality control, mining operations overview etc.), geological formation of the lignite seams and the available sensor data.

The contents of this chapter have been adapted from:

Yüksel, C., Thielemann, T., Wambeke, T., & Benndorf, J. (2016). Real-Time Resource Model Updating for Improved Coal Quality Control Using Online Data. *International Journal of Coal Geology*. doi: <http://dx.doi.org/10.1016/j.coal.2016.05.014>

2.1. INTRODUCTION

This dissertation demonstrates the developed concept in two different case studies. In both of the case studies the challenge originates from the complicated geology that leads to geological uncertainty associated with the detailed knowledge about the coal deposit, in particular with coal quality parameters. This uncertainty causes deviations from expected process performance and affects the sustainable supply of lignite to the customers. The aim is to improve the knowledge over the coal deposit and increase the process performance by applying a resource model updating framework.

The first case study is performed in Garzweiler mine, which is operated by RWE Power AG, Germany. In this case study, the most important challenges are marine and fluvial sand intrusions located in the lignite deposit. Most of the time, these intrusions cannot be captured completely by exploration data and in the predicted deposit models. This lack of information affects the operational process significantly. In this case study, the KOLA system is being used as the sensor data and it measures the material flow reasoning from one excavator.

The second case study is performed in Profen mine, which is operated by MIBRAG mbH, Germany. In this case study, the geology of the field is rather more complex, including multiple split seams with strongly varying seam geometry and coal quality distribution. Moreover, in this case study, lignite production occurs with multiple excavators at different benches. Thus, this case study presents an extension to the first case study, where characteristics from blended material, originating from two or three simultaneously operating extraction faces, are measured. The challenge tackled in this case study is the updating of local coal quality estimates in different production benches based on measurements of a blended material stream. A second aspect discussed here is the practical implementation in an operational environment. The resource model updating concept is based on EnKF, which requires ensemble members (realizations). These can be obtained by conditional simulation [24-27], which can be a time consuming effort, requiring expert knowledge. For operational implementations, the process should be rather simple and robust. Therefore, the aim is to investigate whether realizations of a prior model can be obtained rather simple and without loss of updating performance.

To summarize, the real time resource model updating concept is demonstrated in the Garzweiler Mine, where the KOLA system measures the material flow originating from one excavator (presented in Chapter 5) and in the Profen Mine, where the RGI sensor measures the blended material originating from multiple excavators (presented in Chapter 6).

2.2. CASE STUDY – 1: GARZWEILER MINE

2.2.1. Case Description

The defined study area for this case study is the Frimmersdorf lignite seam in Garzweiler mine, which is operated by RWE Power AG. The necessary data related to this research is provided by RWE Power AG.

This case study is a benchmark in a historical mined out area of about 1.5 km², where there are about 71 drill holes. The study area focuses on one bench, where there is one excavator that executes the mining operations of the area. The extraction sequence is reconstructed based on historical production data while KOLA data, which are assumed to represent the reality, is used for the evaluation of results.

2.2.2. Development of Impurities in Garzweiler Mine

2.2.2.1. Geological Formation of the Lignite Seams

In Tertiary (Oligocene) times, the subsidence of the Central Graben in the North Sea created the Lower Rhine Embayment (LRE) as southernmost extension of the Central Graben [28]. A new sedimentary basin was created. The LRE contains up to 1,600 m of these Oligocene to Pleistocene siliciclastic sediments with intercalated lignite attaining a thickness of up to 100 m [29]. The lignite is of considerable economic importance and has been exploited in open cast mines and near-surface operations since the 18th century, at locations where the seams were easily accessible [30]. Since then, the exploitation of the coal by RWE Generation SE - formerly Rheinbraun AG - is forming a vital basis of German power supply.

Sedimentation in the LRE was mainly influenced by fault block tectonics and variations in sea level. In Upper Oligocene, a 70 Ma long phase of high sea levels came to an end. Short term sea level fluctuations became typical [31]. As a consequence, sequences of marine sands (representing a sea level high) intercalated with terrestrial silts, clays and lignite seams (sea level low) were sedimented. 18 Ma ago, in lower Miocene times (Burdigalian) the uplift of the surrounding highlands named “Rhenish Schiefergebirge” relative to its foreland slowed down. This decreased the sedimentary flows being accumulated in the LRE. At the same time, the climate warmed up. The temperature of North Sea shallow waters rose to 16 °C [32]. Higher precipitation led to a subtropical climate and rising groundwater tables [33]. Vegetation could gain ground extensively and left behind peat, which gradually was converted into lignite.

The place of this research area, the mine Garzweiler, was part of the Venlo block. During two marine regressions, 17 and 15 Ma ago, the deposition of the later lignite seams Morcken (named 6A after [34]) and Frimmersdorf (named 6C) took place. They were separated by the marine Frimmersdorf sands (named 6B). Additionally, as the area of the mine Garzweiler was close to the shore line during that period, the seam Frimmersdorf (6C) faced numerous marine sand intrusions.

These irregular sand partings within 6C and their predictability are part of this research project described here. On top of the seam 6C, the marine Neurath sands (named 6D) were sedimented similar to today's Wadden Sea sedimentation. On top, the seam Garzweiler (6E) was formed during a period of marine regression. In upper Miocene times, the climate cooled down gradually and the LRE underwent a faster downlift. This enhanced the downward gradient and enforced the competence of rivers from the South. Thick fluvial and limnic sediments were deposited, named horizons 7 and 8 after [34]. Their clastic burden led to an easy consolidation of the peat to form lignite.

2.2.2.2. Development of Sand Intrusions in Seam 6C, Mine Garzweiler

The Garzweiler open cast mine is located west of Grevenbroich and is moving westward in the direction of Erkelenz. The mine mainly touches Rhein county Neuss, Rhein-Erft county and Heinsberg county. The lignite is deposited in three seams which together are 40 m thick on average. The coal lays some 40 to max 210 m below the earth's surface.

The Frimmersdorf lignite seam 6C contains multiple sand intrusions (Figure 2.1). The shape and size of these sand partings are irregular and both characteristics are showing a large variability. However, there is not a common idea about the origin of the sand partings. Several possible scenarios for their origin are shortly described below. The first three scenarios are describing a syn-sedimentary process, as opposed to the fourth scenario, which describes a post-sedimentary process:

- An environment of marine transgression
- A rising sea level led to relatively homogeneous sand bodies in the peat. This marine environment arose slowly. Hence, sand partings developed over a longer period of time.
- Accidental injection of heterogeneous sand bodies
- Rough weather and wild sea conditions could accidentally inject a volume of sand within the peat. These events can happen quickly; a daily or hourly event may suffice. Currently, these kinds of events are seen at the German coast near Wilhelmshaven.
- An environment of marine regression and increasing fluvial impact
- A decreasing sea level could strengthen the impact of fluvial conditions. "Crevasse splay" - a situation of a broken embankment causing flooding in the adjacent swampy area - could lead to sand partings within the lignite.
- Coalification
- The geochemical process of coalification can be simplified by the following equation:
- peat + water + CO₂ = lignite

- Here, incidental CO₂ release could be accompanied by large volume relocation. This event could remobilize 6C sand or cause an intrusion of 6D sand into the 6C lignite.

To better predict the quality of lignite to be produced, the genesis of sand partings is rather of second importance. For an improved coal quality control, more important is the combination of data of the existing geological model with production data, GPS data of the excavator's position at one time and data of analytical results of the coal composition. The theoretical formulization of the mentioned data fusion is provided in Chapter 3. Application of this fusion in the Frimmersdorf lignite seam will be provided in Chapter 4.

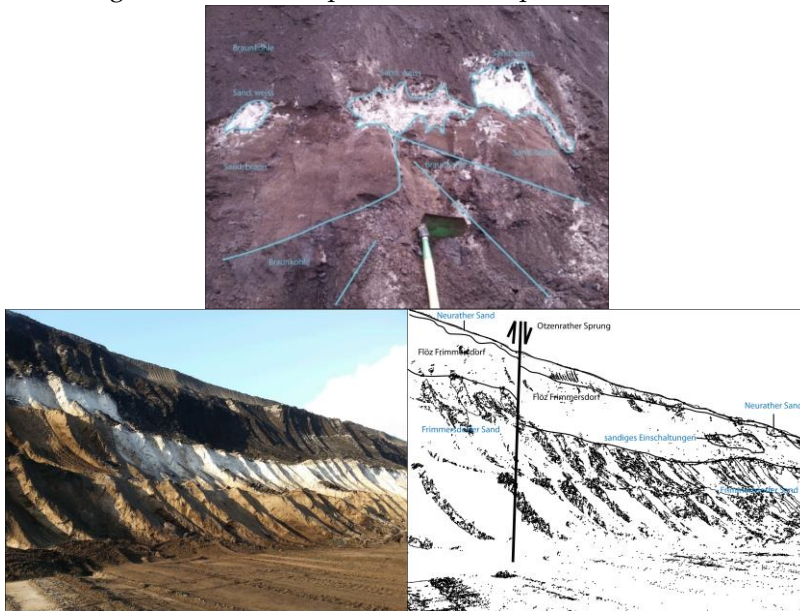


Figure 2.1: The 'trappy' sand of seam Frimmersdorf (Source: RWE)

2.2.3. Available Sensor Data

There are two different online-sensor measurement systems available to characterize the lignite produced from the Frimmersdorf seam.

The KOLA - an abbreviation for Kohle OnLine Analytics - system [1] is the first data type available for a more extensive modeling of the sand parting in the 6C Frimmersdorf lignite seam. It applies X-Ray diffraction in order to accurately assess the components of the produced lignite. The analyzed components are inter alia iron, sulfur, potassium, calcium and - of importance in the context of this research - the ash content of the produced lignite. The Garzweiler opencast mine operates multiple KOLA measuring stations, of which two are analyzing the coal from the Frimmersdorf lignite seam.

The second available source is the radiometric measuring system of RGI data (Figure 2.2) [1]. This system allows an online determination of the ash content of the mass flow directly on the conveyor belt, without requiring any sampling or sample processing. It is installed directly on the excavator that produces lignite from the Frimmersdorf seam and, consequently, the ash content of the produced lignite can be provided by online values during the process of monitoring and controlling the production process. However, calibration of this system is strongly dependent on the composition of the coal.

The presented full case study in Chapter 5 only used the KOLA measurement data as the representative measurement of the produced lignite due to the calibration problems of the RGI measurements.

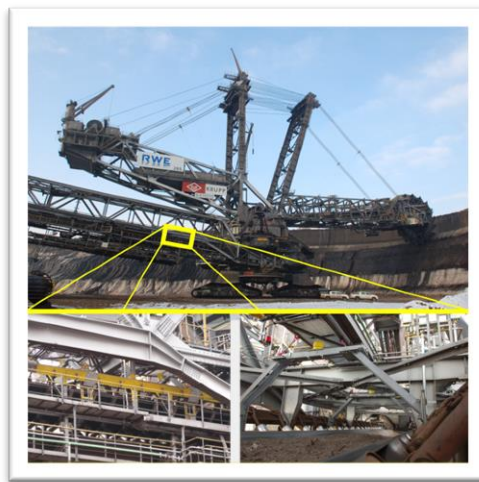


Figure 2.2: Radiometric sensor measurement from excavator 285 (Source: RWE)

2.3. CASE STUDY – 2: PROFEN MINE

2.3.1. Case Description

The case study is performed on a lignite mining operation in Profen mine, Germany, where the geology of the field is complex, including multiple split seams with strongly varying seam geometry and coal quality distribution (Figure 2.3). Profen mine is operated by MIBRAG mbH.



Figure 2.3: Complicated geology in the lignite mine

For this case study, which aims to demonstrate potential improvement, the target area has been defined in an already mined out area of 25 km², where there are about 3000 drill holes. Mining operations are executed by six excavators, each working on a different bench. Among these six excavators, only five of them are continuously working on a lignite seam. Generally, the maximum number of excavators that are working at the same time is three. For this reason, the case study will apply cases where either only one excavator is working, or two excavators are working or three excavators are working at the same time.

The produced materials are being transported through conveyor belts. All conveyor belts merge at a central conveyor belt leading to the coal stock and blending yard, which is further connected to a train load. Figure 2.4 presents the mentioned six benches in black lined blocks, conveyor belts in blue lines, drill holes as green points. The orange point represents the online measuring system (RGI), which was initial described in Chapter 2 (Figure 2.6).

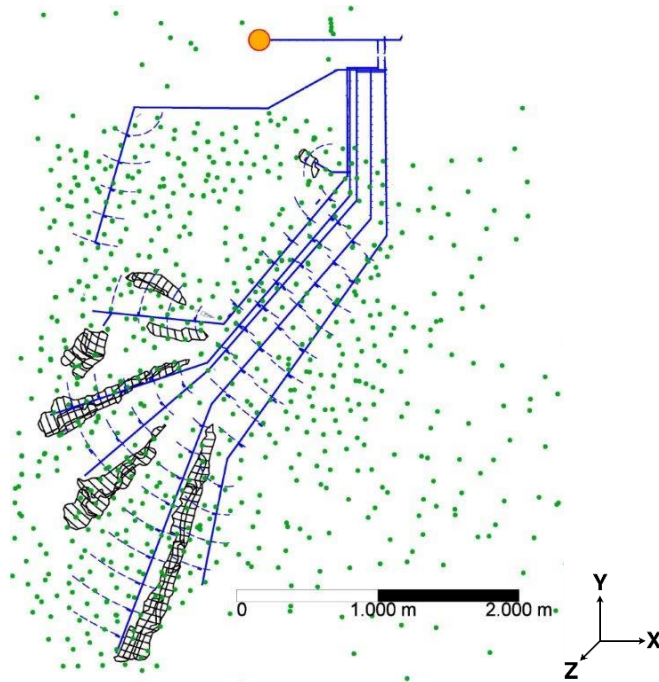


Figure 2.4: Production benches, belt system and drill holes on the study area

2.3.2. Development of Impurities in Profen Mine

2.3.2.1. Regional Geology, External Form of the Deposit [35]

In terms of regional geology, the mining areas at Profen and Schleenhain are located in the Weiße Elster river basin. The deposit was formed by epirogenic-subrosive processes. Almost all of the pre-Tertiary subsoil consists of Zechstein carbonate and anhydrit rock. Subrosion processes which differed in extension and time before and during the Tertiary and Quaternary produced large thickness fluctuations and subsidence in all Tertiary beds. The three lignite seams in the deposit are:

- the Saxon-Thuringian underlying split (seam 1), age - 38 million years
- the Thuringian main seam (seam 23), age - 36 million years
- the Böhlen overlying split (seam 4), age - 33 million years

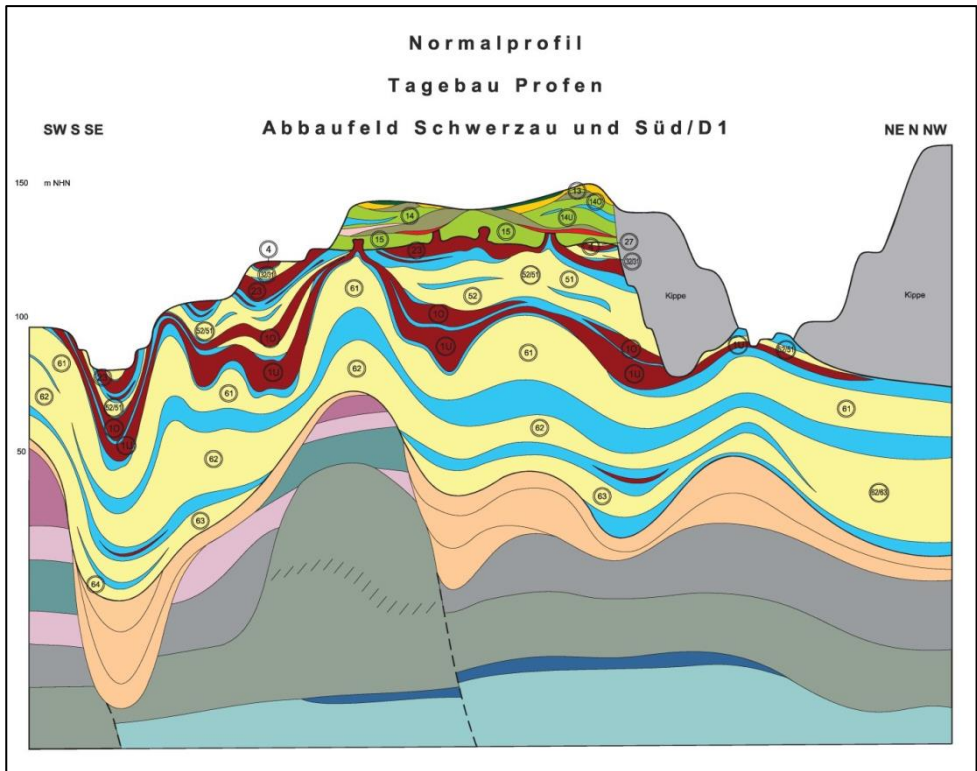


Figure 2.5: Profen open-cast mine standard section, Schwerzau field (Source: MIBRAG)

Particular at the Schwerzau mining field, seam 1 has been partly reduced or completely removed by glacial fluvial effects. In normal stratification, the seam 1 is 2 - 5m thick, in depressions about 40 m, the max. being 50 m. Seam 1 is mostly split in Seam 1U and Seam 1O.

Above seam 1 there is an approx. 20 m thick parting of older Zeitz river sand and Luckenau clay.

Seam 23 is unsplit at the mining field Schwerzau with an average thickness of about 12 m and characterized mostly by postgenetic subsidence which has formed beds. In this field, the originally deposited seam 23 was almost completely removed in its western part by the Döbris channel, resulting in larger seamless areas. The average thickness is about 8 m.

Next are the Domsen sands with thicknesses between 4 m and 20 m.

Seam 4 in the mining fields was not evenly spread originally and spared from erosion only in postgenetic subsidence structures and is mostly split into two layers (4O and 4U) by a clayey parting.

The superposed marine sediments of the Rupelian series also occur in the a.m. subsidence structures.

The Quaternary sediment sequence starts with early Elster ice period gravel, followed by deposits of Leipzig banded clay as a basis for the Elster ground till. Except for the Domsen field, the early Saale glacial gravel terrace of the Weiße Elster river covers most of the mining field. To the south, the erosion level partly extends below seam 1.

Whereas Böhlen banded clay appears sporadically, the ground till from the icing of the Saale river is more widespread. The last sediment is a mantle of Weichsel glacial period loess which is up to 10 m thick.

2.3.3. Available Sensor Data

Similarly, in the Profen Mine, the RGI online-sensor measurement system is available to characterize the produced lignite quality [36]. However, in this mine, it is installed on the central conveyor belt just before the coal stock and blending yard (Figure 2.6). This system allows an online determination of the ash content of the blended mass flow directly on the conveyor belt, without requiring any sampling or sample processing.

For demonstration purposes, the presented full case study in Chapter 6 assumes the RGI values to be accurate.



Figure 2.6: Radiometric sensor measurement device, installed on the conveyor belt, measuring blend of coal resulting from multiple excavators, just before the stock Pile (Source: MIBRAG)

PROBLEM SPECIFICATION

3. METHODOLOGICAL APPROACH

This chapter provides the theoretical background of the adopted algorithmic approach, which allows for full utilization of the available online data to improve prediction of (impurities related) ash content.

The contents of this chapter have been adapted from:

Section 3.1 and Section 3.2: Yüksel, C., Thielemann, T., Wambeke, T., & Benndorf, J. (2016). Real-Time Resource Model Updating for Improved Coal Quality Control Using Online Data. *International Journal of Coal Geology*. doi: <http://dx.doi.org/10.1016/j.coal.2016.05.014>

Section 3.3: Yüksel, C., Benndorf, J., Lindig, M., & Lohsträter, O. (2017) Updating the coal quality parameters in multiple production benches based on combined material measurement: A full case study. *International Journal of Coal Science & Technology*.

3.1. INTRODUCTION

In lignite mining, similar to other branches of mining, the initial step, prior to mining activities, is creating a resource model based on exploration data, such as drill hole data. Traditionally in order to produce a valuable representation of the coal seam geometry and quality attributes of the seam, such as ash content, geostatistical interpolation methods are used. Based on this resource model, a short-term production plan is created and mining activities will be executed according to this plan. In case of discovering unexpected waste intrusions in the coal seam during production, the short-term model has to be renewed. Currently, by using off-line analysis and modelling techniques, this may take days or sometimes even weeks. Using online-sensor techniques for coal quality characterization in combination with rapid resource model updating, a faster reaction to the unexpected deviations can be implemented during operations, leading to increased production efficiency. Figure 3.2 illustrates this conceptual workflow that basically integrates the online-sensor data into the resource model, as soon as they are obtained. This concept was initially proposed by [2] similar to a closed-loop framework as introduced in the petroleum industry (Figure 3.1) [37, 38].

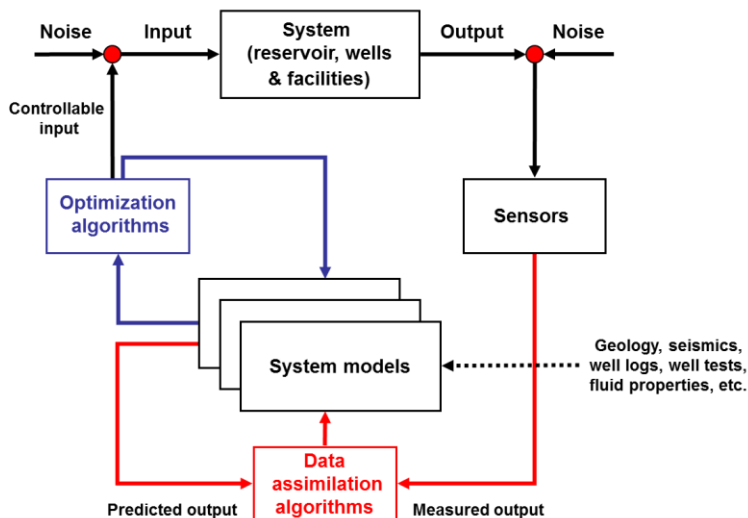


Figure 3.1: Reservoir management represented as a model based closed-loop controlled process [37]

The closed-loop framework continuously compares model-based predictions with observations measured during production monitoring, using inverse modelling or data assimilation approaches to improve the model forecast for subsequent time intervals and combines it with optimization aimed at better decisions for production control and medium-term planning [39]. In this

dissertation, Chapters 3 to 6 focus on the methodology and the application of the data assimilation part of the closed-loop framework in lignite mining. The 7th Chapter adds the optimization part of the framework and closes the loop.

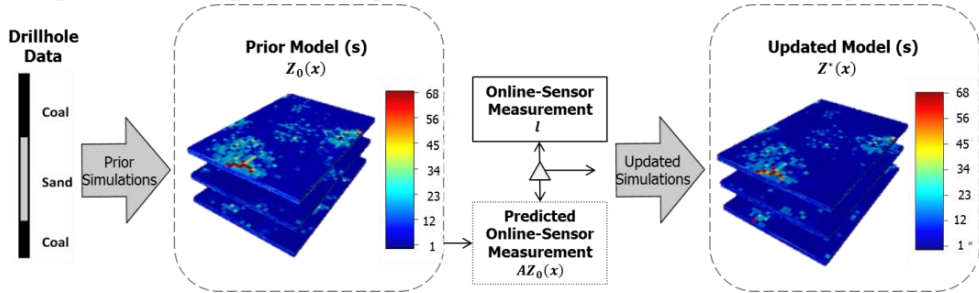


Figure 3.2: An overview of the EnKF based resource model updating concept

Predicting the initial resource model, so-called prior model, is traditionally done by Interpolation methods such as Kriging. Kriging provides the best estimate which is close to reality, yet it is much smoother and doesn't represent the in-situ variability fully. For this reason, it is essential to model the spatial uncertainty by generating multiple realizations of the joint distribution of the ash values in seam using stochastic simulation. Sequential Gaussian simulation (SGS) is a very efficient method for risk assessment applications in the mining industry.

The resource model updating concept compares the predicted measurement values based on the prior prediction (realizations) and the actual online-sensor measurement values per produced block. Once prior models are available, predicted measurement values are required to be calculated according to the production sequence or using material tracking systems, based on prior predictions. The difference between this predicted measurement value and the actual online-sensor measured value per produced block will be fed back to the resource model, in order to create the updated resource model, the so-called posterior model (Figure 3.2). It is important to mention that in general, sensor measurements will have an error component.

For rapid updating of the resource model, sequentially observed data have to be integrated with prediction models in an efficient way. In related fields, methods of data assimilation found many successful applications.

Data assimilation can be defined as the fusion of observations into the prior knowledge (e.g. estimation, simulations) in order to improve the predictions. Thus, this definition translates in mining as the process of combining online-sensor measurement data with the prior model to produce a more accurate prediction of the resource model, the so-called posterior model.

Sequential data assimilation methods use a probabilistic framework and provide estimates of the whole system state sequentially, by propagating information only forward in time [40]. The main sequential methods are the Kalman Filter (KF) [41] ([42]) and the various filters that have been derived from

the basis of the KF, such as; the extended Kalman filter (EKF), the ensemble Kalman filter (EnKF) [43-48], the ensemble transform Kalman filter (ETKF) [49] and the ensemble square root filter (EnSRF) ([50]).

The (KF) is an optimal recursive data assimilation method that combines all available data, such as prior knowledge about the system and measurements, in order to produce an estimate of the desired variables in such a manner that the error rate is minimized statistically. The KF works in two stages. The first stage solves forecast equations, where the prior knowledge is represented by a model to the time of an observation. In our case, these forecast equations represent a mine forward simulation. The mine forward simulation applies a mine plan on the resource model in order to create the model based predictions. The GPS data and material tracking systems are used to estimate the location and the quantity of the produced materials. The second stage is the “sequential updating” stage, where the online-sensor measurements are assimilated into the prior model. This is done according to a ratio of errors in the prior model and in the observations. The difference between the sensor measurements and the predicted measurements is multiplied by a weighting factor (based on the mentioned ratio of errors) and this weighted difference is added to the prior model. An updated resource model is then produced. A detailed explanation on Kalman Filter is given in [51], [52] and [53], the following will focus on the application of the Kalman filter in geosciences.

A framework with a similar aim has been recently proposed by [54] to update the conditional simulations at minimal cost. The proposed conditional simulation update formula is derived by two already well-established approaches called the residual kriging algorithm [55] and the kriging update formulae [56, 57]. Their conditional simulation update formulae offer significant computational savings when the number of conditioning observations is large, and quantify the effect of the newly assimilated observations on already simulated sample paths. Yet, the application of this method in resource model updating using online data case would not be as efficient since the change of support technique is not taken account. In coal production, the obtained quality measurements represent only a small ratio of the entire production block. For this reason, it is essential to apply change of support methods in order to correct the online-sensor measurements in a way to represent a whole production block.

3.2. A FORMAL DESCRIPTION OF THE UPDATING ALGORITHM

The developed framework based on KF is initially validated on the estimated prior model then it is extended to use the SGS method for creating realizations of the prior model. The following formulation is given based on the first investigation study, [22].

Let $\mathbf{Z}(\mathbf{x})$ be the state vector of a stochastic process modelling the spatial distribution, where \mathbf{Z} refers the local ash content at excavation locations \mathbf{x} , then the updated resource model, $\mathbf{Z}^*(\mathbf{x})$, is calculated by the following equation:

$$\mathbf{Z}^*(\mathbf{x}) = \mathbf{Z}_0(\mathbf{x}) + \mathbf{K}(\mathbf{I} - \mathbf{A}\mathbf{Z}_0(\mathbf{x})) \quad (3.1)$$

where $\mathbf{Z}_0(\mathbf{x})$ is the prior resource model, \mathbf{I} is sensor based measurements vector, \mathbf{A} represents the production sequence matrix, so the term $\mathbf{A}\mathbf{Z}_0(\mathbf{x})$ represents the predicted measurements based on the prior block model. Matrix \mathbf{A} describes the contribution of each of the mining blocks at \mathbf{x}_i to the total production at a certain time interval \mathbf{t}_j , with $j = 1, \dots, m$

$$\mathbf{A} = \begin{bmatrix} a_{1,1} & \cdots & a_{1,m} \\ \vdots & \ddots & \vdots \\ a_{n,1} & \cdots & a_{n,m} \end{bmatrix} \quad (3.2)$$

The elements a_{ij} can be interpreted as contributions of each mining block i to the produced material being on the conveyor belt, which will be eventually observed at some sensor station at time j . Matrix \mathbf{A} is herein called production matrix and can be interpreted as an observation model, which links the block model $\mathbf{Z}(\mathbf{x})$ with sensor observations.

The Kalman gain, \mathbf{K} , calculates a weighting factor based on the prediction and measurement error covariances. The Kalman gain matrix indicates the reliability of the measurements, this is done in order to decide "how much to change the prior model by a given measurement" and can be derived from a minimum variance estimate, which leads to the KF providing an optimal solution by minimizing the cost function.

$$\mathbf{K} = (\mathbf{A}^T \mathbf{C}_{zz} \mathbf{A} + \mathbf{C}_{ll})^{-1} \mathbf{A}^T \mathbf{C}_{zz} \quad (3.3)$$

Kalman gain can be calculated as in Equation (3.3). As mentioned above, it contains two different error sources, \mathbf{C}_{zz} , the model prediction error and \mathbf{C}_{ll} , the measurement error. The model prediction error is basically the covariance matrix of the prior resource model, which is propagated through the lignite mining by the production sequence matrix \mathbf{A} . The measurement error is the covariance matrix of the sensor-based measurement. The term $\mathbf{A}^T \mathbf{C}_{zz}$ in Equation (3.3) denotes the model-based prediction, as previously defined.

$$\mathbf{C}_{zz}^* = (\mathbf{I} - \mathbf{KA})\mathbf{C}_{zz} \tag{3.4}$$

The improvement in model prediction can be determined as the updated model error covariance, \mathbf{C}_{zz}^* , which is provided in Equation (3.4). Clearly, this leads to a decrease in the uncertainty of the resource model blocks, not only for the currently excavated ones but also for the adjacent blocks which are spatially correlated. Figure 3.3 illustrates an overview of the KF based resource model updating concept.

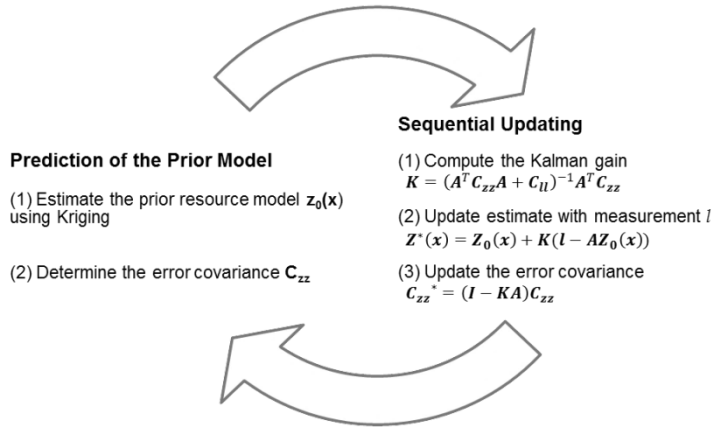


Figure 3.3: An overview of the KF based resource model updating concept

It is obvious that the KF offers large potential in improving resource recovery by combining online data with the resource model and consequently decreasing its uncertainty. However, there are different challenges to solve in order to comprehend the source of the difference between sensor measurement and the resource model, and feed the gained knowledge back to the resource model. The main challenges to solve are the size of the estimated resource model (in the order of multiple millions of grid nodes), non-Gaussian behavior of data, the different support of observations and resource model blocks and a possible non-linear relationship between the observations and model attributes.

The (EnKF) provides a comprehensive solution for large-scale applications when explicit storage and manipulation of the covariance matrix is impossible or not feasible [58]. Moreover, EnKF is able to deal with the non-linear systems. The developed framework with ENKF uses SGS in order to create the ensemble of realizations, also called prior ensemble $\mathbf{Z}_0(\mathbf{x})^e$, where $e = 1, \dots, N$ is the number of realizations/ensembles. Next, the algorithm continues recursively, using the following recurrence relations;

$$\mathbf{Z}^*(\mathbf{x})^e = \mathbf{Z}_0(\mathbf{x})^e + \mathbf{K}^e(\mathbf{I}^e - \mathbf{A}\mathbf{Z}_0(\mathbf{x})^e) \quad (3.5)$$

$$\mathbf{K}^e = (\mathbf{A}^T \mathbf{C}_{zz}^e \mathbf{A} + \mathbf{C}_{ll}^e)^{-1} \mathbf{A}^T \mathbf{C}_{zz}^e \quad (3.6)$$

$$\mathbf{C}_{zz}^{*e} = \overline{(\mathbf{Z}(\mathbf{x})^e - \overline{\mathbf{Z}(\mathbf{x})^e})(\mathbf{Z}(\mathbf{x})^e - \overline{\mathbf{Z}(\mathbf{x})^e})^T} \quad (3.7)$$

where $\mathbf{Z}(\mathbf{x})^e$ and \mathbf{I}^e respectively consist of an ensemble of block models and the measurements. In Equation (3.7) \mathbf{C}_{zz}^{*e} refers to the updated error covariance of the resource model, where the overbar denotes the expected values of the ensembles. The covariance matrices represent the whole ensemble and the Kalman gain \mathbf{K}^e is derived from these.

Two measures are suggested by [59] to reduce computational time of Kalman gain calculations. The first measure is related to the neighborhood. The size of the \mathbf{C}_{zz} matrix is in the order of the number of cells that are in the defined updating neighborhood. The second measure is a Cholesky decomposition which is implemented to avoid an explicit computation of the inverse in Equation (3.6). This results in significant computational speed ups.

Blended measurements and differences in the scale of support are dealt with by the forecast and observation error covariances. These covariances are computed empirically from the field and predicted observations [59]. This Monte Carlo based approach allows for a convenient/flexible connection between the blended measurements and their corresponding source location.

To deal with the non-gaussianity of the data, a new approach NS-EnKF is proposed by Zhou [60] which transforms the original state vector into a new vector that is univariate Gaussian at all times. Gaussianity is achieved by applying a normal-score transformation to each variable for all locations and all time steps, prior to performing the updating step in EnKF.

The NS-EnKF approach follows the same steps as the standard EnKF, except the NS-EnKF has additional pre - and post processing steps. Local grades at grid nodes will be normal score transformed before application of the EnKF, and once the update is complete, the normal score transformed data will be transformed back (Figure 3.4). Readers are referred to [61] for information about the normal score transformation.

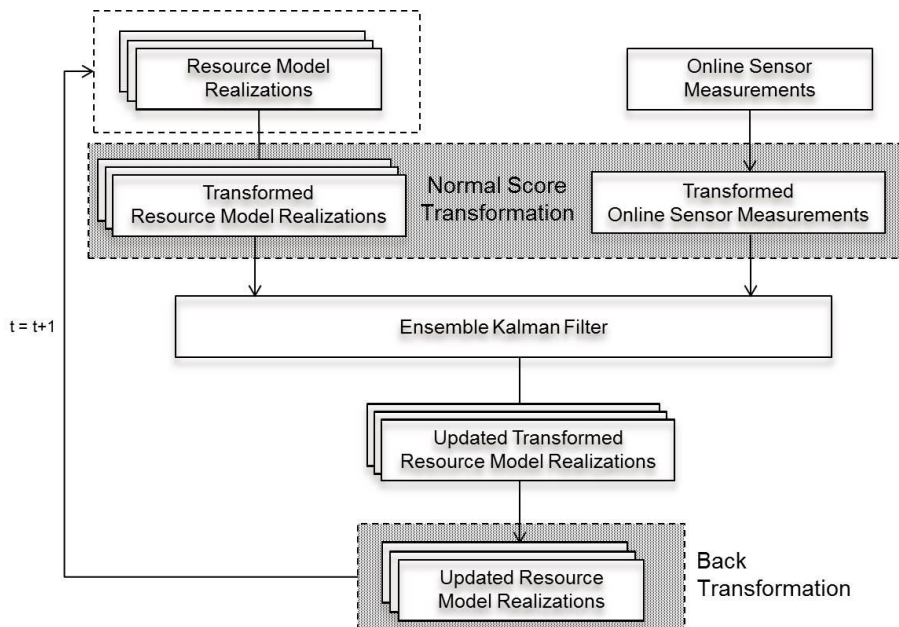


Figure 3.4: Real-time updating algorithm based on NS-EnKF approach, modified from [60]

With the goal of continuously updatable coal quality attributes in a resource model, a framework based on the NS-EnKF approach was tailored for large-scale mining applications. It is based on an implementation from [62]. Figure 3.5 gives a general overview of the operations which are performed to apply the resource model updating framework. The concept initially starts with resource modelling, by using conditional simulation to generate a prior ensemble. This is the first required input consisting of ensemble members to be updated. The input consists of the production data and their related actual sensor measurements. The production data provides the excavated block information, e.g. names and quantities. The actual online-sensor measurement values are collected during the lignite production and they represent the excavated material. The third input is a data set consisting of a collection of actual and predicted sensor measurements. The predicted measurements are obtained by applying the production sequence as a forward predictor to prior resource model realizations. Once all of the input data are provided, the updated posterior resource model will be obtained. This process will continue as long as new online-sensor measurement data is received.

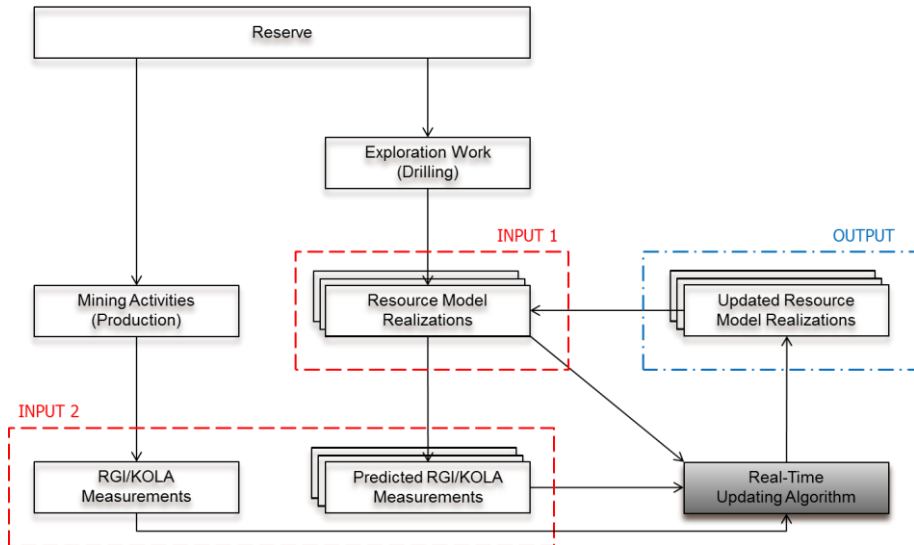


Figure 3.5: Configuration of the real-time resource model updating concept, modified from [62]

3.3. A SIMPLIFIED PRIOR MODEL

As mentioned earlier, the first input needed to apply the resource model updating framework is a collection of resource model realizations, also called the prior model. This requires the application of sophisticated geostatistical methods, such as conditional simulation (such as the application in Chapter 5). However, this requires expert knowledge and adds an additional step prior to using the updating framework. Moreover, generating a new resource model might create disarray between geology and mine planning departments in the company, since they already have a resource model created by their own team. For these reasons, in order to apply the updating framework in real mining environment, a more practical and simplified application of the framework is required. The proposed simplification obtains the required prior model realizations by adding fluctuations around the company’s short-term block model. This short-term model is created by the mining engineers, based on applying the defined block geometries (Figure 3.6) on the company’s estimated block model. In this way, each block will have an estimated ash value. Figure 3.7 compares both of the prior model generation processes.

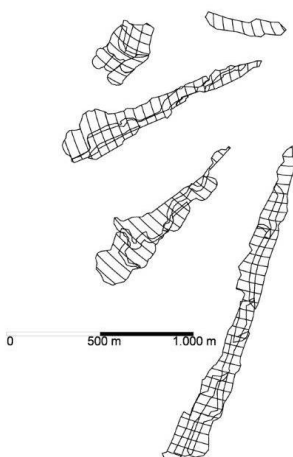


Figure 3.6: Planned block geometries in the production benches

In order to create the quality model based on short-term model, the following strategy is employed:

1. Short-term block model values are generally available for each block and they deliver the prior estimation of block attributes (E-type estimate).
2. A conditional simulation is applied to production blocks that were in the short-term block model. For this application, the previously calculated block scaled variogram model is used. Drill hole locations with zero ash content are used as the reference point while running the simulations. This creates fluctuations with zero mean capturing variability on a block

- scale conditioned on data locations. This can be done in “black-box” type module.
3. After this, simulated data on the production blocks refer to the uncertainty and they will be added on prior estimations of block attributes.
 4. The short-term model based on the simulations is now ready to be imported into the algorithm as the first main component (prior model).
 5. The updated resource model (posterior model) will be split in a mean part, which will be written back to update the short-term block model, and an uncertainty related part which will be written back in the ensemble part.

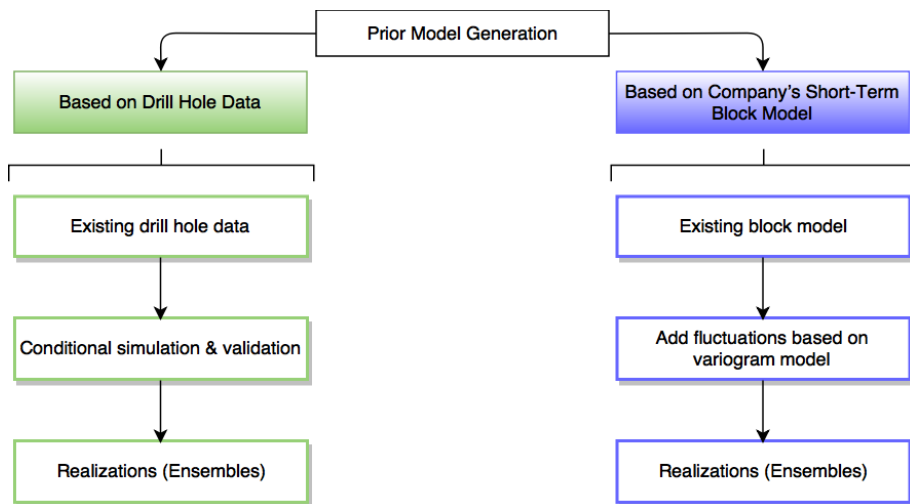


Figure 3.7: Flow chart of prior model generation

As long as new measurement data is obtained, these steps need to be applied recursively. The process can easily be automated by using a previously calculated variogram model and some interfaces. In this way, there will be no requirement for an additional complex process of creating conditional simulations since they are not part of the daily work flow. Moreover, there will be no disarray between a company’s short-term model and the input prior model of the updating approach; the integration will be smooth. Additional to that, no expert knowledge will be required when applying the framework due to the automated process, contrary to conditional simulation application. All of these simplifications on application are very significant since it is important to benefit from the framework in a real mining environment.

This approach will be applied in the case study of Chapter 6.

4. METHOD VALIDATION IN A 2D CASE STUDY

In this chapter, a 2D case study has been performed in order to validate the introduced concept in a fully controllable environment. This case study validates if performing a real-time update on a resource model leads to more accurate resource models for future processes. This chapter will describe the set-up of the experiments, explain some details about performance measures and finally, provide the results of the case studies.

The contents of this chapter have been adapted from:

Yüksel, C., Thielemann, T., Wambeke, T., & Benndorf, J. (2016). Real-Time Re-source Model Updating for Improved Coal Quality Control Using Online Data. *International Journal of Coal Geology*. doi: <http://dx.doi.org/10.1016/j.coal.2016.05.014>.

4.1. EXPERIMENTAL SET-UP

All of the experiments presented in this chapter are performed in a completely known and fully controllable environment; a well-known geostatistical dataset, called Walker Lake dataset [63]. The dataset originally contained digital elevation data from the Walker Lake area (California-Nevada border), in our case those will be interpreted as the concentration values. An exhaustive dataset is chosen in order to benchmark the obtained results against reality.

The virtual exploration data is created by sampling the dataset in a spacing of 32m x 32m x 20m. Realizations of the block model are created by conditional simulation. The blocks were defined with a dimension of 16m x 16m x 10m. The density is assumed 2 t/m³, which leads a tonnage of 5120t for one mining block.

No availability of real sensor data requires the generation of virtual sensor data. In order to mimic real sensor data, the artificial sensor data are composed of three components; true block value, dispersion variance and sensor error. Component one is the true block grade taken from the exhaustively known data set. Component two captures the volume variance relationship and corrects the block value support to a smaller measured support by adding the corresponding dispersion variance [63-65]. The third component represents the precision of the sensor and, for this case study, varies between 1, 5 and 10%.

It is assumed that the excavated material is discharged on a conveyor belt positioned on the benches in the mining area. The conveyor belts then combine the material flow at the central mass distribution point. The combined material flow is scanned by a sensor positioned above the conveyor belt.

The mining system is assumed to consist of, either one, two, three or four bucket-wheel excavators positioned at different benches with different digging rates. In the case of one excavator, the mine design assumes that the excavation starts from the south-west corner of the block model and continues through the east direction until the entire row is mined (Figure 4.1). When the excavation of the first row is completed, the excavator moves to the northern row and continues to excavating in a western direction. In case of two excavators, the second excavator starts at the south-eastern corner of the northern half of the field. In the case of three and four excavators, the field is divided in three and four parts respectively.

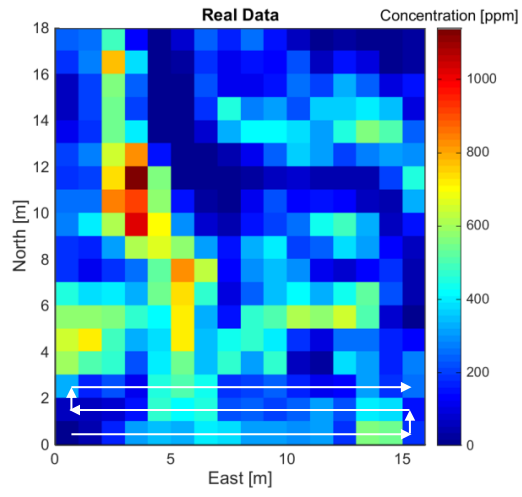


Figure 4.1: Mining sequence

4.2. RESULTS AND DISCUSSION

A series of experiments is performed in order to analyze the performance of the updating concept. This section provides some representative results from the performed experiments. In the influence area of updating three different performance measures are used in order to present the results of the performed experiments.

The first measure is an empirical error measure so called mean square difference, or mean square error (MSE). MSE compares the difference between estimated block value $\mathbf{Z}^*(\mathbf{x})$ and real block value $\mathbf{Z}(\mathbf{x})$ from the exhaustive data set and it can be calculated as follows:

$$MSE = \frac{1}{N} \sum_{i=1}^N (z^*(\mathbf{x}_i) - z(\mathbf{x}_i))^2 \tag{4.1}$$

The second measure is the theoretical block variance (BV), which can be approximated by the EnKF Equation (3.7) or:

$$BV \cong \frac{1}{N-1} \sum_{i=1}^N ((z(\mathbf{x}_i) - \overline{z(\mathbf{x})})(z(\mathbf{x}_i) - \overline{z(\mathbf{x})})^T) \tag{4.2}$$

Both of the mean square error and block variance bar plots are illustrated relative to the prior model in order to make a good comparison. This “relative illustration” refers to scaling the MSE and the BV values by the prior model. Each plot contains four bars, from left to right; prior model, mined blocks, adjacent blocks and indirect blocks (two blocks away).

Table 4.1: MSE and BV plots for 1 excavator case – 2D Case study

	Mined Blocks	Adjacent Blocks	Indirect Blocks
MSE	<p>1</p>	<p>2</p>	<p>3</p>

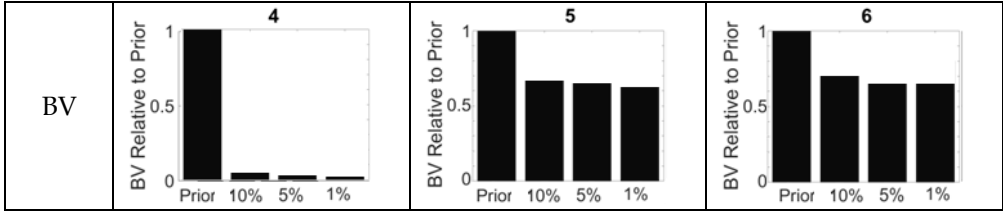


Table 4.1 gives the MSE and BV plots for one excavator case. The graphs are obtained under the following conditions: one excavator was operating, undergoing measurements every 10 minutes and updating the resource model every hour. The following observations can be made based on the graphs given in Table 4.1:

- For mined blocks, the uncertainty almost vanishes while the sensor error decreases. This is expected because in case of one excavator the sensor measurements can be clearly tracked back to the source block. Residual uncertainties can be caused by the sensor precision and also interpreted as the limit of the filter for this special application.
- Adjacent blocks are updated resulting in a significant improvement compared to the prior model. This improvement is due to the positive covariance between two adjacent blocks. In addition, the sensor precision effect can be observed from the results.
- Blocks in the second next row are still updated. As expected, the error in prediction increases when moving further away from the point of measurement (from mined block, to adjacent and indirect blocks).

Finally, the third measure is a representative map of the study area which indicates the differences between the real value and updated values of the area (Figure 4.2).

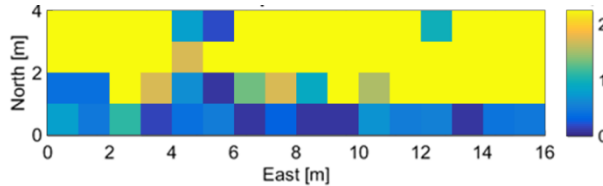


Figure 4.2: Difference map between the real data and updated model on 50th simulation.

The experiment was designed to update only the blocks in the first row, by integrating their relative measurements. Figure 4.2 indicates almost no difference between reality and the updated model. In the second row, it is still possible to observe the updates by investigating the small differences between reality and the updated models. Once again, the difference maps prove that the developed framework is suitable for this specific application.

In addition to the above results, the MSE and BV plots for the two excavators case are given in Table 4.2. The graphs are obtained under the following

conditions: two excavators were operating, undergoing measurements every 10 minutes and updating the resource model every hour. The following observations can be made based on the graphs given in Table 4.2.

- For mined blocks, the uncertainty increases with a trend similar to the one excavator case. The observed increase in the uncertainty is expected since the sensor measurements cannot be clearly tracked back to the source block anymore. Yet, even with this increase in the MSE, the results shown significant improvement compared to the prior model.
- Adjacent blocks are updated which results in a significant improvement compared to the prior model. A slight decrease in the uncertainty is observed in the results compared to the one excavator case. This can be explained due to positive correlation between the increased amount of measurement data and the adjacent blocks. Moreover, the sensor precision effect can also be observed from the results.
- Blocks in the second next row are still updated with an increased uncertainty (relative to the one excavator case). Again, MSE and BV behave similarly and the sensor precision effect can be observed from the results.

Table 4.2: MSE and BV plots for 2 excavators case – 2D Case study

	Mined Blocks	Adjacent Blocks	Indirect Blocks
MSE	<p>1</p>	<p>2</p>	<p>3</p>
BV	<p>4</p>	<p>5</p>	<p>6</p>

Results show the validity of the real-time resource model updating concept in a 2D example. The consistency is reduced when the update moves from mined blocks to indirect blocks, as is expected. Moreover, the observed results match and show similar behaviors between the theoretical measure (BV) and the empirical measure (MSE), which indicates good calibration of the model parameters.

4.3. VALIDATION OF THE DEVELOPED FRAMEWORK

Results in the previous section indicated a significant level of improvement in the resource models by incorporating sensor data. A reduction of uncertainty is observed after the data assimilation. In order to continue, the method is benchmarked against a proven and well-studied, however computationally expensive method of rejection sampling.

The rejection sampling method is chosen for validation purposes due to its simplicity. Similar applications of this method can also be found in reservoir engineering [66-69]. Rejection sampling is a Monte Carlo method that proposes a sample from some relatively simple distribution, after which a test is applied to decide whether or not to accept it. It is based on the fact that the posterior is a subset of the prior distribution, and therefore it can be evaluated by sub-sampling the prior [70]. All accepted samples are truly independent since the accept/reject criteria do not depend on the most recent sample.

To implement this method, 1000 realizations were created by using the Sequential Gaussian Simulation method, to generate the prior models. The developed updating framework was applied to the 1000 prior models in order to generate 1000 updated realizations (updated posterior models). As the rejection sampling proposes that the posterior is a subset of the prior distribution, it is expected that one can obtain the updated posterior distributions by applying rejection sampling to our prior models.

To generate realizations from the target probability density $f(\mathbf{Z}(\mathbf{x}))$, we let $h(\mathbf{Z}(\mathbf{x}))$ be a probability density of one single realization and suppose that there is some constant c such $f(\mathbf{Z}(\mathbf{x})) \leq ch(\mathbf{Z}(\mathbf{x}))$ for all m .

- 1: randomly **draw** realization m^* from 1000 prior models pdf $h(\cdot)$
- 2: randomly **draw** a decision variable u from $U(0, ch(\mathbf{Z}(\mathbf{x}))^*)$
- 3: **if** $u \leq f(\mathbf{Z}(\mathbf{x}))^*$
 accept proposed model
 else
 reject proposed model
- 4: **return** to step 1
- 5: **end**

The conditional probability density $f(\mathbf{Z}(\mathbf{x}))$ is provided by Bayes rule and can be calculated as follows,

$$f_{(\mathbf{Z}(x)^e|l^e)(\mathbf{Z}(x)|l)} = \frac{f_{(l^e|\mathbf{Z}(x)^e)(l|\mathbf{Z}(x))} f_{\mathbf{Z}(x)^e}(\mathbf{Z}(\mathbf{x}))}{\int f_{(l^e|\mathbf{Z}(x)^e)(l|\mathbf{Z}(x))} f_M(\mathbf{Z}(\mathbf{x})) \mathbf{1Z}(\mathbf{x})} \quad (4.3)$$

$$\propto \exp\left(-\frac{1}{2}(\mathbf{AZ}_0(x) - \mathbf{I})^T \mathbf{C}_{\parallel}^{-1} (\mathbf{AZ}_0(x) - \mathbf{I})\right) \times \exp\left(-\frac{1}{2}(\mathbf{Z}_0(x) - \mu)^T \mathbf{C}_{zz}^{-1} (\mathbf{Z}_0(x) - \mu)\right) \quad (4.4)$$

where $\mathbf{AZ}_0(x)$ is the predicted observation and $\mathbf{Z}_0(x)$ is the prior model and μ is the mean value of the prior model. \mathbf{C}_{\parallel} and \mathbf{C}_{zz} are the measurement error covariance and the prior model covariance respectively.

Figure 4.3 illustrates the performed experimental scheme. The given algorithm is applied to both 1000 prior models and 1000 updated posterior models. Around 290 of 1000 prior models were accepted, while 950 of 1000 updated posterior models were accepted. The fact that almost all of the updated posterior models are accepted shows a significant improvement over the prior models (from 29% to a 95% acceptance rate). This indicates that the updated posterior models are closer to reality than the prior models.

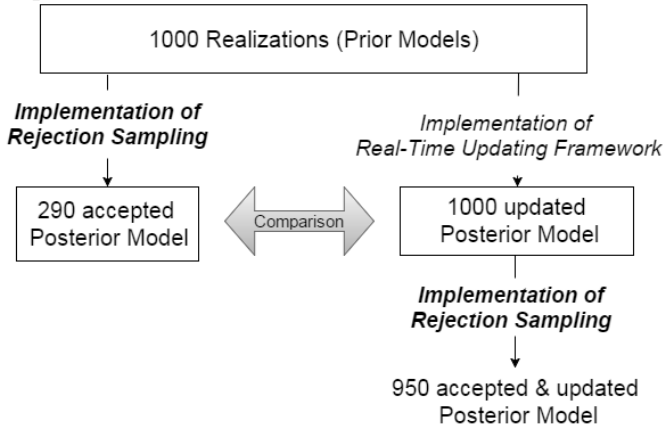


Figure 4.3: Validation experiment scheme

The 290 accepted posterior models and 1000 updated posterior models are compared to each other in order to investigate the similarities. Therefore, the average of mean and variance of the distributions are compared.

Figure 4.4 and Figure 4.5 show the average of mean and variance of the posterior models obtained from rejection sampling and updating framework, respectively. It can be seen that the average mean and variance of accepted prior models (290) and updated prior models (1000) are very similar to each other.

Figure 4.6 is provided for a better comparison between the accepted posterior realizations from rejection sampling (290) and updated posterior realizations from the real-time update framework (1000). The deviations between two models are very small. One can conclude that the updated posterior realizations from the real-time update framework are reproduced through rejection sampling.

In addition, MSE and BV graphs of mined, adjacent and indirect blocks from the accepted posterior models by rejection sampling (290) are given to provide the

empirical and theoretical measures (Table 4.3). As mentioned in the previous section, both of the plots are prepared relative to the prior model in order to provide a good comparison. Again, each plot includes four bars, from left to right; prior model, mined blocks, adjacent blocks and indirect blocks.

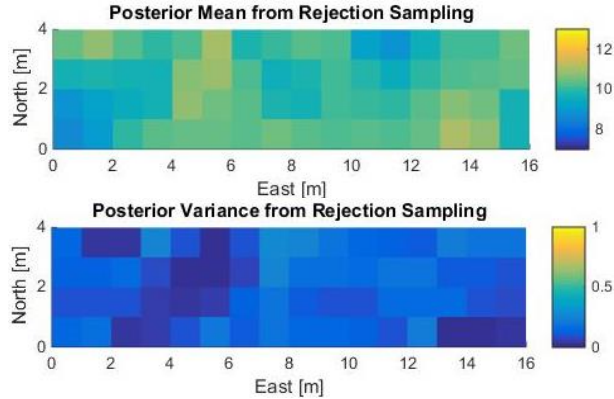


Figure 4.4: Average mean (left) and variance (right) maps of 290 posterior realizations accepted according to rejection sampling method

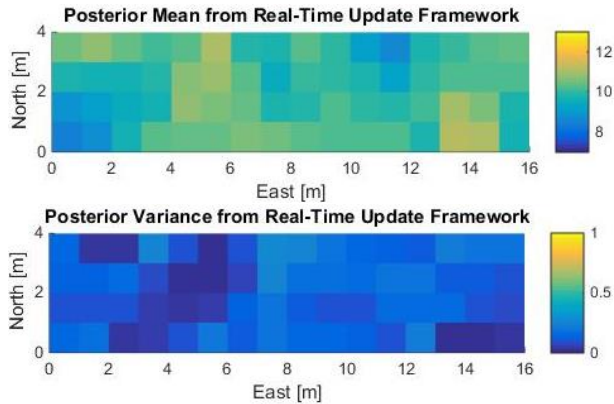


Figure 4.5: Average mean (left) and variance (right) maps of 1000 posterior realizations updated with real-time update framework

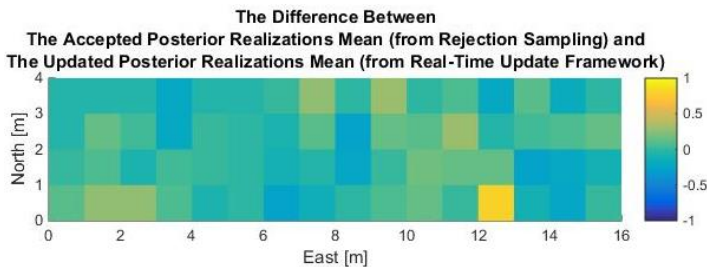


Figure 4.6: Difference map between the accepted posterior realizations from rejection sampling and updated posterior realizations from real-time update framework

Table 4.3: MSE and BV plots - Rejection sampling

	Mined Blocks	Adjacent Blocks	Indirect Blocks
MSE			
BV			

When BV values in Table 4.3 (MSE and BV plots of the accepted posterior models from rejection sampling) are compared to the ones in Table 4.1 (MSE and BV plots of the updated posterior realizations), similar trends are observed except relatively higher values in Table 4.3. The general behavior of both tables is the increase of the block variance moving from mined blocks to indirect blocks, and the decrease of it when the sensor error is smaller. For the MSE values, an increase in the error rate is observable when moving from mined blocks to indirect blocks, yet the increase is not very significant. This is because the nature of rejection sampling does not take into account the weight of distances.

The mentioned similarities in the comparison of empirical error and theoretical variance of the accepted posterior realizations from rejection sampling and updated posterior realizations from real-time updating framework, once again, indicate that the accepted models through rejection sampling are truly reflecting the updated models. This section concludes that the presented results validate the developed real-time updating framework in a simple 2D setting and that it is a promising method for reaching the targets aimed for in a more complex 3D environment.

5. DEMONSTRATION AND PROOF OF CONCEPT IN AN INDUSTRIAL ENVIRONMENT - CASE 1

This chapter demonstrates the applicability of the developed framework during an industrial application, in Garzweiler mine, Germany. The application in continuous mining test case is illustrated and sensitivity analysis experiments are performed. Findings of the study are then presented. Key findings of the study are discussed and summarized.

The contents of this chapter have been adapted from:

Section 5.1, 5.2 and 5.3: Yüksel, C., Thielemann, T., Wambeke, T., & Benndorf, J. (2016). Real-Time Resource Model Updating for Improved Coal Quality Control Using Online Data. *International Journal of Coal Geology*. doi: <http://dx.doi.org/10.1016/j.coal.2016.05.014>.

Section 5.4: Yüksel, C., Benndorf, J. (2017) Performance analysis of continuous resource model updating in lignite production *Geostatistics Valencia 2016* (pp. 431-446): Springer.

5.1. EXPERIMENTAL SETUP

First, the geological model (Figure 5.1) of the defined coal seam is created in a 32x32x1 m block model based on the roof and floor information of the seam. Second, a 32x32x1 m quality model that indicates the wet ash content in percentages is represented with 24 simulations and an estimation, based on the provided drill hole data. The simulated and estimated ash values are imported into previously defined coal seam. These are the first input file, the prior quality (ash) model.

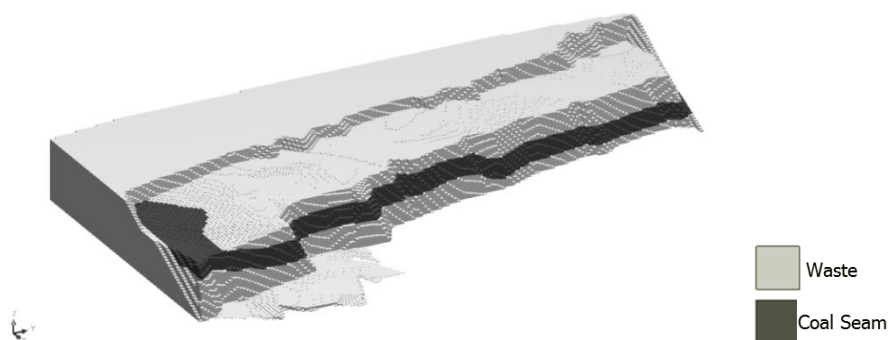


Figure 5.1: Geological model

Predicted measurements are obtained by averaging the simulated ash values from each simulation set, which falls into the defined production block boundaries. The online RGI sensor measurement data and KOLA data are provided for the time corresponding to extraction. In order to determine the location of the received RGI and KOLA data, in other words to track back where the measured material comes from, the GPS data is matched with the measurement data based on the given timecodes. The located measurements in coal seams are then imported into the previously defined block model.

The second input file for the algorithm is written to a file containing the following information: the block ID, central block location (X, Y, Z coordinates), a series of real and predicted measurements.

A study bench produced for 15 days is defined by considering all the available data (topography, RGI, GPS and production data). Later, the study bench is divided into so-called "production blocks". This was necessary to reproduce the excavated production blocks. The horizontal divisions (or production slices) are based on the movements of the excavator during production, which is based on GPS data. The vertical divisions are based on the changes in the Z coordinates in the GPS data. In the end, the defined production bench is divided into 28 blocks and 5 slices, which gives 140 production blocks. Once the study bench is divided both in vertical and horizontal, the production blocks are now ready to be updated.

The defined study bench is divided into blocks and their respective related block ID numbers are given in Figure 5.2. As a start the 2nd slice of block number 1 is chosen to be updated, based on the KOLA measurements taken from that block. The series of updating experiments will continue until the 10th block. The update range is defined based on the variogram of the data as 450m in X and Y direction and 2.5m in Z direction. The range of expected improvements is marked as the circled area.

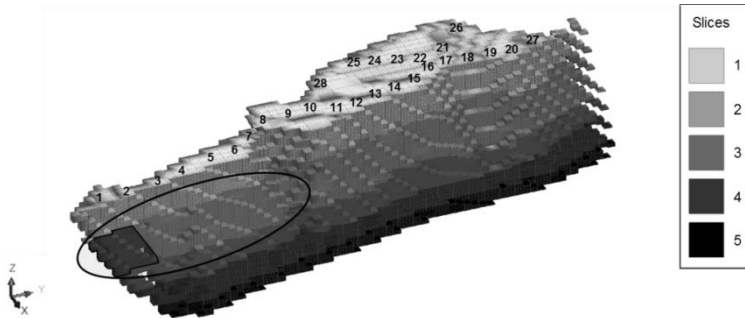


Figure 5.2: Production blocks

5.2. RESULTS AND DISCUSSIONS

This section presents the results of the previously defined experiment. The added value of this application will also be discussed.

The first experiment uses the KOLA measurement, received from the 1st block's production, in order to update the neighborhood blocks of the 1st block. Figure 5.3 illustrates the first experiment, where prior, posterior and measurement values are given. The averaged ash values from the prior simulation are represented with round dots and the related KOLA measurement values are given square marks. The light grey cloud of updated simulations covers the model uncertainty, while the long dashed line represents the average of the simulations. The vertical red line indicates which block's KOLA data has been used for that experiment.

Figure 5.4 to Figure 5.6 presents results of similar experiments, except the base of the update is moving forward from 1st block till the 9th block, as if the production moves. In each graph, the mined out area is indicated with an arrow. Among results of 7 experiments, only four of them (1st, 2nd, 4th and 7th) are presented here since they adequately represent the rest.

It is clearly seen from the Figure 5.3 that the average of the prior simulations dramatically underestimates the actual KOLA measurements. This happens because the prior simulations are created based on the coal samples in the drill holes, while the KOLA measurements measure higher ash values due to the sand intrusions in the coal seam. Integrating the KOLA measurement of the 1st block updates the first nine blocks to some higher values. As expected, the update effect decreases while moving away from Block 1.

Already from the second experiment (updating the ash values based on the measurement of the Block 2), the KOLA data is well covered by the range of uncertainty in the updated neighborhood. While the integrated measurement number increases (experiment 2, 3, ..., 7) it is observed that the uncertainty in the near neighborhood gets slightly smaller and more of the actual KOLA measurements are captured by this uncertainty range.

The improvements from the very initial averaged prior simulation to the most recent updated simulations are clearly observable

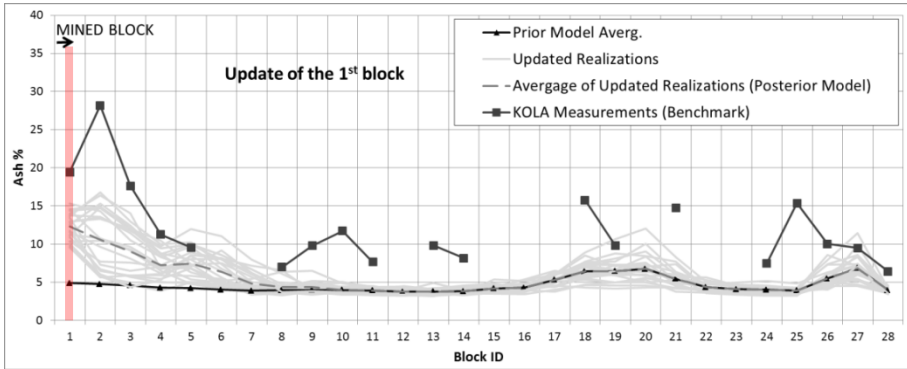


Figure 5.3: Experiment 1 - Updating: 2nd slice of the 1st block

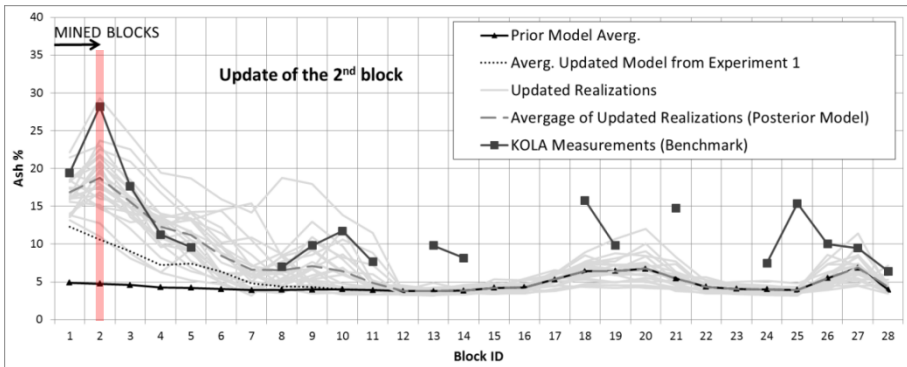


Figure 5.4: Experiment 2 - Updating: 2nd slice of the 2nd block

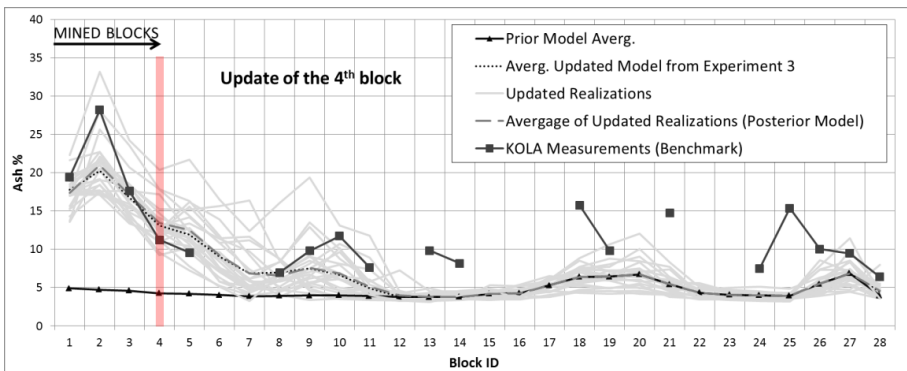


Figure 5.5: Experiment 4 - Updating: 2nd slice of the 4th block

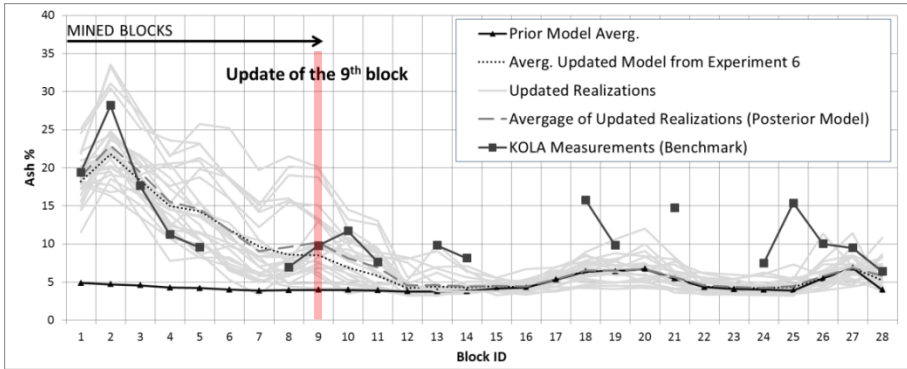


Figure 5.6: Experiment 7 - Updating: 2nd slice of the 9th block

The presented experiment demonstrated a resource model updating case study in a large open pit mining operation using the actual measurements, the so called KOLA data. The results have shown that the developed updating algorithm works well in a real-3D case.

Figure 5.7 gives the calculated MSE values for each performed experiment. Since this is a real case, the real block values are unknown. For this reason, the MSE compares the difference between estimated block value $Z^*(x)$ and measured KOLA value (v). Once more, they are calculated relative to the prior averaged simulation. Figure 5.7 clearly indicates the improvements. The biggest improvement is observed on the first experiment, where the MSE value drops to 0.33 from 0.64. For the next experiments, the update is slightly smaller, yet observable. MSE values drop from 0.33 to 0.27 during the experiments between 2 and 7. This indicates in the order of 70% improvement while integrating online measurement data into the resource model.

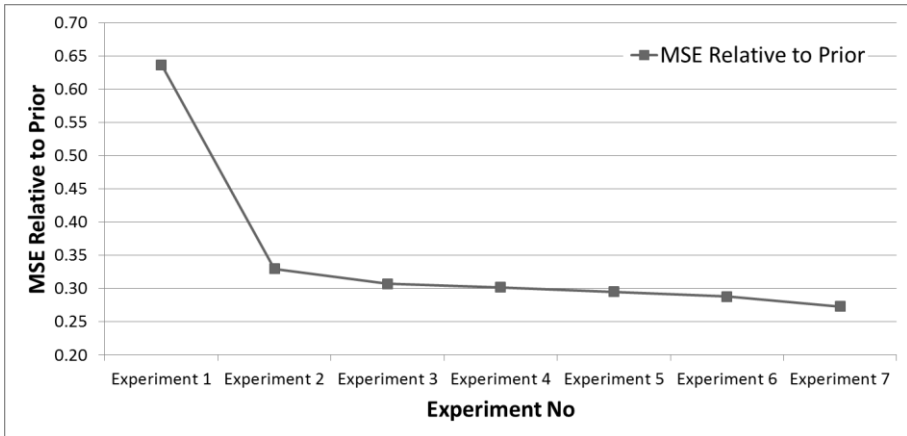


Figure 5.7: MSE Graph for performed experiments

5.3. SENSITIVITY ANALYSIS

The aim of the case study presented in this section, is to analyze the performance of the resource model updating framework method by performing sensitivity analysis on main parameters, including; the ensemble size, localization and neighborhood strategies and the sensor precision.

5.3.1. Identification of Main Parameters

5.3.1.1. Number of Ensemble Members

The first sensitivity analysis focuses on investigating the optimal realization number (subsequently used as ensemble size) by performing resource model updating experiments with differently sized ensembles. Defining the ensemble size that will acceptably represent the orebody is a very delicate problem. A large amount of research in literature [6, 71] focuses on the optimum ensemble size investigation and usually concludes that the analysis error decreases as the number of ensembles (realizations) increases. Contrary, the computational costs increase with the ensemble size. Therefore a sensible size of the ensemble is required.

5.3.1.2. Localization

The second sensitivity analysis focuses on investigating the effects of localization strategies and neighborhood size on the given case. As mentioned, one of the limiting factors in EnKF based applications is the restrained ensemble size. Having an insufficient number of ensemble numbers, the empirical way to compute the covariance matrixes needed might cause long range spurious correlations. In order to avoid these spurious correlations, a covariance localization technique is applied to the updating framework by [59]. The term 'spurious correlations' refers to the correlations between quality attributes that are at a significant distance from one another where there is no spatial relation. Moreover, these correlations can lead to inbreeding and filter divergence. Covariance localization modifies update equations by replacing the model error covariance by its element-wise (Schur) product with some distance-based correlation matrix [72, 73]. This replacement increases the rank of the modified covariance matrix and masks spurious correlations between distant state vector elements [58].

5.3.1.3. Sensor Error

The final sensitivity analysis focus on testing the effect of the sensor precision. In most cases errors are involved when taking measurements, due to calibration issues of sensor technologies. For each experiment, different amounts of standard error is added to the actual measurement values. The standard error can be calculated as;

$$SE_{\bar{x}} = \frac{\sigma}{\sqrt{n}} \quad (5.1)$$

where σ is the standard deviation of the actual measurements and n is the size (number of observations) of the actual measurements. For this study, the actual measurement data set contains 700 observations, which values correspond to coal extracted from 28 mining blocks. This leads to approximately 25 actual measurement data per block. Therefore, according to Equation (5.1), where the added standard error is 0.1% ash, the absolute standard deviation will be 0.5% ash and the variance will be 0.25%² ash.

Similarly, when the added standard error is 0.2% ash, the standard deviation will be 1% ash and the variance will be 1%² ash. The variance of the actual measurements will be 6.25%² ash and the standard deviation will be 2.5% ash when the added standard error is 0.5% ash. The variance will be 25%² ash when the added standard error is 1% ash. The variance of the averaged prior model for 48 ensemble members is calculated as 0.99.

To give a clear view, the mentioned standard deviations are converted to relative error of the measurements. The average measurement value is calculated as 12% ash. This leads around 4% ash relative error in measurement values when the added standard deviation is 0.5% ash. Similarly, when the added standard deviation is 1% ash, this indicates around 8% ash relative error in measurement values. In the same way, when the added standard deviation is 2.5% ash, this indicates around 20% ash relative error in measurement values. Finally, when the added standard deviation is 5% ash, this indicates around 40% ash relative error in measurement values.

5.3.2. Experimental Set-Up

To apply the resource model updating algorithm, the input data needs to be prepared. For the experiments performed in this section, multiple sets of block model realizations are generated with each having a different number of simulations (24, 48, 96, 192 and 384). To apply the double helix approach as suggested by [59], the initial simulation number is an even number. Double helix approach is used in order to avoid problems of inbreeding, a pair of sequential updating cycles is configured by [59] so that the assimilation of data into one set of realizations employs the weights calculated from the other one. The simulation numbers following the initial simulation number are doubled for each set. The details of generating the block model (with 24 realizations) for Case 1 are explained in Section 5.1.

Figure 5.8 illustrates the prior model of 48 simulations, the averaged ash values of those simulations and related sensor measurement values, per block. A significant underestimation of the actual measurement data is observed in the

prior model. This is because the prior model is created based on the drill hole data, where the local sand intrusions are not fully captured. True variability of the coal seam is captured by the online sensor measurements.

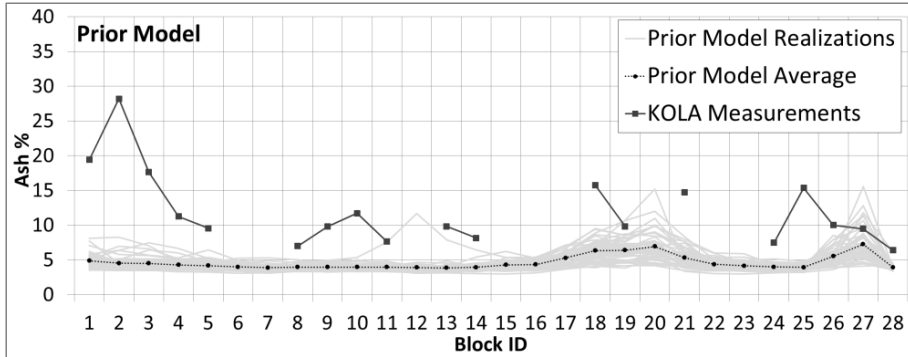


Figure 5.8: Prior model and measurement data (before updating)

The preparation of the predicted measurements, located KOLA measurements, second input file and the study bench are done in an exactly identical experimental set-up as given in Section 5.1.

First the 1st block of the 2nd slice is updated, based on the KOLA measurements taken from that block. The series of updating experiments included seven updating experiments and continued until the 9th block (since there are no KOLA data obtained on 6th and 7th block, 7 experiments are performed to update until the 9th block). In each updating experiment, only one block is updated based on the related measured KOLA value.

As introduced in the Section 4.2., the empirical error measure MSE (Equation (4.1)) is also used in this case study in order to present the results of the performed experiments. The mean square error graphs are calculated relative to the averaged prior model of 384 ensembles, in order to make a good comparison.

5.3.3. Experiments with Respect to Main Parameters

Table 5.1 provides a complete overview of the parameters used to perform the experiments. The obtained results of these experiments are provided in the next chapter. In every experiment performed for every parameter, one parameter is varied and the others remain fixed Table 5.1.

Table 5.1: Experimental scheme

	Experiment #	Ensemble Size	Localization Option on/off and Size (X,Y,Z) (m)	Neighborhood Size (X,Y,Z) (m)	Relative Sensor Error (%)
Ensemble Size Experiments	1	24	on, 125,125,3	225,225,6	0
	2	48	on, 125,125,3	225,225,6	0
	3	96	on, 125,125,3	225,225,6	0
	4	192	on, 125,125,3	225,225,6	0
	5	384	on, 125,125,3	225,225,6	0
Localization & Neighborhood Strategies Experiments	6	48	off	225,225,6	0
	7	48	on, 225,225,3	450,450,6	0
	8	48	off	450,450,6	0
	9	48	off	900,900,6	0
	10	48	on, 450,450,3	900,900,6	0
	11	48	on, 450,450,6	900,900,6	0
Sensor Error Experiments	12	48	off	450,450,6	4
	13	48	off	450,450,6	8
	14	48	off	450,450,6	20
	15	48	off	450,450,6	40

5.3.3.1. Number of Ensemble Members

With a view towards the real-time application of the updating resource model, the industrial case presented in the previous sections of this chapter (Section 5.1, 5.2 and 5.3) focused on small - and moderate - sized ensembles (24). For the investigation of the optimum ensemble size, updating experiment series are performed with 24, 48, 96, 192 and 384 ensembles. All of the simulations are created by using SGS with same seed number and same variogram parameters.

5.3.3.2. Localization

The initial neighborhood size is defined as 450m in X and Y direction and 6m in Z direction based on the variogram of the drill hole data. For the experiments,

three different neighborhood sizes (225, 450 and 900 m) are tested while the localization option was not being used. Three more experiment are performed while the localization option was being used in order to test the effect of designed localization, with varying localization and neighborhood sizes. For the experiments where the localization option was used, the localization neighborhood was assumed as half of the defined neighborhood size, except for the 10th experiment. In the 10th experiment, in the X and Y direction, localization sizes were assumed as half of the defined neighborhood size. In the Z direction, the localization size remained the same. Reasons of this preference will be explained in the discussion section.

5.3.3.3. Sensor Error

For each experiment, a different amount of standard error is added to the actual KOLA measurement values. In total, five experiments are performed, where the relative measurement error varies between 4%, 8%, 20% and 40%.

5.3.4. Results and Discussion

5.3.4.1. Results

5.3.4.1.1. Ensemble Size

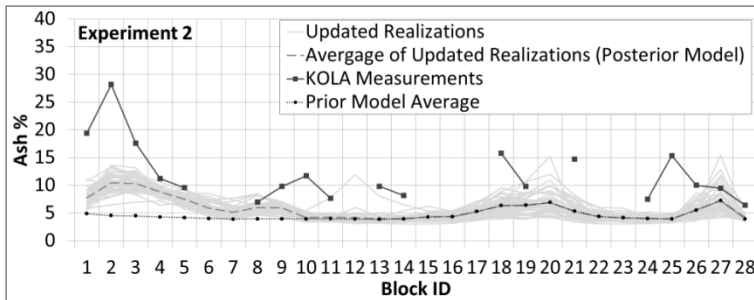


Figure 5.9: Experiment 2 – Ensemble size: 48

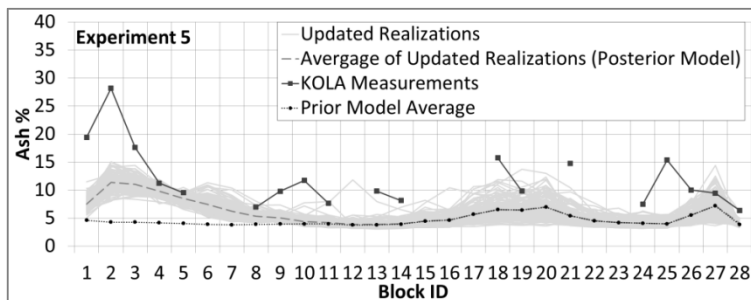


Figure 5.10: Experiment 5 – Ensemble size: 384

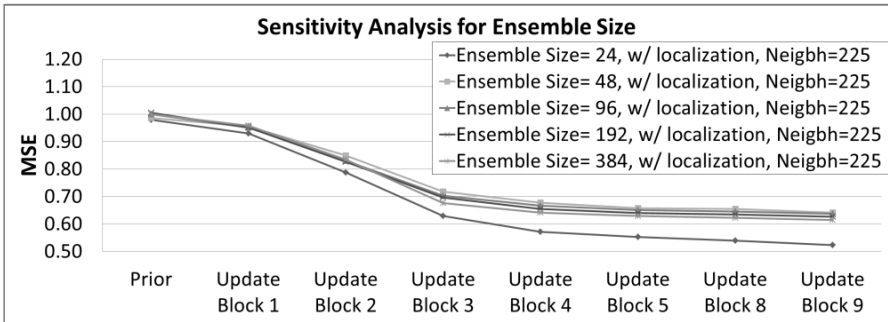


Figure 5.11: Comparison graph for different ensemble sized experiments

5.3.4.1.2. Localization and Neighborhood Strategies

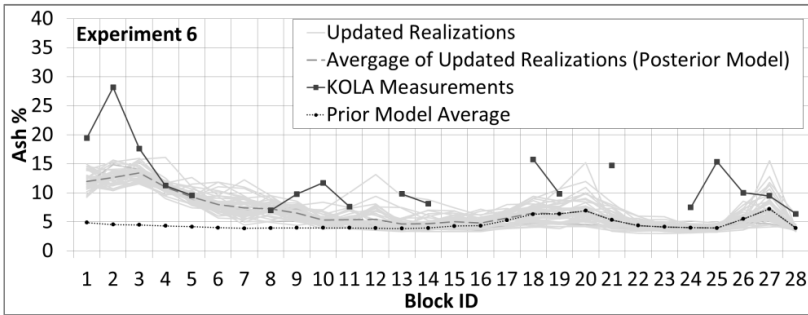


Figure 5.12: Experiment 6 - Localization option off, Neighborhood size: 225,225,6 m

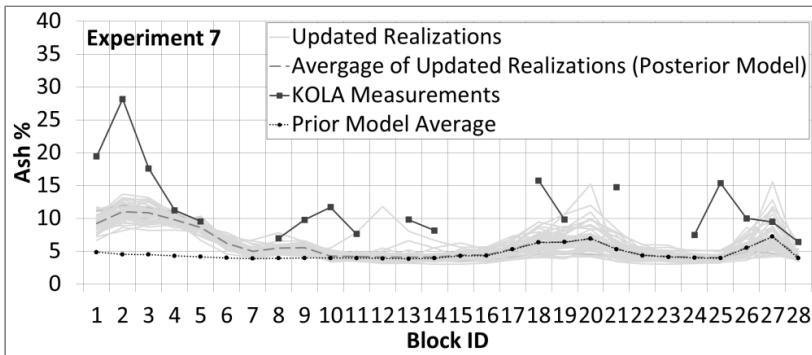


Figure 5.13: Experiment 7 - Localization option on (225,225,3 m), Neighborhood size: 450,450,6 m

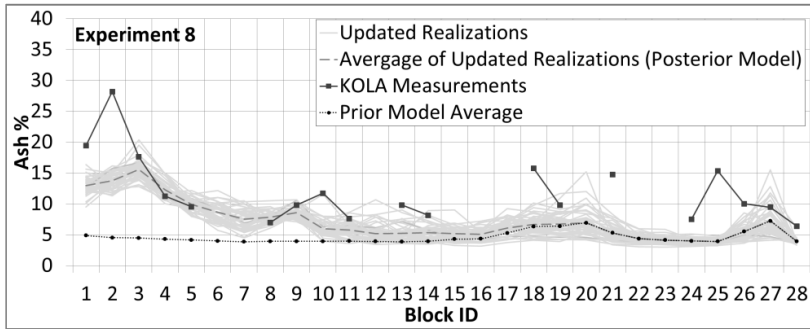


Figure 5.14: Experiment 8 - Localization option off, Neighborhood size: 450,450,6 m

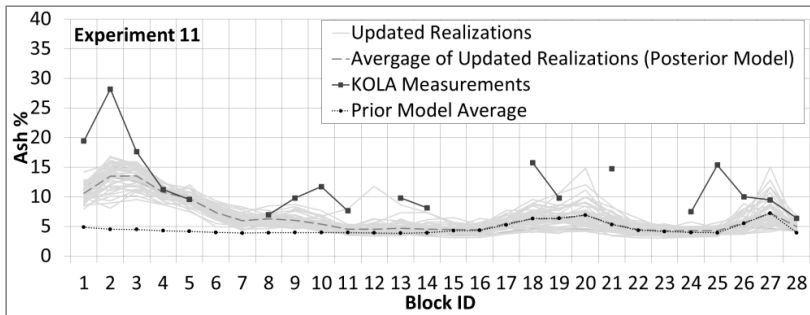


Figure 5.15: Experiment 11 - Localization option on (450,450,6 m), Neighborhood size: 900,900,6 m

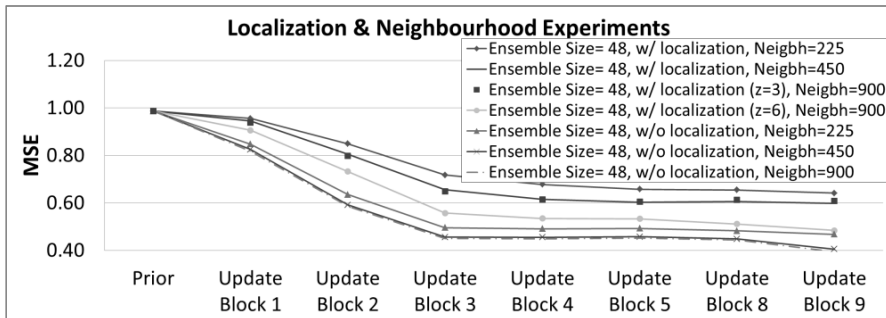


Figure 5.16: Comparison graph for different localization and neighborhood strategies experiments

5.3.4.1.3. Sensor Precision

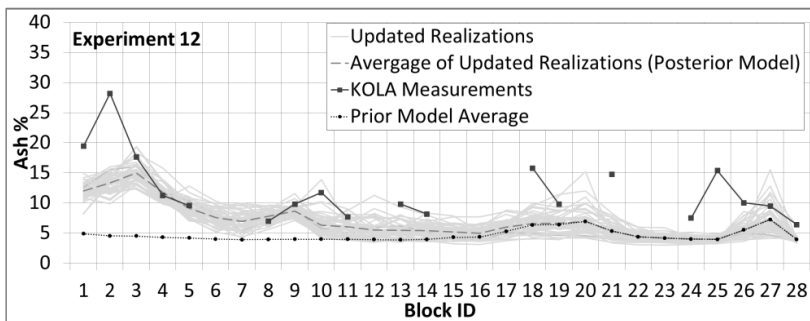


Figure 5.17: Experiment 12 – Relative sensor error: 4%

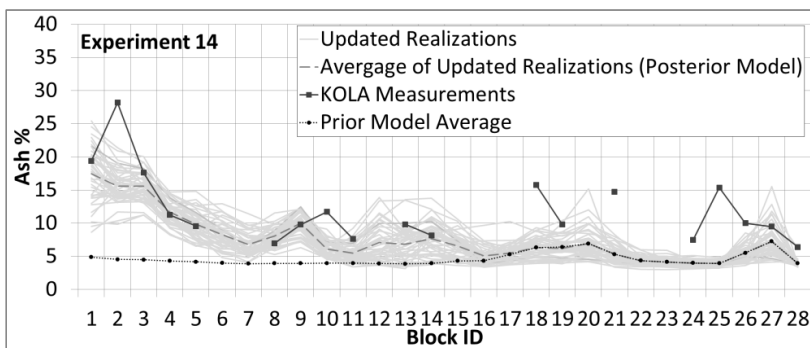


Figure 5.18: Experiment 14 – Relative sensor error: 20%

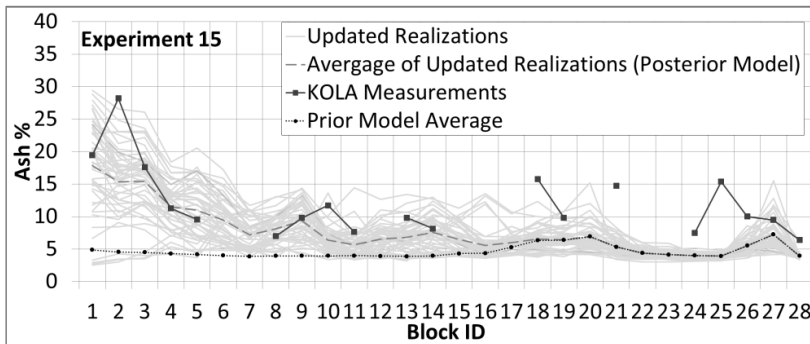


Figure 5.19: Experiment 15 – Relative sensor error: 40%

5.3.4.2. Discussion

The previous section presented sensitivity analysis results for each parameter. The following section will be discussing the key findings of the study for each parameter.

5.3.4.2.1. Ensemble Size

Figure 5.9 and Figure 5.10 present results of the updating process from the 1st block until the 9th block, for some of the representative ensemble sizes. For these experiment series, the localization strategies were applied, the neighborhood size was 225,225,6 m for X,Y,Z directions and no sensor error was assumed.

It can be seen that the average of the prior simulations substantially underestimates the actual KOLA measurements. This is caused by the data effect. The prior simulations are created based on the coal samples from drill holes spaced multiple hundred meters apart, while the KOLA measurements measure higher ash values due to the sand intrusions in the coal seam. Integrating the KOLA measurement in to the first nine blocks, updates the neighborhood blocks to some relatively higher values. As expected, the update effect decreases while moving away from the last updated block, Block 9.

For all different ensemble sizes, a clear improvement is observed towards the KOLA data when considering the average of the initial simulations, so called prior model.

Figure 5.11 presents the relative MSE values to the prior model for each experiment performed with different ensemble sizes. The biggest reduction of the error occurs in the update of the first block. While the skewness behavior of the each MSE graphs is similar, the biggest error behavior to the smallest is as follows: 48 ensemble members, 96 ensemble members, 192 ensemble members, 384 ensemble members and 24 ensemble members. Except for the results from 24 ensemble, the rest of the listing supports the literature. It is expected to observe a decrease in the MSE values while the ensemble size gets larger since the representativeness gets higher. However, to increase the computational efficiency and to apply the updating framework in real-time during production, an economic ensemble size is required.

At first glance, the higher initial variance of the 24 ensemble members explains the very low MSE values. Nevertheless, a further investigation is performed in order to understand the phenomenon better. Five different newly derived sets of 24 ensemble members are generated with SGS, by using different random seeds for each set. New series of updating experiments are performed with the new series of 24 ensemble members and the results are compared. The comparison shows a high variety among results. MSE values obtained from the 9th block's update varied between 0.52 - 0.69. In addition, the new sets of MSE values were equal to, lower or higher than the 48 ensemble members, 96 ensemble members,

192 ensemble members and 384 ensemble members. This big variety, which is caused by different seed numbers, shows that 24 ensemble members were not sufficient to represent a statistical stable estimate of the mentioned lignite seam.

When considering the 48 ensemble, even though the 48 ensemble has the highest MSE values by comparing to the 96 ensemble, 192 ensemble and 384 ensemble, the MSE dropped from 1.0 to 0.64. In his research Yin, Zhan [74] found that improvements while using larger ensemble sizes (after the optimum ensemble size) are relatively insignificant. Likewise, the improvements between 48, 96, 192 and 384 ensembles are obvious, yet not very significant. For this reason, this study concludes that the optimal ensemble size for this specific study is 48 ensemble members.

5.3.4.2.2. Localization and Neighborhood Strategies

Figure 5.12 to Figure 5.15 presents results of the updating process from the 1st block until 9th block, for different localization strategies and neighborhood sizes. Experiment 2 (Figure 5.9) and 6 (Figure 5.12), Experiment 7 (Figure 5.13) and 8 (Figure 5.14) are comparable to each other when investigating the localization option. Experiment 6 (Figure 5.12), 8 (Figure 5.14) and 9 are comparable to each other when investigating the neighborhood size.

Figure 5.16 compares all of the experiments performed in this section by plotting MSE values of each. Higher MSE values are observed when localization strategies are applied and the neighborhood size is defined as 225,225,3 m. The MSE values become lower when the neighborhood size is increased and localization option is not used. This is expected because the neighborhood size was initially defined as 450,450,6 m based on the variogram, so performing the experiments with 225,225,3 m sized neighborhood was not enough to cover the seam continuity. Minor changes are observed between the MSE values of the 450,450,6 m neighborhood sized experiment and the 900,900,6 m sized experiment due to a lack of spatial correlation between the attributes.

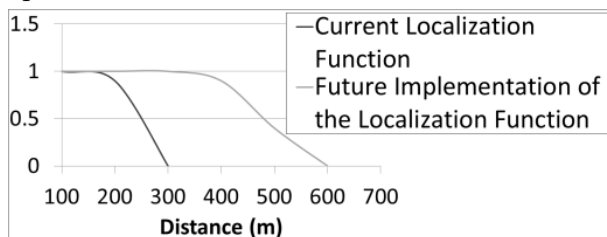


Figure 5.20: Localization function illustrations

The reason that applying the localization strategies did not provide any improvement in our case is due to the definition of the localization function.

Figure 5.20 illustrates the currently used function. Since the production block size is varying for each block, sometimes the plateau phase of the used function

cannot cover a full block which is in the neighborhood. This creates un-updated values in a block and consequently the updating process of the entire block fails. For this reason, better results are obtained while the localization strategies were not in use. Future study may improve this drawback by developing the localization function in a way that it can define the block boundaries and acts according to those distances.

Experiment 10 uses the localization option with the following dimensions: 450,450,6 m in X,Y,Z directions. The used neighborhood size was 900,900,6 m. As mentioned before, the initial intention was to use a localization size half the size of the neighborhood size. Yet, since the depth of a production block is 6 m, limiting the localization by 3 m decreased the expected improvements. By running the same experiment, only changing the Z localization size parameter from 6 m to 3 m, the same results as found in Experiment 6 (Figure 5.12) are obtained. This can be observed in Figure 5.16, by comparing the related MSE values.

5.3.4.2.3. Sensor Precision

Figure 5.17 to Figure 5.19 present the final results of the updating process from the 1st block until 9th block, for different relative sensor errors. For all the experiments performed in this section, the average prediction quality gets better in the sense that they become closer to the KOLA measurement values.

When the relative sensor error gets higher, the posterior variance appears to increase significantly. This is mainly because the KOLA measurement values are almost out of the range of the prior model (Figure 5.8) and the variance of the prior model significantly underestimates the KOLA measurement values. By integrating the KOLA measurements which have lower precision (applied relative error varies between 4% to 40% ash), the algorithm opens up the option to decide whether the KOLA data can be right or the prior model. Subsequently, this inflates the posterior uncertainty.

5.4. CONCLUSIONS

This chapter illustrated significant improvements in predictions, leading to a potential increase of coal recovery and process efficiency by controlling the decisions continuously in a mining operation. The results from the full scale application validated the applicability of the method in a continuous mine environment and presented significant prediction improvements in the resource model.

Some limitations might be influencing the results. A first potential limitation could be the quality of the provided data from RWE. For example, the accuracy and the representativeness of the received measurement data can highly effect the improvement of the results.

In Section 5.4, the performance of the resource model updating framework was analyzed by performing sensitivity analysis on main parameters, including the ensemble size, the neighborhood size, localization strategies and the sensor precision. The results should assist in future applications by determining the impact of the different parameters.

The findings of ensemble size sensitivity analysis supported the results from existing literature [6, 71]: more accurate updates are achievable by using a bigger ensemble size. Although 24 ensemble members provided the best results in terms of MSE, they are not chosen as the optimum ensemble size since they were not representative enough of the lignite seam. Instead of an ensemble of 48 members was chosen because it was second best and was more representative of the lignite seam.

The sensitivity analysis of the localization and neighborhood strategies concluded that the applied localization strategies need to be improved and the neighborhood size needs to remain as 450,450,6 m in X,Y,Z directions, as previously defined in the variogram modelling.

Sensitivity analysis for different sensor precision showed that a lower sensor precision increases the uncertainty of the posterior model, due to a significant difference between prior model and the actual sensor data.

In general, the KOLA data is well covered by the range of uncertainty in the updated neighborhood. It is observed that the uncertainty in the near neighborhood gets slightly smaller and more of the actual KOLA measurements are captured by this uncertainty range.

The research presented in this chapter was limited to a case where only one excavator is operating. Next chapter applies a case study where two or three excavator are operating. This will require updating the coal quality parameters in different production benches based on one combined material measurement.

6. DEMONSTRATION AND PROOF OF CONCEPT IN AN INDUSTRIAL ENVIRONMENT - CASE 2

This chapter demonstrates an industrial application of the developed framework in the Profen mine, Germany and discusses two different aspects. First, it tests the performance of the resource model updating framework while the sensor is observing a blend of coal resulting from multiple excavators. Second, it simplifies and semi-automates the framework for easier application in a real mining environment.

The contents of this chapter have been adapted from:

Yüksel, C., Benndorf, J., Lindig, M., & Lohsträter, O. (2017) Updating The Coal Quality Parameters in Multiple Production Benches Based on Combined Material Measurement: A Full Case Study. *International Journal of Coal Science & Technology*, 2017:p. 1-13.

6.1. DATA PREPARATION

To apply the resource model updating framework, preparation of input data is required (Figure 3.5). The first data set is the prior model, which contains a collection of the resource model realizations. For the case study, two different prior models are prepared based on different approaches.

6.1.1. Prior Model: Based on Drill Hole Data

A prior model based on drill hole data refers to generation of prior realizations by conditional simulation based on the given drill hole data. First, the geological model of the defined coal seam is created on a 25x25x1m dimensioned block model based on the roof and floor information of the lignite seam. Second, a 25x25x1m dimensioned quality model capturing the wet ash content in percentages is generated by 25 simulations based on the provided drill hole data. The simulated ash values are then merged with the previously defined coal seam. After this, the block model realizations are ready to be imported into the algorithm as the first input.

6.1.2. Prior Model: Based on Short-Term Model

A prior model based on the short-term model refers to generation of prior realizations by adding fluctuations on a short-term mining model of the company. A detailed explanation of this application was given in Chapter 3.

The updating experiments are performed both for drill hole based prior model realizations and short-term model based prior model realizations. This is done in order to compare the performance of the updating framework while updating differently generated prior models. The aim of this performance comparison is to investigate the question: "If the updating framework uses a non-geostatistical set of simulations as a prior model, would the updated models still be improved?"

The second data set consists of the production data and their related actual sensor measurements. The material travelling time from each production location (excavator & bench location) to the RGI location is calculated. In order to determine the location of the received RGI measurement data, in other words: "to track back where the measured material comes from", the production data is linked with the RGI data based on given timecodes (material travel delays are taken into account). The second input file for the algorithm is written to a file containing the following information: timecode, actual sensor measurement (RGI data), excavated block₁ id, excavated block₁ mass, excavated block₂ id, excavated block₂ mass, ..., excavated block_n id, the excavated_n block mass; where $b = 1, \dots, n$ is the excavated block number in the given time span.

The third data set consists of a collection of actual and predicted sensor measurements. An ensemble of predicted values is obtained by the forward simulator applying the digging location and the material transport model to each realization. The third input file for the algorithm is written to a file containing the

following information: the block ID, central block location (X, Y, Z coordinates), a series of real measurements and predicted measurements.

6.2. EXPERIMENTAL SET-UP

The experiments that are performed both with drill hole based and short term plan based prior model realizations, fall into two different categories. The first category involves different time span based experiments, where updating of the prior model is performed every 2 hours, 1 hour, 30 minutes, 15 minutes and 10 minutes. Thus, this category includes either one, two or three excavators producing at the same time, depending on the actual production scheme. For these experiments, the related RGI and production data are linked to each other (for every minute) and averaged for each indicated time span.

The second category involves experiments that are based on the number of excavators producing coal at a given time period. It investigates the capability of the updating framework when updating multiple benches based on a blend of material measurements. For these experiments, the data set that is prepared for every two hours of updating is taken as the base data and divided into three different data sets. This division is done based on the number of excavators that are producing coal at a given time span such as; 1 excavator, 2 excavators and 3 excavators.

For each criterion introduced above, an experiment is performed. Each experiment initially updated the prior model for a four day time period. Based on this resulting posterior model, forward simulator is used to generate predicted posterior model values for the future mining operations (for the next two days). These predictions are then compared with the related RGI data. Chosen time spans are representative for any time span that might be chosen in the future.

The updating neighborhood size is chosen as 900m x 900m x 10m in X,Y,Z directions based on the variogram model range, which was calculated during geological modelling. A 225,225,5m sized localization is applied for each experiment to prevent long range spurious correlations.

6.3. RESULTS AND DISCUSSION

6.3.1. Results

This section presents representative results of the previously defined experiments. The following graphs provide representative information where the X-axis refers to the mentioned time spans, $i = 0, 1, 2, \dots, n$. Instead of writing the full date and time information, it is decided to use time span codes for simplicity. For example for the case where the updating is every 2 hours; if $i=0$ refers to 01.01.2014 at 00:00, $i=10$ refers to 20 hours later, which is 01.01.2014 at 20:00. Y-axis refers to the ash%. The presented graphs consist of the following information:

1. Posterior Model Box Plots: Box plot representation of posterior model simulations which are updated based on a given criterion (e.g. updating every 2 hours, 1 hour, 30 minutes, 15 minutes or 10 minutes; or updating while 1 excavator, 2 excavators or 3 excavators are producing).
2. Posterior Mean: Represents the mean of the updated models in the learning period. Essentially, it is the mean of the posterior model that is updated based on a given criterion.
3. Predicted Mean: Represents the mean of the predictions in the prediction period. Basically, it is the prediction of future mining blocks, based on the four-day-long-updated model.
4. Prior Mean: Mean of the prior model that is created based on either the drill hole data or short-term model. The prior model is "mined" according to different operation files based on a given criterion (e.g. updating every 2 hours, 1 hour, 30 minutes, 15 minutes or 10 minutes; or updating while 1 excavator, 2 excavators or 3 excavators are producing).
5. RGI: The averaged RGI data for a given time span.
6. White area: Represents the learning period, where posterior models are produced as a result of updating the prior model, by using the RGI data.
7. Green area: Represents the prediction period, where the mining operations are executed on the four-day-long-updated model.

In these graphs the prior model is updated for four days. Based on this updated prior model, the posterior model, further mining operations are performed for the next two days. The operation file "mines" through the posterior model and highlights the area as green.

6.3.1.1. Results: Using a Prior Model that is Based on Conditional Simulation

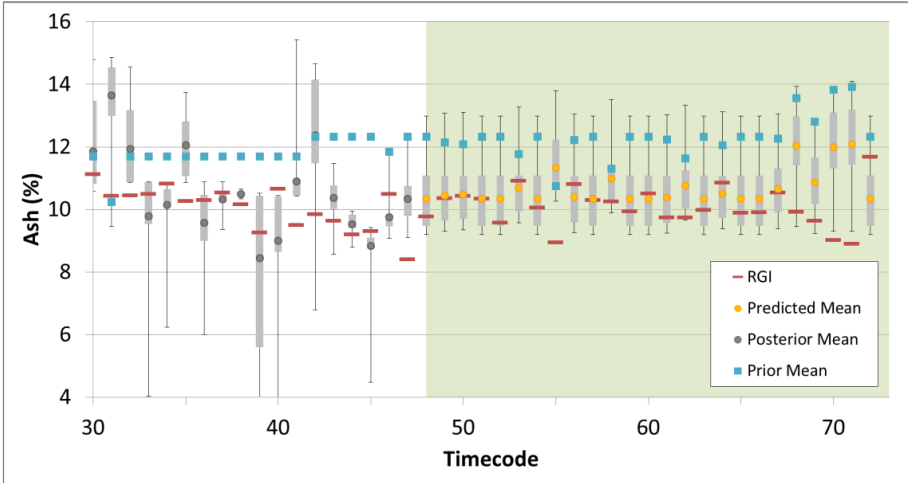


Figure 6.1: Results based on conditional simulation: Updating every 2 hours for 4 days. The green area represents the prediction period. The white area represents the learning period.

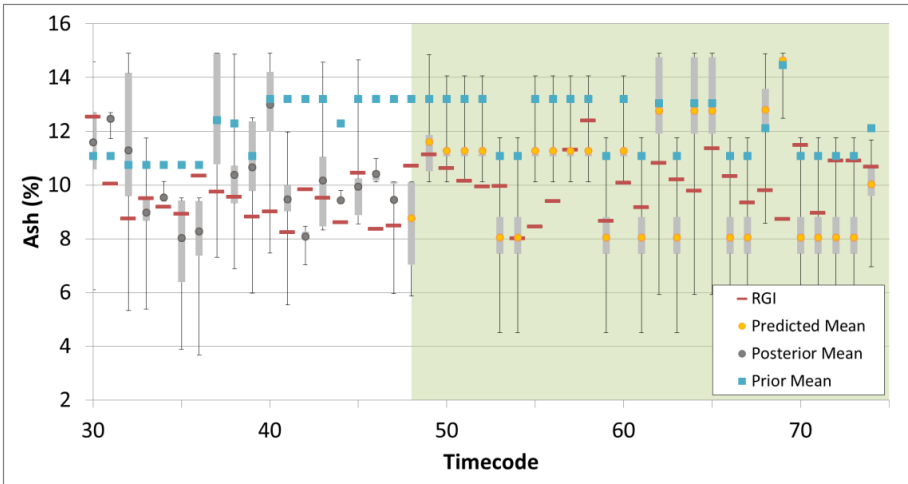


Figure 6.2: Results based on conditional simulation: Updating every 2 hours for 4 days, 1 excavator producing. The green area represents the prediction period. The white area represents the learning period.

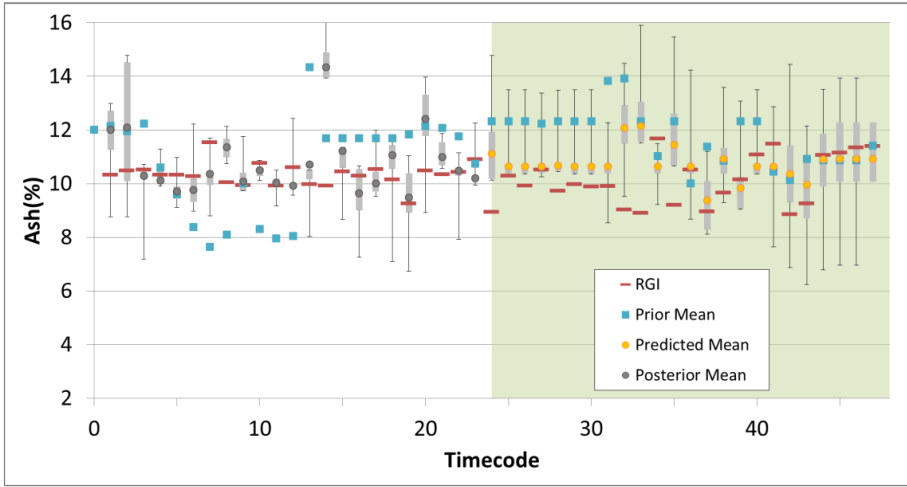


Figure 6.3: Results based on conditional simulation: Updating every 2 hours for 4 days, 2 excavators producing. The green area represents the prediction period. The white area represents the learning period.

In this case study, the achieved improvements are numerically evaluated using an absolute error measure for an easier interpretation. The absolute error measure is used due to the relatively bigger scale of the experiments compared to the case studies in the previous chapters. Moreover, the results obtained from the previous chapters were directly measuring the MSE of a block, whereas in this case study, due to the blended material flow, the absolute error is measured per each iteration (timecodes). The absolute error is defined as the absolute difference between the measured value of a quantity and its actual value. In our case, absolute error refers to the absolute difference between the measured RGI value l of produced coal at a given time span and its prior $\mathbf{Z}_0(\mathbf{x})$ (or posterior $\mathbf{Z}^*(\mathbf{x})$) value, calculated by the following equation:

$$AE = \frac{1}{n} \sum_{i=0}^n |l_i - \mathbf{Z}^*(\mathbf{x})_i| \quad (6.1)$$

The absolute error values are calculated for each experiment iteration at a given time span $i = 0, \dots, n$ and eventually averaged when the update of the block model is completed for the defined study case.

Table 6.1 provides the calculated absolute errors for prior models and predictions that are illustrated in the green area of the graphs. In addition to that, it indicates the improvement (IMPROV) in percentages when comparing prior's and predictions' absolute errors. Improvements indicate the decrease of the absolute errors and it can be calculated as;

$$\text{IMPROV}(\%) = \frac{\text{Prior Model}_{\text{Absolute Error}} - \text{Predicted Model}_{\text{Absolute Error}}}{\text{Prior Model}_{\text{Absolute Error}}} \quad (6.2)$$

Table 6.1: Calculated absolute errors for predictions- Prior model is based on drill hole data

	Prior Model	Predictions originated from Posterior Model	
	Absolute Error	Absolute Error	IMPROV %
2 hr	2.25	0.82	64%
1 hr	2.82	1.03	43%
30 mins	1.20	1.14	5%
15 mins	2.59	2.08	20%
10 mins	2.57	2.39	7%
1 Exc	2.22	1.87	16%
2 Exc	1.72	0.96	44%
3 Exc	1.12	0.92	18%

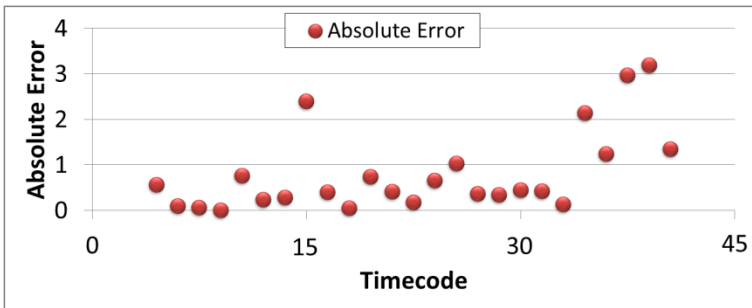


Figure 6.4: Absolute error predictions (for the next 2 days) of after updating every 2 hours for 4 days

Moreover, Figure 6.4 presents the calculated absolute error for the following two days after updating the prior model every two hours for four days. Red dots illustrate the calculated absolute errors for each time span.

6.3.1.2. Results: Using a Prior Model that is Based on Short-Term Model

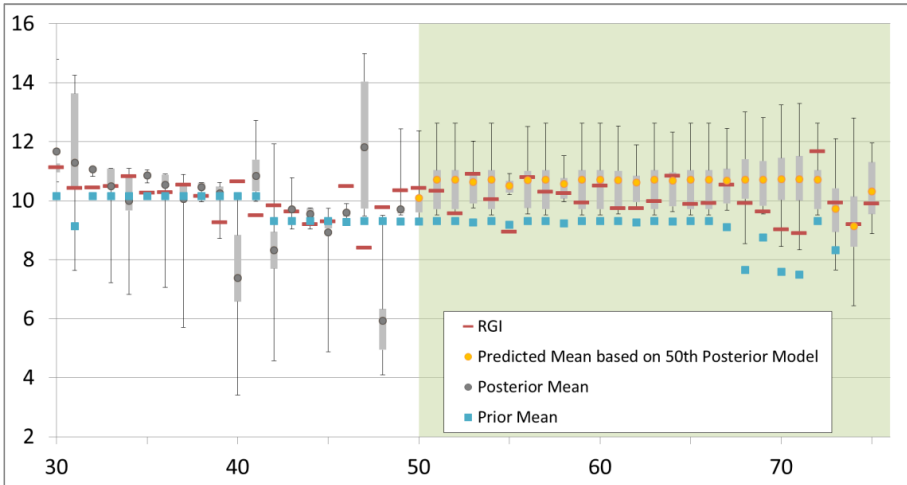


Figure 6.5: Results based on short-term model: Updating every 2 hours for 4 days. The green area represents the prediction period. The white area represents the learning period.

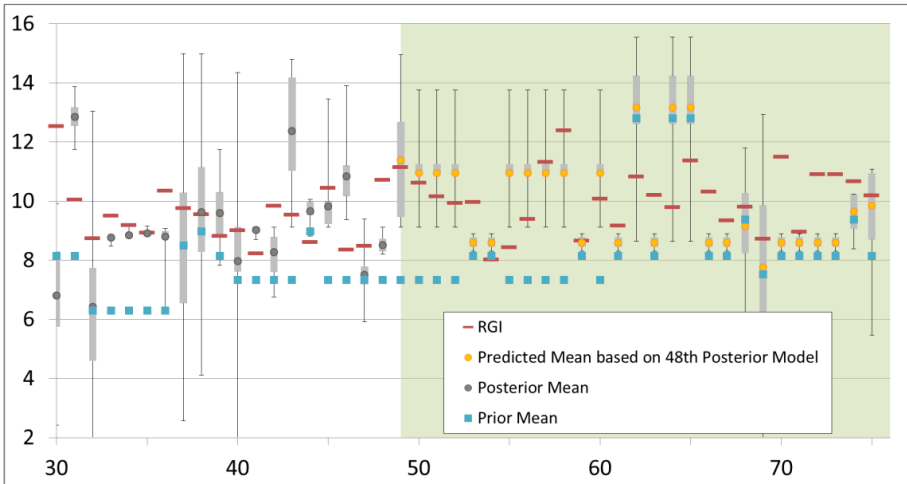


Figure 6.6: Results based on short-term model: Updating every 2 hours for 4 days, 1 excavator producing. The green area represents the prediction period. The white area represents the learning period.

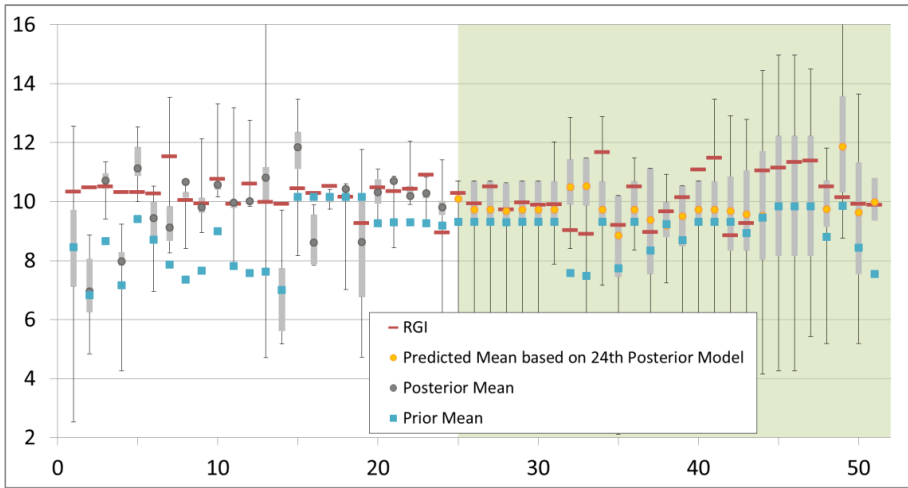


Figure 6.7: Results based on short-term model: Updating every 2 hours for 4 days, 2 excavators producing. The green area represents the prediction period. The white area represents the learning period.

The achieved improvements are presented using “absolute error” as previously introduced. Table 6.2 provides the calculated absolute errors for prior models and predictions. The improvement percentages (IMPROV) are calculated by comparing the absolute errors of prior and prediction models.

Table 6.2: Calculated absolute errors for predictions - Prior model is based on short-term model

	Prior Model	Predictions originated from Posterior Model	
	Absolute Error	Absolute Error	IMPROV %
2 hr	1.09	0.70	36%
1 hr	0.99	0.84	14%
30 mins	1.49	1.27	15%
15 mins	4.37	1.17	73%
10 mins	4.24	1.59	63%
1 Exc	2.10	1.36	35%
2 Exc	1.13	0.91	19%
3 Exc	1.18	0.89	25%

Moreover, Figure 6.8 presents the calculated absolute error for the following two days after updating the prior model every two hours for four days. Red dots illustrate the calculated absolute errors for each time span.

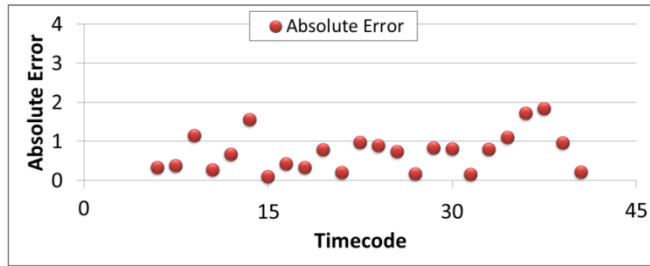


Figure 6.8: Absolute error predictions (for the next 2 days) after updating every 2 hours for 4 days

6.3.2. Discussion

6.3.2.1. Improvements of Predictions

Figure 6.1, Figure 6.2 and Figure 6.3 illustrate the improvement of the ash% predictions in the posterior model, where updating of the prior model (developed from drill hole data) is applied based on RGI data for four days. The ensuing posterior model is “mined” according to production data. The predictions of the posterior model while mining the neighborhood blocks are then compared with the actual ash% (in this case RGI measurements are assumed as reality) and prior model. Representative graphs are provided.

Figure 6.1 presents the case where the prior model (based on drill hole data) is being updated for every two hours for four days. The following green area represents a period of two days, where orange points represent the averaged prediction behavior of the posterior model which is updated for four days. In this time period, it can be observed that posterior model predictions are mostly following the trend of the RGI data (red lines). Moreover, when comparing the posterior model predictions with the prior model (blue square points), significant improvements are observed in the posterior predictions. Based on Table 1, the averaged absolute error for those predictions is 0.82, while it is 2.25 for prior model. This indicates a 64% improvement.

Figure 6.2 presents the case where the prior model (based on drill hole data) is being updated every two hours when only 1 excavator is operating for four days. Similarly, in the green area, orange points represent the averaged prediction behavior. Between the 50th-52nd and the 55th-58th timecodes, posterior model predictions are remaining stable due to production of the same mining block at each time. This stable prediction averages around the reality (RGI data). Moreover, the uncertainty of predictions (box plot whiskers) covers the reality (RGI data) better than the prior model. After the 63rd timecode, posterior model predictions follow a similar trend as the prior model due to spatial variability of the lignite seam. Furthermore, since this experiment focused on a case with only one excavator producing, the application was not limited to only one bench. As a result, after updating four days in three benches, using only the times where one

excavator is working, could only improve the future predictions for a limited time. The authors believe that for this case, the quality and the lifetime of the predictions can be improved by extending the learning phase (more than four days).

Figure 6.3 presents the case where the prior model (based on drill hole data) is being updated every two hours when 2 excavators are operating for four days. By using 2 excavators at the same time, already more information becomes available about the lignite seams that are being worked on and this leads to a longer time of good quality improvements. This can be seen by comparing Figure 6.2 and Figure 6.3.

Figure 6.5, Figure 6.6 and Figure 6.7 apply the same experiments as above, however in these figures the prior model is based on the short-term model. With these experiments similar results as before were achieved. In Figure 6.5, where the updating of the prior model is every 2 hours, predicted ash% values are almost always aligned with the reality (RGI data). Figure 6.6 presents a case with 1 excavator and Figure 6.7 presents a case with 2 excavators. As above, when looking to those two graphs, better predictions are observed when using 2 excavators.

For both cases, Figure 6.4 and Figure 6.8 are provided in order to investigate the behavior of the absolute error values obtained from predictions. The absolute error values are initially very low (between 0 and 12th timecode), but after approximately one day period (12th timecode) they indicate an increase over time. When the distance between the mined block and the neighborhood blocks increases, it is expected to see less improvement for the neighborhood blocks. This occurs due to the lower spatial correlation. Moreover, when predicting the neighborhood blocks there might be some blocks that are not updated in the learning period. This causes not only an increase in the absolute error over the time, but also outliers in the early phases of the prediction period. For example, see timecode 55 in Figure 10 or see timecode 51 and 54 in Figure 6.8. These outliers can be observed and the reason that they occur can be explained as follows: at each individual timestamp there are different blocks being mined from different benches. If a block gets mined in the prediction period and it has not been mined in the learning period or if it has not been in the neighborhood of any other mined blocks, it has never been updated. Thus, it still has the prior model's value assigned to it. This results in a prior biased prediction and an increase of the absolute error.

6.3.2.2. Time Based Experiments

Different time span based experiments are performed (every 2 hour, 1 hour, 30 minutes, 15 minutes and 10 minutes) for updating the prior model based on drill hole data. In overall, significant improvements (up to 64%) are obtained while updating the prior model with measured RGI values and predicting neighborhood blocks' qualities (Table 6.1). A comparison among the performed experiments

between the most frequent update (every 10 minutes) and the least frequent update (every 2 hours), shows that highest improvements are achieved by the least frequent updates of this case (every 1 hour and 2 hours updating cases).

Similar to the above experiments, different time span based experiments are also performed for updating the prior model based on the short-term model. All the experiments show satisfactory improvements (up to 73%) (Table 6.2). In this case, the highest improvements are achieved by the most frequent updates (every 15 minutes and 30 minutes).

However, calculating these absolute errors does not necessarily indicate the best parameters to use. It only validates the applicability of the method for the given parameters. It should not be forgotten that the calculated absolute errors for predictions can vary depending on the quality of the posterior model that is chosen as the base of the predictions. For each case this chapter has chosen the posterior models that are obtained after four days of updating the prior model. Other experiments are also applied to test this issue and they all recorded significant but varying amounts of improvements.

6.3.2.3. Excavator Number Based Experiments

Experiments based on a different number of working excavators are performed in order to investigate the capability of the updating framework. The previous case study presented in Chapter 5, in which the study area was limited to one bench and one producing excavator, produced successful results. The RGI online-sensor was positioned on the producing excavator, so that the measured material was the produced material from that excavator. However, in this case study, there are three different benches and three different producing excavators (one excavator for each bench). The online RGI sensor is positioned on one of the conveyor belts just before the stock yard. Therefore, the RGI sensor measures blended material produced from different benches. The aim of performing the mentioned experiments in this section is to test the performance of the updating algorithm in when the observations are measured from a blended flow.

By looking at Table 6.1, a range of 16-44% improvement is observed when using a varying amount of excavators in the updating experiments with a drill hole based prior model. This shows that the algorithm can handle a situation where the blended measurement data is fed into different benches where the material is originally produced.

By looking at Table 6.2, a range of 19-35% improvement is observed when using a varying amount of excavators in the updating experiments with a short-term model based prior model. The obtained improvements are significant considering the benefits of automation while using a short-term model based prior model. Once again, the results indicate that the algorithm can handle a situation where the blended measurement data is fed into different benches where the material is originally produced.

6.4. HYPOTHESIS TESTING

The previous experiments in Chapter 6 tested the performance of the resource model updating framework while the sensor is observing a blend of coal originating from multiple excavators and concluded that the updating framework improves the resource model with the given conditions. These experiments are performed for a time period of 15 days. Within these 15 days, the experiments focused on periods of 4 days close investigation. However, it is decided that any conclusions derived from the 15 days of data might not be sufficient to prove the performance of the updating framework. To achieve more definitive results, this section applied a hypothesis testing approach.

A hypothesis test is a statistical test that is used to determine whether there is enough evidence in a data sample to infer that a certain condition is true for the entire population. Further information on hypothesis testing can be found in [75].

When applying hypothesis testing for the presented case study in this chapter, the null hypothesis (H_0) states that the average improvement in the future predictions is equal to zero. This means that the real-time resource model updating framework is not working as it is supposed to, which would mean that there is no improvement recorded in the predictions of the future. On the contrary, the alternative hypothesis (H_A) states that the average improvement in the predictions is greater than zero. This means that the real-time resource model updating framework improves the predictions so that the average improvement percentages are greater than zero. Thus, the parameter μ_{IMPROV} represents the average number of the prediction improvements calculated after updating the prior model by using resource model updating. The two hypotheses in question are as follows:

$$H_0 : \mu_{IMPROV} = 0$$

$$H_A : \mu_{IMPROV} > 0 \text{ (an upper-tailed test).}$$

A test statistic is a test where the standardized value, which is calculated from sample data during a hypothesis test, is used for determining whether or not to reject the null hypothesis. The null hypothesis will state that the expected value μ has a particular numerical value, the null value, which we will denote by μ_{IMPROV} . Let x_1, x_2, \dots, x_n represent the predicted improvements of the resource model with size n . Then the sample mean \bar{x} has an expected value $\mu_{\bar{x}} = \mu$ and standard deviation $\sigma_{\bar{x}} = \sigma/\sqrt{n}$. When H_0 is true, $\mu_{\bar{x}} = \mu_{IMPROV}$. The statistical test, known as the t-test, can be calculated as:

$$T = \frac{\bar{x} - \mu_{IMPROV}}{\frac{\sigma}{\sqrt{n}}} \quad (6.3)$$

When the data shows strong evidence against the assumptions in the null hypothesis, the magnitude of the test statistic becomes large and the test value can become small enough to reject the null hypothesis.

After calculating the T-value, the T-value can be converted to a P-value by simply using the table of T, which can be found in any statistics book. The P-value is the probability, which calculated with the assumption that the null hypothesis is true, of obtaining a value of the test statistic at least as contradictory to H_0 as the value calculated from the available sample [75]. More generally, the smaller the P-value, the more evidence there is in the sample data against the null hypothesis and for the alternative hypothesis.

To define if the P-value is sufficiently small or not, a significance level is selected. The significance level is the largest acceptable probability of committing a false rejection of H_0 and is denoted by α , where $0 < \alpha < 1$ [76]. The case study presented in this section is performed at level 0.05 and this refers to a 95% confidence interval. If the P-value is less than or equal to the α , H_0 is rejected and the claim of H_A is supported; if it is greater than the α , this means there is not enough support to claim that H_A is correct so we keep H_0 .

The following results in Section 6.5.1. are obtained while updating the prior model until the day that is indicated in the first column of the results tables (Table 6.3 and Table 6.4). Then, based on this most recent updated model (posterior model), the next one, two or three days are predicted. The achieved improvements are then presented using "absolute error" as previously introduced in Section 6.4.1. Table 6.3 and Table 6.4 provide the calculated absolute errors for prior models and predictions. The improvement percentages (IMPROV) are calculated by comparing the absolute errors of the prior models and prediction models. Moreover, Table 6.5 and Table 6.6 present the calculation of the test statistics. These results will be evaluated in Section 6.5.2.

6.4.1. Results

Table 6.3: Calculated absolute errors for predictions (for 23 days) - Prior model is based on drill hole data

Day #	Mining for next 1 day			Mining for next 2 days			Mining for next 3 days		
	Prior Model	Predictions originated from Posterior Model		Prior Model	Predictions originated from Posterior Model		Prior Model	Predictions originated from Posterior Model	
	Abs Error	Abs. Error	IMPROV %	Abs. Error	Abs. Error	IMPROV %	Abs. Error	Abs. Error	IMPROV %
Day 1	2.30	1.33	42%	1.51	1.17	22%	1.30	1.08	16%
Day 2	0.72	0.47	35%	0.77	0.63	18%	0.86	0.83	4%
Day 3	0.78	0.69	11%	0.91	0.80	12%	0.84	0.77	9%
Day 4	0.95	0.78	18%	0.87	0.78	10%	1.04	0.98	6%
Day 5	0.70	0.50	28%	1.15	1.06	8%	1.84	1.62	12%
Day 6	1.79	1.35	25%	2.46	2.45	1%	2.42	2.36	2%
Day 7	3.08	2.34	24%	2.67	2.39	11%	2.31	2.24	3%
Day 8	2.34	1.52	35%	1.95	1.7	15%	1.97	1.95	1%
Day 9	1.55	0.84	46%	1.72	1.30	25%	1.72	1.35	22%
Day 10	1.89	1.66	12%	1.82	1.62	11%	1.99	1.37	31%
Day 11	1.58	1.30	18%	1.98	0.92	54%	1.81	1.30	28%
Day 12	2.38	0.77	67%	1.92	1.36	29%	1.55	1.48	4%
Day 13	1.54	0.81	47%	1.17	0.93	20%	1.03	0.96	6%
Day 14	0.71	0.56	22%	0.70	0.56	20%	0.86	0.72	17%
Day 15	0.76	0.48	38%	1.00	0.88	12%	1.20	0.96	20%
Day 16	1.21	0.92	24%	1.40	1.06	24%	1.72	1.16	33%
Day 17	1.59	0.53	66%	2.03	0.94	54%	1.70	0.78	54%
Day 18	2.70	0.73	73%	1.77	0.83	53%	1.73	0.97	44%
Day 19	1.16	0.55	52%	1.42	0.70	51%	1.50	1.08	28%
Day 20	1.69	0.64	62%	1.68	1.04	38%	1.78	1.06	41%
Day 21	1.67	0.65	61%	1.77	1.04	41%	N/A	N/A	N/A
Day 22	1.97	1.13	42%	N/A	N/A	N/A	N/A	N/A	N/A
Day 23	1.77	0.38	78%	N/A	N/A	N/A	N/A	N/A	N/A

Table 6.4: Calculated absolute errors for predictions (for 23 days) - Prior model is based on short-term model

	Mining for next 1 day			Mining for next 2 days			Mining for next 3 days		
	Prior Model	Predictions originated from Posterior Model		Prior Model	Predictions originated from Posterior Model		Prior Model	Predictions originated from Posterior Model	
Day #	Abs. Error	Abs. Error	IMPROV %	Abs. Error	Abs. Error	IMPROV %	Abs. Error	Abs. Error	IMPROV %
Day 1	1.47	1.42	3%	1.30	1.27	2%	1.44	1.32	8%
Day 2	1.13	0.75	34%	1.42	0.97	32%	1.34	1.32	1%
Day 3	1.65	0.74	55%	1.41	0.89	37%	1.29	0.88	32%
Day 4	1.25	1.15	8%	1.18	1.05	11%	1.39	1.33	4%
Day 5	0.97	0.87	10%	1.50	0.91	39%	1.41	0.88	38%
Day 6	1.73	0.21	88%	1.65	0.74	55%	1.54	0.97	37%
Day 7	1.14	1.02	11%	1.22	1.09	10%	1.33	1.28	4%
Day 8	1.37	1.22	11%	1.42	1.4	2%	1.55	1.53	1%
Day 9	1.47	1.07	27%	1.59	1.49	6%	1.50	1.50	0%
Day 10	1.78	1.24	30%	1.52	1.49	2%	1.62	1.61	1%
Day 11	1.11	0.98	12%	1.49	1.21	19%	1.29	1.01	22%
Day 12	1.87	1.48	21%	1.37	1.00	27%	1.50	1.18	22%
Day 13	0.97	0.81	16%	1.34	0.93	30%	1.64	0.96	41%
Day 14	1.79	0.50	72%	1.92	0.50	74%	2.19	0.58	74%
Day 15	2.18	1.23	44%	2.50	1.29	49%	2.37	2.10	12%
Day 16	2.80	2.19	22%	2.46	2.44	1%	2.44	2.24	8%
Day 17	2.11	0.85	60%	2.23	1.19	46%	2.24	1.58	29%
Day 18	2.40	0.73	69%	2.32	0.49	79%	2.34	0.73	69%
Day 19	2.27	0.50	78%	2.31	1.09	53%	2.00	1.42	29%
Day 20	2.36	0.87	63%	1.86	1.43	23%	2.08	1.87	10%
Day 21	1.26	1.12	11%	1.80	1.61	11%	N/A	N/A	N/A
Day 22	2.53	1.89	25%	N/A	N/A	N/A	N/A	N/A	N/A
Day 23	2.59	0.62	76%	N/A	N/A	N/A	N/A	N/A	N/A

Table 6.5: Test statistics calculation - Prior model is based on drill hole data

	Mining for next 1 day	Mining for next 2 days	Mining for next 3 days
\bar{x}_{IMPROV}	40.3%	25.1%	19.1%
σ	0.20	0.17	0.16
N	23	21	20
T-value	9.5	6.87	5.47
P-value	1.48E-09	3.35E-07	0.00
α	0.05	0.05	0.05
Decision	P-value < α : H _A is proven	P-value < α : H _A is proven	P-value < α : H _A is proven

Table 6.6: Test statistics calculation - Prior model is based on short-term model

	Mining for next 1 day	Mining for next 2 days	Mining for next 3 days
\bar{x}_{IMPROV}	36.8%	28.9%	22.1%
σ	0.27	0.24	0.22
N	23	21	20
T-value	6.5	5.59	4.55
P-value	7.67E-07	6.45E-06	0.00
α	0.05	0.05	0.05
Decision	P-value < α : H _A is proven	P-value < α : H _A is proven	P-value < α : H _A is proven

6.4.2. Discussion

Table 6.3 and Table 6.4 provide the calculated absolute errors for the prior models and the predictions based on these model, during a updating period of 23 days, for both of the cases where the prior model is based on drill hole data and the short-term model, respectively. To give an example, in Table 6.3, after continuously updating the prior model during the first day, a posterior model is obtained by the end of the "Day 1". Based on this resulting posterior model, a forward simulator is used to generate predicted posterior model values for the future mining operations (for the next one, two or three days). After this, the absolute errors (Equation (5.1)) are calculated both for the prior and the mentioned posterior model. Later, the improvement percentages (IMPROV) (Equation (6.1)) are calculated by comparing the absolute errors of the prior and prediction models. Since the absolute error of the prior model was 2.30 and the absolute error of the posterior model became 1.29 after updating for an entire day, a 44% improvement in the predictions can be calculated from this comparison. A similar process is applied for each experiment. For example, while updating the prior model for 20 days, the resulting posterior model indicated a 50% improvement for the next day's predictions. This improvement percentage decreased while moving to the predictions of the second and third day (35% and 14% respectively).

In Table 6.5 and Table 6.6 the test statistics for both of the mentioned cases are calculated. The calculated parameters are given and in the last row the decision making process is illustrated.

In the case where the prior model is based on drill hole data (Table 6.5), the alternative hypothesis is accepted for the predictions of the next three days. This means that the real-time resource model updating framework increased the average accuracy of the resource model for the mining of the next three days with 95% confidence. As expected, in general, a decreasing trend is observed among the results when moving from the first mining day to third mining day.

Similarly, in the case where the prior model is based on the short-term model (Table 6.6), the alternative hypothesis is accepted for the predictions of the next three days. The fact that we can use a the short-term model based prior model provides a major operational benefit and allows for increasing the production efficiency during mining operations.

In both Table 6.5 and Table 6.6, it is possible to observe that the average improvement percentages are decreasing when moving away from the updated area while mining. As discussed in previous chapters this can be expected. Moreover, similar results are obtained in similar experiments of which the results are presented in Section 6.4.1.

Overall, for both of the cases where a prediction is made for the next three mining days after updating for various time spans, the hypothesis that has been tested is accepted with 95% confidence. This indicates more accurate predictions of a resource model for the following mining days.

6.5. CONCLUSIONS

This chapter provided a full-scale case study into the application of an Ensemble Kalman based resource model updating framework, with the aim of simplifying the application process.

To offer an easy application of the updating framework in a real mining environment, a simplified application method is created. This simplified application method involves creating the prior realizations based on the company's short-term model. Improvement percentages, on average, were not significantly different when the case study results are compared with the results obtained from a case study where the prior realizations are generated with geostatistical simulations. This paper validates that the automation of the developed framework during real applications can be done based on a short-term model without any additional process being required in order to prepare the prior model.

Moreover, significant improvements are observed while using blended material measurement data in order to update different production locations in different benches. This provides great flexibility for future applications.

Furthermore, the hypothesis testing performed in this case study (which has a duration of almost a month) has once again shown that the real-time resource model updating framework significantly improves the future predictions. The obtained results from the case , where the prior model is based on drill hole data, are slightly better than the case where the prior model is based on the short-term plan. However, both of the cases behaved similarly and showed an average improvement of about 29%. This is valuable for highlighting the practicality of the framework. However, in the future, depending on the application location and the accuracy of the measurement data used, this might change. Nevertheless, in both cases, significant improvement are observed.

The next chapter will focus on the value of introducing additional information in the short-term model during the production phase.

7. VALUE OF INFORMATION

In this chapter, the added value of the real-time resource model updating concept is evaluated by using a value of information (VOI) analysis. The expected economical and environmental benefits of additional information (due to the integration of the online-sensor measurements into the resource model) are compared to a case where there is no additional information integrated into the process.

The contents of this chapter have been adapted from:

Yüksel, C., Minnecker, C., Shishvan, M.S., Benndorf, J., & Buxton, M. (2017). Value of Information Introduced by a Resource Model Updating Framework. *Mathematical Geosciences*. (submitted)

7.1. INTRODUCTION

The previous chapters provided a validation and a demonstration of the real-time updating framework in full scale lignite production. The previous chapters presented the improvements in predictions achieved by applying the updating framework. However, so far, none of those studies investigated whether the improvements in predictions truly have economical and environmental effects. This chapter indicates the economical and environmental impacts determined by application of the resource model updating framework.

One of the most well-known tools for assessing the value of additional information added into the system is the Value of Information (VOI) [77-79]. In the last decades, VOI gained high popularity in many different fields. A few applications are documented in mining industry. Peck and Gray [80] make no explicit reference to VOI, yet they discuss the potential benefits to decision makers of gathering information in the mining industry. Barnes [81] applied VOI to incorporate a geostatistical estimation into mine planning. More recently, Phillips, Newman [82] provided a case study where a VOI decision framework was applied to provide guidance for mine managers regarding the purchase of ore grade scanners. Contrary to the mining industry, the VOI approach has found more applications in related fields, such as the oil and gas industry. Bratvold et al. [83] provided an extensive overview on oil and gas industry applications. Bhattacharja et al. [84] integrated the decision-analytic notion of VOI with spatial statistical models, similar to this paper's application work. Barros et al. [85] proposed a new methodology to perform a VOI analysis within a closed-loop reservoir management framework, which is similar to the resource model updating framework, except it is applied in reservoir engineering. Further applications in the oil and gas industry can be found in: [86], [87], [88], [89], [90] and [91].

The essence of the technique is to evaluate the benefits of collecting additional information before making a decision [83]. When using the resource model updating framework, this decision making process would be changing the short-term mining plan by using a mine optimizer. If the resource model always provides correct coal quality attributes it delivers Perfect Information, otherwise it is known as Imperfect Information. The latter is usually the case in geoscience applications, since the reality is unknown. The resource model updating framework aims to carry forward the current situation from Imperfect Information to an "Improved" Imperfect Information state, where the current situation lies somewhere between the Perfect Information and previous Imperfect Information (Figure 7.1). Every updating iteration brings the previous Imperfect Information closer to Perfect Information.

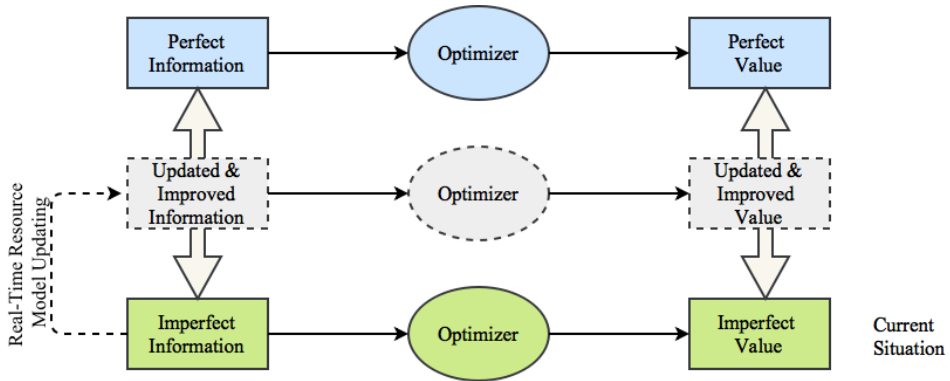


Figure 7.1: Aim of the resource model updating framework

The expected benefit of additional information (integration of the online-sensor measurement into the resource model) is compared to a case where there is no additional information integrated into the process. These benefits are evaluated in two main categories: economical and environmental. Economical aspects include the monetary values such as cost per shift. Environmental aspects focus on emissions of pollutants. Typical emissions in the coal industry are carbon dioxide (CO₂), sulphur dioxide (SO₂), nitric oxide (NO). This research focuses on CO₂.

This chapter addresses the following question, what is the value of integrating real-time production measurements into the resource model and executing an optimized mine plan, considering economical and environmental aspects?

7.2. ECONOMICAL AND ENVIRONMENTAL ASPECTS IN LIGNITE MINING

This section discusses the economical and environmental aspects in lignite mining and introduces the related Key Performance Indicators (KPIs) for the following sections.

Economical aspects in lignite mining mainly refer to monetary values. This dissertation focuses on the costs of deviating from the target quality (ash %) during production. Calculation of this KPI is given in the following: Let the costs of deviating from the target production quality when executing the mine plan on the prior model be C_{prior} (€), the costs of deviating from the target product quality per ton of coal is D_{prior} (€/ash% × t), the amount of the deviation in quality is d_{prior} (ash%) and, finally, the amount of the deviated coal is t_{prior} (ton). Similarly, when executing the mine plan on the posterior model, the previously defined parameters are; $C_{\text{posterior}}$, $D_{\text{posterior}}$, $d_{\text{posterior}}$ and $t_{\text{posterior}}$ respectively. Then, the costs of deviating from the target production is:

$$C_{\text{prior}} = D_{\text{prior}} * d_{\text{prior}} * t_{\text{prior}} \quad (7.1)$$

Environmental aspects in lignite mining refer to emissions of pollutants and energy consumption. Typical emissions in the coal industry are carbon dioxide (CO₂), sulphur dioxide (SO₂), nitric oxide (NO). However, with modern mining methods, the biggest problem remaining is the large amount of CO₂ emissions. Thus, this dissertation focuses on CO₂ emissions. The main two source of CO₂ emissions during coal mining and energy producing from coal are: the emissions from the excavators during mining activities and the emissions from the power plant. Due to the complexity of the process, defining an approximate KPI measure for the environmental aspects is very difficult. Too many assumptions need to be made and in the end, these assumptions will not reflect reality. Thus, a verbal discussion is made of the environmental aspects.

Each power plant is designed to work efficiently with a specific quality range (ash%) of coal. Having higher ash values than the specified ash% range will cause serious efficiency losses due to lower calorific value of the high ash content coal. Then, the power plant needs to burn more coal to produce the same amount of energy that it could have produced with lower ash content coal. This will cause more CO₂ emissions.

7.3. A STOCHASTIC BASED MINE PROCESS OPTIMIZER

This research uses a stochastic based mine process optimizer in order to calculate the expected benefit of the updating framework. The mentioned mine process optimizer is used as a transfer function needed for the VOI concept as introduced in Figure 7.1.

The stochastic based mine process optimizer is created within the RTRO-Coal project in work package 1 and 5 by Mollema [92]. It is a form of optimizer where the efficiency of a set of decision variables is simulated through a simulation model, which in this case represents a complex continuous mining operation [92]. The stochastic based mine process optimizer optimizes the task schedule of the excavators at a given sequence with a minimal penalty value.

In this case study, the mine process optimizer finds the best mining schedule based on a predefined target daily ash value for a given resource model. Thus, it translates the resource model uncertainties into penalty calculations based on an optimized mine schedule.

In this research the optimized variable is the schedule of the six excavators. The schedule for each excavator is a list with three shifts per day of the simulated period. For each shift the excavator is either scheduled to work or not active. This is represented with a one or a zero in the schedule. The input for a single simulation is thus a two-dimensional array with six rows and $3 \cdot n$ columns, where n is the number of simulated days. An example of a schedule with the ones and zeroes being represented by green and red blocks respectively is shown in Figure 7.2. [92]

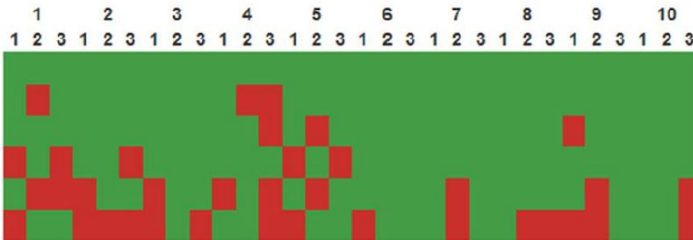


Figure 7.2: Visual representation of a series of schedules, with the 10 simulation days and the shift for each day in the first two rows. A red block means the excavator is not schedules, a green block means the excavator is scheduled to work. [92]

The total activity time of an excavator is never 100% of the time it is scheduled. The activity time is simplified to a single percentage per excavator by dividing the total active time of the excavators (corrected for downtimes) in the historical data by the total time of this data. This gives the following percentages per excavator (Table 7.1). The number of active minutes in a shift that is used in the simulation model is obtained by multiplying the activity factor with 480, the total number of minutes in an eight hour shift. [92]

Table 7.1: Activity factors for excavators [92]

Excavator	Activity factor
Bg.1580 (excavator 1)	0.592
Bg.1511 (excavator 2)	0.601
Bg.1553 (excavator 3)	0.667
Bg.351 (excavator 4)	0.518
Bg.1541 (excavator 5)	0.630
Bg.309 (excavator 6)	0.513

As mentioned earlier, the stochastic based mine process optimizer works with a penalty function to calculate the fitness of a solution. A KPI is optimized in this research; the daily ash value. Any deviation from the defined target ash value will increase the penalty value. The implemented penalty function works with several configurable parameters. The parameters are as follows: [92]

- - Coal quality daily target T_q
- - Coal quality minimum penalty deviation $P_{q\ min}$
- - Coal quality penalty factor P_q

The minimum penalty deviation is the maximum acceptable deviation of the target value before a penalty is applied. This gives for the daily penalty calculation the following formula, where S_q is the simulated quality. [92]

For the daily quality penalty value $PV_{quality}$:

$$PV_{quality} = \begin{cases} (|S_q - T_q| - P_{q\ min}) \times P_q, & |S_q - T_q| > P_{q\ min} \\ 0, & |S_q - T_q| \leq P_{q\ min} \end{cases} \quad (7.2)$$

The total penalty value of a solution is the sum of both the quality and tonnage penalty value for all the days of simulation.

In this chapter, the defined decision variables are the resource model and mining schedule. The constraints of this optimization problem are; the scheduled maintenance, the daily production target and the daily quality target. The scheduled maintenance is one of the problem constraints since each excavator requires specific amounts of maintenance. These scheduled maintenance are defined as the following; for Excavator 1580, none; for Excavator 1511, 4 shifts; for Excavator 1553, 3 shifts; for Excavator 351, 6 shifts; for Excavator 1541, 10 shifts and for Excavator 309 is 18 shifts. The defined daily coal production is 12,000 ton with a 3,000 ton deviation. The defined coal quality target is 9% of ash with a 1% ash deviation.

For a detailed information on the used mine process optimizer, the readers are referred to [92].

7.4. VALUE OF INFORMATION

In the context of this dissertation, the value of information (VOI) concept is used to understand what is gained by integrating the online-sensor measurement data into the resource model when using the updating framework. In general, VOI is calculated as following [83]:

$$VOI = \left[\text{Expected value with} \right] - \left[\text{Expected value without} \right] \quad (7.3)$$

additional information additional information

The concept analyzes the value of the resource model updating framework's ability to improve the prediction of coal quality parameter, namely the ash percentage (ash%). For this, the expected value of the posterior model ($V_{\text{posterior}}$) is compared to the prior model's expected value (V_{prior}). Eventually, in our application, calculation of VOI translates Equation (7.3) as following:

$$VOI = V_{\text{posterior}} - V_{\text{prior}} \quad (7.4)$$

A similar calculation can be applied in a case where the mine plan is applied to the posterior model. Finally, one can calculate the economical VOI as following:

$$VOI_{\text{economical}} = |C_{\text{posterior}} - C_{\text{prior}}|. \quad (7.5)$$

The VOI concept considers the value of perfect and imperfect information. Perfect information refers to perfectly reliable information, thus it contains no uncertainties. Perfect information rarely exists, but it provides a best-case scenario for the value of an information and it defines an upper limit on the value of additional information [82]. In the context of this dissertation it would answer the question: 'How much better would the economical and environmental aspects of an optimized mine plan be executed after knowing the coal seam geometries and coal quality distributions?'. However, since the case study presented here is a real case study, the reality remains unknown. Thus for this case study, there can be no VOPI defined.

As indicated in Figure 7.1, the experiments performed within this chapter, will compare the calculated VOIs of the Imperfect Value and Updated & Improved Value. These values will be calculated after applying the mine optimizer on the prior and posterior (updated) models.

Next section will explain further the experiments that will be performed in order to calculate the VOI.

7.5. CASE STUDY

7.5.1. Experimental Set-Up

This case study is performed in the Profen mine, Germany. The description of this mine area, various updating experiments with different parameters (including their results) and a hypothesis testing case study are presented in Chapter 6.

The experiments performed in this chapter calculate the expected values for different resource model based experiments (Figure 7.3). One of these resource models is without any additional information. This is the base case and the resource model in this case is the prior model. The other resource models are with additional information. These are the updated cases and the resource model in this case is the posterior model. There are five different posterior models which are updated within different time periods:

- The posterior model which resulted from updating the prior model over the 19 July – 1 August period.
- The posterior model which resulted from updating the prior model over the 19 July – 4 August period.
- The posterior model which resulted from updating the prior model over the 19 July – 7 August period.
- The posterior model which resulted from updating the prior model over the 19 July – 10 August period.
- Finally, the posterior model which resulted from updating the prior model over the 19 July – 13 August period.

The latter is assumed as the most precise model since this is the most up-to-date resource model and it serves as a benchmark.

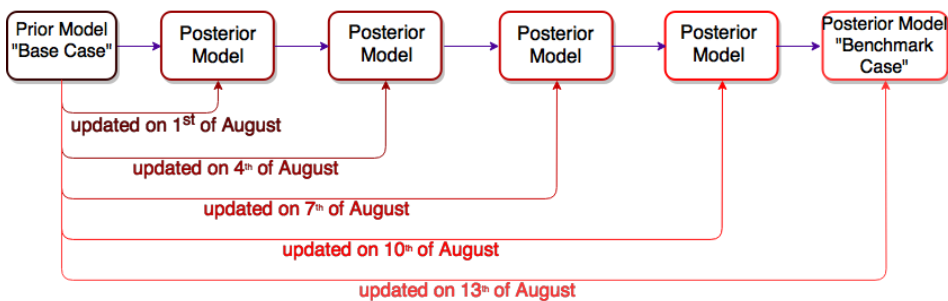


Figure 7.3: Resource models that are used in the experiments

The mine optimizer, which is introduced in Section 7.3, is applied to all of resource models above for the following 5 days after their updating periods. For the base case and the benchmark case, the mine optimizer is applied for 5 days after the each updating period. These dates will be: 2-6 August, 5-9 August, 8-12 August and 11-16 August. For these dates there are different best schedules

optimized based on the prior model, the updated model and the real model. To be precise, in total there are twelve different best schedules for different time spans. These best schedules are:

1. Best schedule for 2-6 August, achieved by applying the optimizer to the prior model.
2. Best schedule for 2-6 August, achieved by applying the optimizer to the posterior model (which is updated between 19 July - 1 August).
3. Best schedule for 2-6 August, achieved by applying the optimizer to the real model (which is updated between 19 July - 13 August).
4. Best schedule for 5-9 August, achieved by applying the optimizer to the prior model.
5. Best schedule for 5-9 August, achieved by applying the optimizer to the posterior model (which is updated between 19 July - 4 August).
6. Best schedule for 5-9 August, achieved by applying the optimizer to the real model (which is updated between 19 July - 13 August).
7. Best schedule for 8-12 August, achieved by applying the optimizer to the prior model.
8. Best schedule for 8-12 August, achieved by applying the optimizer to the posterior model (which is updated between 19 July - 7 August).
9. Best schedule for 8-12 August, achieved by applying the optimizer to the real model (which is updated between 19 July - 13 August).
10. Best schedule for 11-16 August, achieved by applying the optimizer to the prior model.
11. Best schedule for 11-16 August, achieved by applying the optimizer to the posterior model (which is updated between 19 July - 10 August).
12. Best schedule for 11-16 August, achieved by applying the optimizer to the real model (which is updated between 19 July - 13 August).

Next, these obtained best schedules are applied to the benchmark model (Figure 7.4). This is done in order to see the improvements during the mining operations, when using the prior model, the most current model and the benchmark model. As mentioned in the previous section, the case study presented here is a real case study and thus, there can be no VOPI defined for this case study. For this reason, since the benchmark model is the most up-to-date resource model and thus, the most precise model, this case study assumes it is the reality. In this way, an approximation of VOPI can be calculated between the benchmark and the prior model whereas the VOI is calculated between the posterior model and the prior model. A comparison of this would answer the following questions: "What would be the result of the mining activities if we didn't have additional information?", "How did the additional information affect the mining activities?" and finally "What would happen if we knew the reality and performed the mining activities mine based on that?". Of course, the latter one is only for comparison and in reality we can never have this information beforehand.

Once the best schedules are applied to the benchmark model, the expected costs of deviating from the target quality (ash %) values will be calculated as explained in Section 7.2. The expected values are then compared to each other and the VOI is calculated. This comparison and the results are provided in Section 7.5.2.

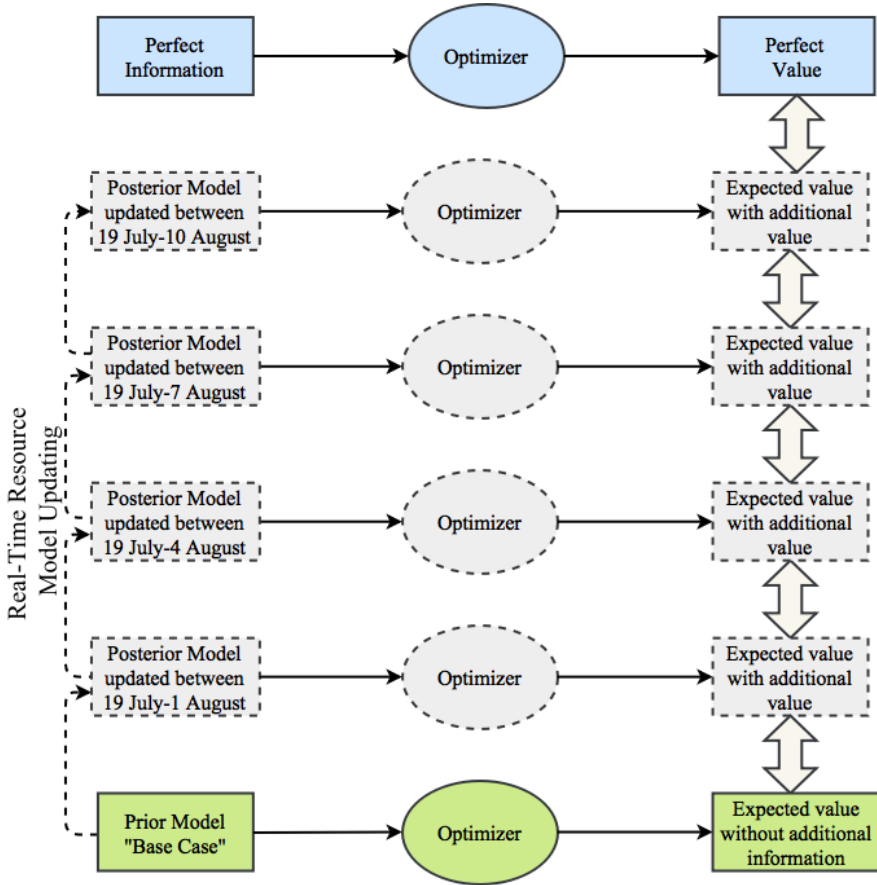


Figure 7.4: VOI - Experimental scheme

This experimental scheme is applied to six different case studies in order to investigate the VOI for the resource model updating concept with different prior models. These prior models are created based on different information sources in order to test different exploration strategies and other replacement options (such as using the short-term mining model as the prior model). These case studies are:

- Case 1: The first case study used a prior model with 25 realizations which were created by geostatistical simulations (SGS) on 25x25x1m grid. A detailed explanation is provided for this prior model in Section 6.2.1. The

posterior model of this case study is created simply by applying the resource model updating algorithm on the prior model of this case study.

- Case 2: The second case study used a prior model with 25 realizations which were created by adding fluctuations to a short-term mining model of the company. A detailed explanation is provided for this prior model in Section 6.2.2. The posterior model of this case study is created simply by applying the resource model updating algorithm to the prior model of this case study.
- Case 3: The third case study used a prior model with 25 realizations which were created by geostatistical simulations (SGS) on block based. In the context of this dissertation, block based simulation indicates performing SGS on the central coordinates of the production blocks. In this case study, all of the drill holes (100 percent) were used when performing the SGS. The posterior model of this case study is created simply by applying the resource model updating algorithm to the prior model of this case study.
- Case 4: The fourth case study used a prior model with 25 realizations which were created by geostatistical simulations (SGS) on block based. In this case study, only 50 percent of the drill holes were used when performing the SGS. The posterior model of this case study is created simply by applying the resource model updating algorithm to the prior model of this case study.
- Case 5: The fifth case study used a prior model with 25 realizations which were created by geostatistical simulations (SGS) on block based. In this case study, only 25 percent of the drill holes were used when performing the SGS. The posterior model of this case study is created simply by applying the resource model updating algorithm to the prior model of this case study.
- Case 6: The sixth case study used a prior model with 25 realizations which were created by geostatistical simulations (SGS) on block based. In this case study, only 10 percent of the drill holes were used when performing the SGS. The posterior model of this case study is created simply by applying the resource model updating algorithm to the prior model of this case study.

All of the case studies presented in this chapter are updated every 2 hours using the same mining sequence and the same RGI data. Overall, all of the updating parameters are kept the same in order to compare the differences caused by feeding different prior models as an input. A summary of the case studies is given in Table 7.2.

In this study, penalties are applied for not meeting the coal quality target (Equation (7.3)). This target production quality is defined as 9 % ash and the penalty is only applied for the realizations above 10.5 ash % and below 7.5 ash %.

The costs of deviating from the targets (the penalties) in this study are calculated by one unit per ton of coal. Hence, these penalties can be interpreted as percentage of deviation from the targets. A penalty of 0.1€/ash % is applied per ton of coal.

Table 7.2: Case summarization for VOI experiments

	Base Case: Prior Model	Updated Case: Posterior Model
Case 1	100% of the drill holes - SGS on grid	Updated prior model using RGI data
Case 2	Short-Term plan + Fluctuations	Updated prior model using RGI data
Case 3	100% of the drill holes - SGS on block based	Updated prior model using RGI data
Case 4	50% of the drill holes - SGS on block based	Updated prior model using RGI data
Case 5	25% of the drill holes - SGS on block based	Updated prior model using RGI data
Case 6	10% of the drill holes - SGS on block based	Updated prior model using RGI data

7.5.2. Results

This section presents some representative results of the previously defined experiments.

Two graphs are provided for each case study. The first graph presents the calculated deviation costs (penalties). This graph calculates the deviations per day for exceeding the upper target values in the simulations. Since the deviations from the lower target value are, in general, insignificant and negligible, the graphs for exceeding the lower target values are not presented.

The second graph presents the calculated VOI for each case study. The VOPI is represented with pink squared lines and the average of those VOPI is represented with a red line. The calculated VOI is represented with light green pointed line and the trendline fitted on these points is represented with a dark green line.

7.5.2.1. Case 1

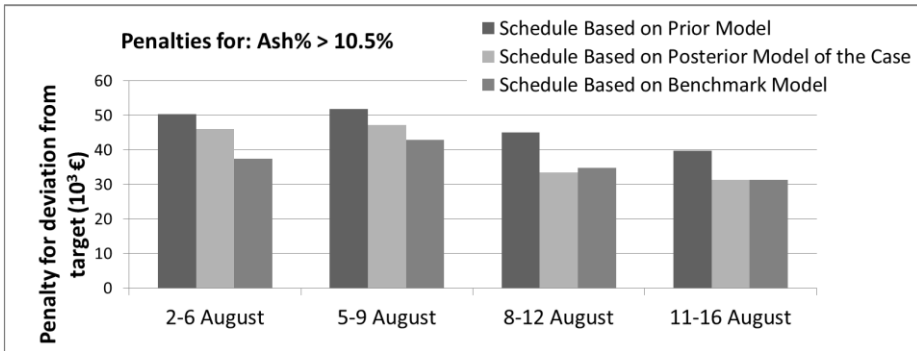


Figure 7.5: Cost calculations of deviating from the target quality (ash %) - Case 1

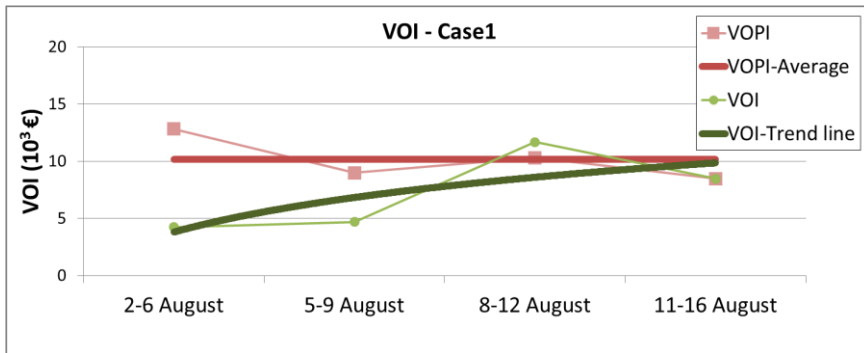


Figure 7.6: VOI - Case 1

7.5.2.2. Case 2

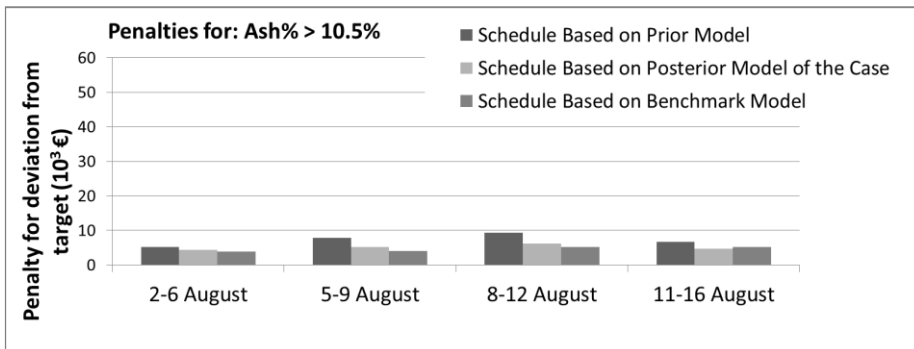


Figure 7.7: Cost calculations of deviating from the target quality (ash %) - Case 2

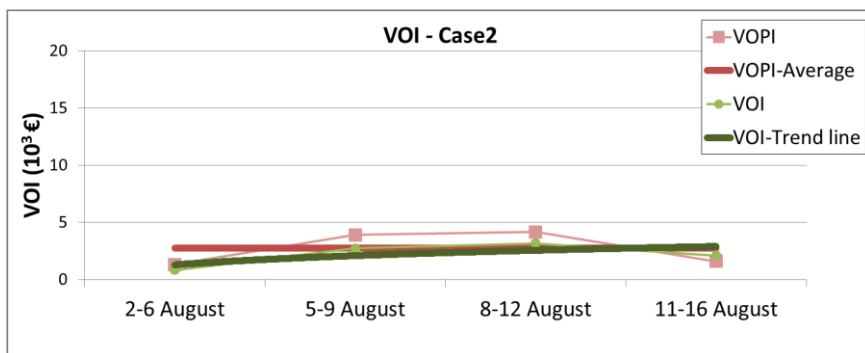


Figure 7.8: VOI - Case 2

7.5.2.3. Case 3

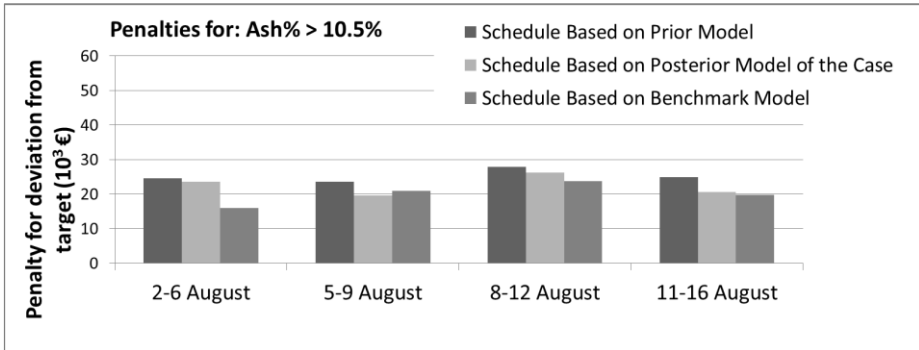


Figure 7.9: Cost calculations of deviating from the target quality (ash %) - Case 3

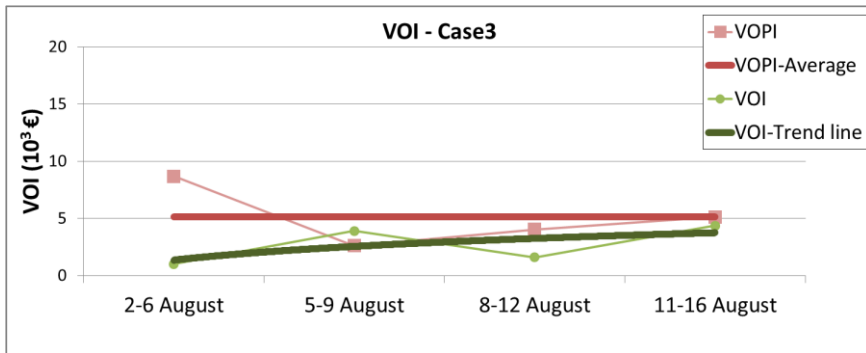


Figure 7.10: VOI - Case 3

7.5.2.4. Case 4

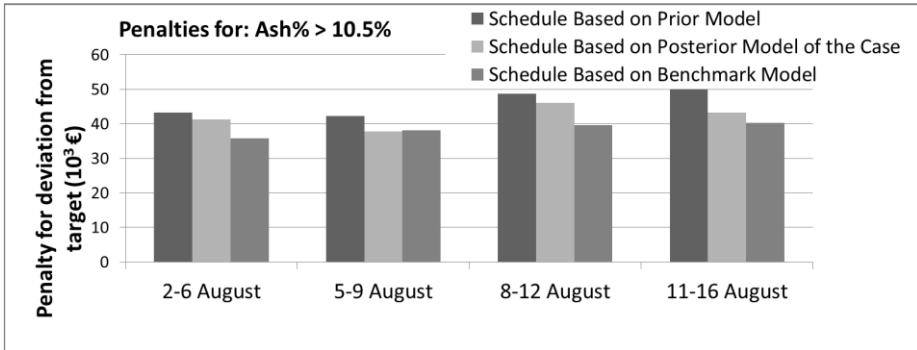


Figure 7.11: Cost calculations of deviating from the target quality (ash %) - Case 4

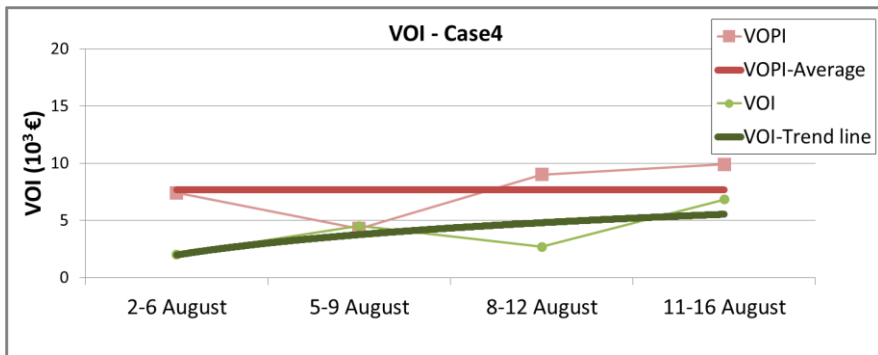


Figure 7.12: VOI - Case 4

7.5.2.5. Case 5

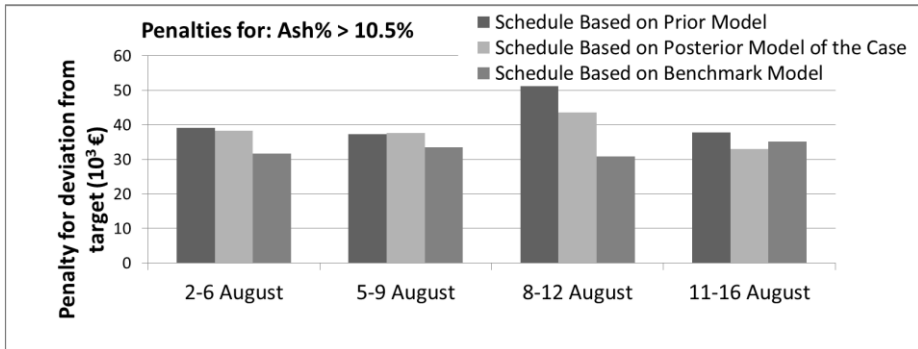


Figure 7.13: Cost calculations of deviating from the target quality (ash %) - Case 5

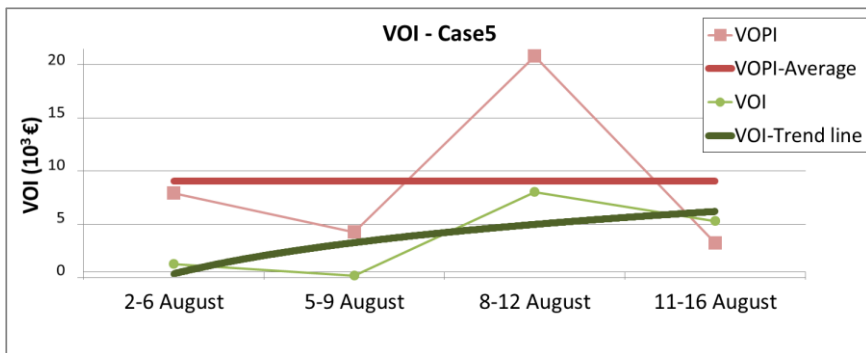


Figure 7.14: VOI - Case 5

7.5.2.6. Case 6

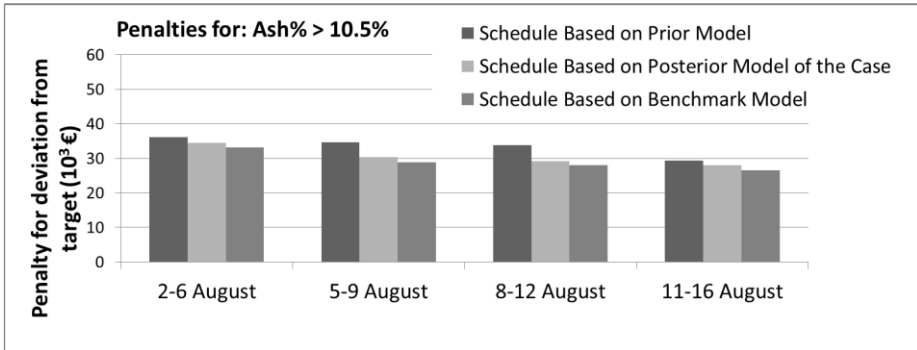


Figure 7.15: Cost calculations of deviating from the target quality (ash %) - Case 6

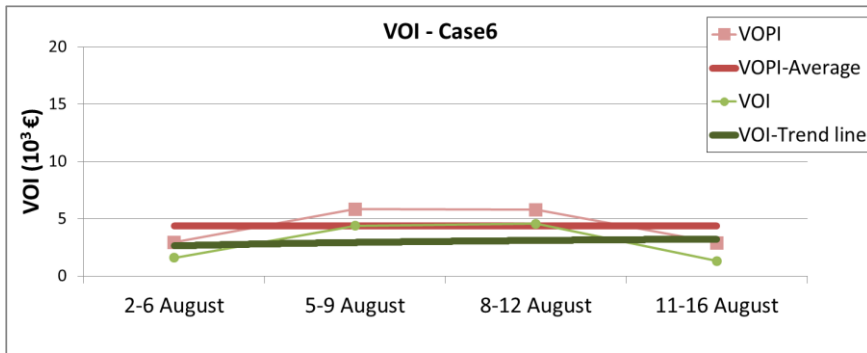


Figure 7.16: VOI - Case 6

7.5.3. Discussion

This section discusses the results presented in the previous section.

In the “cost calculations of deviating from the target quality (ash %)” graphs (Figure 7.5, Figure 7.7, Figure 7.9, Figure 7.11, Figure 7.13 and Figure 7.15), the darkest column represents the calculated penalties for the best schedule which is optimized based on the prior model and later this schedule is applied to the benchmark model. It is expected to observe a constant penalty value with a slight fluctuation for these columns. The reason for that is, the applied best schedule for those columns is based on the same prior model and the model, on which the mentioned schedule is applied, is the same benchmark model. The only changing parameter for these columns is the differentiating application days and this can cause slight fluctuations. The lightest column represents the calculated penalties for the best schedule which is optimized based on the posterior model of that case and later this schedule is applied to the benchmark model. The medium darkest column represents the calculated penalties for the best schedule which is optimized by using the benchmark model and later this schedule is applied to the benchmark model. Similar to the schedule based on prior model cases, a constant penalty value with a slight fluctuation for the schedule based on benchmark model cases is expected.

When evaluating the next five days of mining right after updating the resource model, the following observation can be made from the comparison of all of the experiments that are mentioned above: For all of the case studies, a decrease in the uncertainty range and a better fitting of the average ash values into the target ash value area is observed in general, when the updating interval is increased and the optimized schedule is calculated based on a more accurate/up-to-date resource model.

In overall, each case study indicates penalty reductions for five production days. This leads an increasing VOI towards VOPI. These significant benefits of the resource model updating framework are achieved while using the stochastic based mine process optimizer. It is expected to have higher impacts while using an optimizer which changes the block sequencing as the current one changes the weekly maintenance schedule.

7.5.3.1. Case 1

The prior model of Case 1 was created by geostatistical simulations (SGS) on a 25x25x1m grid, after creating the geological model of the coal seam.

The following observations can be made from Figure 7.5:

- Penalties for the schedule based on the prior model are in average € 47,000, while they vary between € 40,000 to € 52,000.

- Penalties for the schedule based on the posterior model gradually decrease from € 46,000 to € 31,000. However, the penalty for 5-9 August is € 47,000, this is a slight and negligible increase.
- Penalties for the schedule based on the benchmark model are in average € 57,000, while they vary between € 31,000 to € 43,000.
- Thus, for this case study, the calculated VOPI is € 10,000 and the calculated VOI moves from € 4,000 to € 8,000 (Figure 7.6). These calculations of VOI and VOPI are made for only 5 days after each updating period.
- The above mentioned VOI numbers will lead to approximately a € 300,000 to € 600,000 annual cost reduction or saving.

In Figure 7.6, the trend line of the VOI illustrates the benefit of using a combination of the resource model updating algorithm and the mine optimizer (“closed-loop” optimization). With each iteration of updating, the mine schedule optimization penalties decrease, thus VOI increases. In this case study, the VOI trendline is almost merging with the average of VOPI. This is great, however if we had the real VOPI, as expected, our VOI would not have reached it.

7.5.3.2. Case 2

The prior model of Case 2 was created by adding fluctuations on a short-term mining model of the company.

The following observations can be made from Figure 7.7:

- Penalties for the schedule based on the prior model are in average € 7,000, while they vary between € 5,000 to € 9,000.
- Penalties for the schedule based on the posterior model gradually decrease from € 5,000 to € 4,000.
- Penalties for the schedule based on the benchmark model is in average € 4,500, while they vary between € 3,900 to € 5,100.
- Thus, for this case study, the calculated VOPI is € 3,000 and the calculated VOI moves from € 1,000 to € 2,000 (Figure 7.8). These calculations of VOI and VOPI are made for only 5 days after each updating period.
- Above mentioned VOI numbers will lead to approximately € 60,000 to € 250,000 annual cost reduction or saving.
- This case study has the least calculated penalties for exceeding the upper target values in the simulations. The reason for this is that the prior model of this case study is underestimated. In this case study, penalties for exceeding the lower target values in the simulations would be a better graph to evaluate the developments in this case study. However, in order to provide a complete comparison, and since other cases mostly don’t have penalties for exceeding the lower target values in the simulations, these graphs are not provided.

Figure 7.8 presents an increasing VOI (while the penalties are decreasing) with time. In this case study, the VOI trendline is merging with the average of VOPI. Once again, this proves the benefit of using a combination of the resource model updating algorithm and the mine optimizer.

When comparing this case study to Case 1, the calculated VOI is remarkably lower. However, this doesn't indicate a direct correlation between the success of the real time resource updating framework. There are two reasons for this. First, due to the underestimation of the short-term model based prior model. Second, the current optimizer is job scheduling and thus, the effect on the VOI is lower. Larger VOI are expected when using an optimizer which changes the block sequencing.

7.5.3.3. Case 3

The prior model of Case 3 was created by geostatistical simulations (SGS) on block based. In this case study, all of the drill holes (100 percent) were used when performing the SGS.

The following observations can be made from Figure 7.9:

- Penalties for the schedule based on the prior model are in average € 25,000, while they vary between € 24,000 to € 28,000.
- Penalties for the schedule based on the posterior model gradually decrease from € 20,000 to € 26,000.
- Penalties for the schedule based on the benchmark model is in average € 20,000, while they vary between € 16,000 to € 24,000.
- Thus, for this case study, the calculated VOPI is € 5,000 and the calculated VOI moves from € 1,000 to € 4,400 (Figure 7.10). These calculations of VOI and VOPI are made for only 5 days after each updating period.
- Above mentioned VOI numbers will lead to approximately € 70,000 to € 320,000 annual cost reduction or saving.
- Relatively lower penalties (comparing to Case 1) are due to the underestimation of the prior model of this case.

Figure 7.10 presents an increasing VOI (while the penalties are decreasing) with time. In this case study, the VOI trendline is not merging with the average of VOPI. This is not a problem, however, this shows that a few more updating iterations are required to reach the same VOPI level as in the previous cases. This is expected since in this case the prior model was "quickly" simulated on the center points of the blocks. Thus, the accuracy of this prior model is expected to be worse than the previous two cases prior models. Yet, the increase in the VOI still indicates the benefit of using a combination of the resource model updating algorithm and the mine optimizer. It shows that resource models that have different accuracy can be improved until some level (VOPI) and if a longer time

period of updating is possible, the initial knowledge gap between with the prior models can be closed.

7.5.3.4. Case 4

The prior model of Case 4 was created by geostatistical simulations (SGS) on block based. In this case study, only 50 percent of the drill holes were used when performing the SGS.

The following observations can be made from Figure 7.11:

- Penalties for the schedule based on the prior model are in average € 46,000, while they vary between € 42,000 to € 50,000.
- Penalties for the schedule based on the posterior model gradually decrease from € 38,000 to € 46,000.
- Penalties for the schedule based on the benchmark model is in average € 38,000, while they vary between € 36,000 to € 40,000.
- Thus, for this case study, the calculated VOPI is € 8,000 and the calculated VOI moves from € 2,000 to € 7,000 (Figure 7.12). These calculations of VOI and VOPI are made for only 5 days after each updating period.
- Above mentioned VOI numbers will lead to approximately € 150,000 to € 500,000 annual cost reduction or saving.

Compared to the previous cases, the VOI of Case 4 is higher than Case 2 and Case 3. This was explained by Case 2 and Case 3's underestimations, thus there are lower penalties and lower improvement possibilities. This case study shows a great increase of VOI. Therefore it can be concluded that, regardless of the quality of the resource model, it is possible to update each resource model and bring them to a similar accuracy level. Obviously, this accuracy level is closer to the reality than the initial accuracy. Since the accuracy level of this case study's prior model is lower than the previously presented cases, this case study has a higher VOI when comparing with the previous case studies.

7.5.3.5. Case 5

The prior model of Case 5 was created by geostatistical simulations (SGS) on block based. In this case study, only 25 percent of the drill holes were used when performing the SGS.

The following observations can be made from Figure 7.13:

- Penalties for the schedule based on the prior model are in average € 41,000, while they vary between € 37,000 to € 51,000.
- Penalties for the schedule based on the posterior model gradually decrease from € 33,000 to € 44,000.
- Penalties for the schedule based on the benchmark model is in average € 33,000, while they vary between € 31,000 to € 35,000.

- Thus, for this case study, the calculated VOPI is € 8,000 and the calculated VOI moves from € 1,000 to € 8,000 (Figure 7.10). These calculations of VOI and VOPI are made for only 5 days after each updating period.
- Above mentioned VOI numbers will lead to approximately € 50,000 to a € 550,000 annual cost reduction or saving.

Similar to Case 4, Case 5 shows a significant increase of VOI. Even though only 25% of the drill hole data has been used in this case study's prior model, after the updating iterations, the posterior model manages to catch up with the previously calculated VOI. The obtained VOI increased when the accuracy of the prior model being used is decreased. Once again this case study's results show that the updating framework, after a few iterations, manages to decrease these penalties to a similar penalty level obtained from the previous case studies.

7.5.3.6. Case 6

The prior model of Case 6 was created by geostatistical simulations (SGS) on block based. In this case study, only 10 percent of the drill holes were used when performing the SGS.

The following observations can be made from Figure 7.15:

- Penalties for the schedule based on the prior model are in average € 33,000, while they vary between € 29,000 to € 36,000.
- Penalties for the schedule based on the posterior model gradually decrease from € 28,000 to € 34,000.
- Penalties for the schedule based on the benchmark model are in average € 29,000, while they vary between € 26,000 to € 33,000.
- Thus, for this case study, the calculated VOPI is € 4,000 and the calculated VOI moves from € 2,000 to € 5,000 (Figure 7.16). These calculations of VOI and VOPI are made for only 5 days after each updating period.
- Above mentioned VOI numbers will lead to approximately € 100,000 to € 330,000 annual cost reduction or saving.

Finally, when comparing the results of this case study with the previous results, even though the prior model was created by only using 10% of the drill hole data, the VOI trendline is still increasing. However, in this case, the instability of the results indicates that, using only 10% of the drill hole data is not representing the spatial variability. Thus, it can be concluded that using only 10% of the drill hole data is not enough to have stable results.

7.6. CONCLUSIONS

In this chapter, the added value of the real-time resource model updating concept is demonstrated by using a value of information (VOI) analysis. The expected economical benefits of additional information (due to the integration of the online-sensor measurement into the resource model) is compared to different cases where there is no additional information integrated into the process.

Six different case studies are performed in this chapter. Each case study has a prior resource model with a different accuracy level. This is done in order to compare the obtained VOI while the accuracy of the prior model was getting worse. In general, great improvements were achieved for all case studies. The effectiveness of the resource model updating framework is proven due the similar VOI increases after the resource model updating framework was used for a few iterations. This indicates that even if the resource model is initially worse, it can learn from the real-time production data. This shows a great success of real-time resource mode updating framework with a combined use of mine optimizer.

Moreover, by using the resource model updating framework combined with the mine optimizer, performed case studies prove that the deviations from the defined target quality are reduced. In overall, the calculated VOI for five mining days varied between € 2,000 to € 8,000. These numbers will lead to approximately a € 100,000 to € 550,000 annual cost reduction or saving.

This dissertation demonstrates that using the resource model updating framework provides more accurate resource models at each iteration. By having an accurate up-to-date resource model, the daily planning will always be optimal. With the daily planning being optimal, the efficiency of the mining process can be increased significantly. Deviations from the prior model can be processed and adapted to quickly and efficiently. This would result in reaching the target product which needs to be mined more efficiently. Furthermore, if any deviations in the target product are noticed and the plan needs to be changed, it can be done swiftly and will be based on a more accurate prediction of the mining environment.

Moreover, for every minute that the excavator needs to work extra because the mining plan was not optimal, CO₂ will be released unnecessarily. The excavator runs on heavy fuels and produces substantial amounts of CO₂. This is bad not only for environment but also for the cash flow and profits. In modern times, the CO₂ output is taxed with CO₂ credits. For example, the European Union gives a limit amount of CO₂ credits each year. When extra CO₂ is used the company needs to buy credits from companies that did not use their full amount of CO₂ credits. This would result into additional costs whenever the mining plan is not optimal.

Another economical point would be equipment aging. With an optimal mining plan the mining equipment would need to be used for less time compared to a situation where the mining plan is not optimized.

Each case study indicated significant benefits of the resource model updating framework, while using the stochastic based mine process optimizer. It is expected

to have higher impacts while using an optimizer which changes the block sequencing as the current one changes the weekly maintenance schedule.

8. TECHNOLOGICAL READINESS LEVEL & INDUSTRIAL APPLICABILITY

This chapter discusses the technological readiness level and industrial applicability of the real-time resource model updating framework.

8.1. TECHNOLOGICAL READINESS LEVEL & INDUSTRIAL APPLICABILITY

The Technology Readiness Level (TRL) scale is a measure for describing the maturity of a technology. This scale provides a common understanding of the status of a technology and addresses the entire innovation chain. By evaluating a technology project against the parameters for each TRL, one can assign a TRL rating to the project based on its stage of progress. There are nine technology readiness levels; TRL 1 being the lowest and TRL 9 the highest. Although they are conceptually similar, different definitions of TRLs are used in different fields. To describe the status of developed technologies in this research, the following standards, provided in Figure 8.1, as defined by the European Commission in HORIZON 2020 [93] are being referred to.

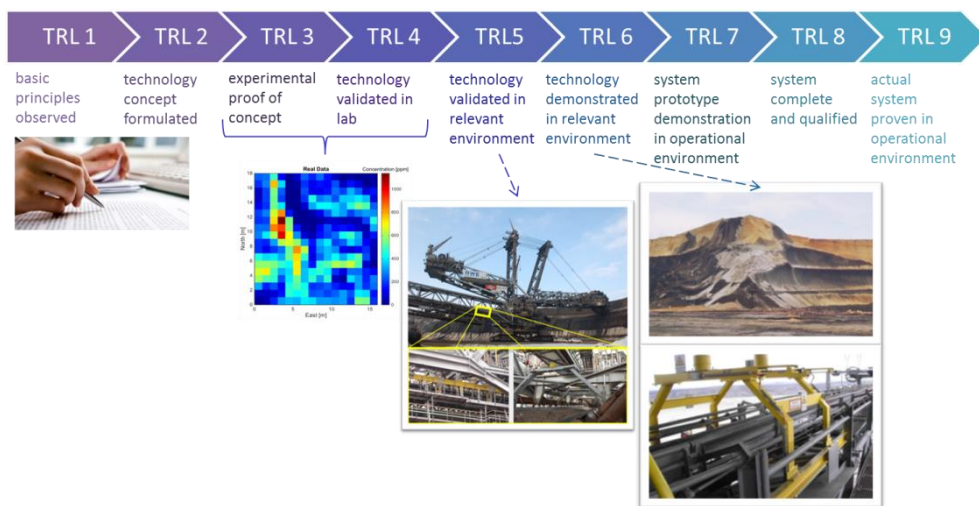


Figure 8.1: Technology readiness levels

TRL 1 refers to the beginning of scientific research where the basic principles are being observed. This is the stage where case specific problems are defined and related literature review is done in order to initiate this research. TRL 2 occurs once the technology concept is formulated. TRL 2 is achieved in Chapter 3, by proving a formal description of the updating algorithm.

When active research and design begin, a technology is elevated to TRL 3. Chapter 4 provided a 2D case study which is performed in a completely known and fully controllable environment. In this way, an experimental proof of concept is constructed as required in TRL 3. Furthermore, the developed technology is benchmarked against a proven and well-studied method in Section 4.3. With this validation, the technology advances to TRL 4.

A full case study is provided in a real lignite mining environment in Chapter 5, this validation in real environment refers TRL 5. Similarly, another yet more

complicated full case study in real environment is presented in Chapter 6. The TRL 6 has been reached by this demonstration in the real lignite mining environment.

Thus, the current resource model updating framework is considered as TRL 6. Further study thus requires a system prototype to be demonstrated in an operational environment. This will be TRL 7. Next, a complete and qualified system is required to reach TRL 8. Once an actual system has been proven in an operational environment, it can be called TRL 9.

9. CONCLUDING REMARKS

This final chapter summarizes the conclusions drawn in this dissertation in view of the scope of the research stated in Chapter 1. Furthermore, suggestions and recommendations are given for future research.

9.1. CONCLUSIONS

In line with the scope of this research as stated in Chapter 1 the achieved objectives are the following:

1. A tailored method, which is adapted to update coal quality attributes in a continuous mining environment, in order to improve the resource model accuracy, is provided.
2. The real-time resource model updating framework is applied to a full scale lignite production environment. The results obtained from the full scale application validate the applicability of the method in a continuous mining environment and presents significant improvements in prediction in the resource model. These improvements are expected to lead to an increase of coal recovery and process efficiency by continuously controlling the decisions in a mining operation.
3. The performance of the resource model updating framework with respect to the main parameters (the ensemble size, the neighborhood size, localization strategies and the sensor precision) was investigated. The results should assist in future applications by determining the impact of the different parameters. The findings of ensemble size sensitivity analysis supported the existing literature [5, 62]; more accurate updates are achievable by using a larger ensemble. Although 24 ensemble members provided the best results in terms of MSE, they are not chosen as the optimum ensemble size since they were not representative enough of the lignite seam. Instead an ensemble of 48 members is chosen, because it is second best and is more representative of the lignite seam. The sensitivity analysis of the localization and neighborhood strategies conclude that the applied localization strategies need to be improved and the neighborhood size needs to remain as 450,450,6 m in X,Y,Z directions, as previously defined in the variogram modelling. The sensitivity analysis for different sensor precision shows that a lower sensor precision increases the uncertainty of the posterior model, due to the significant difference between the prior model and the actual sensor data.
4. The real-time resource model updating framework is applied while the sensor is observing a blend of coal resulting from multiple excavators. Significant improvements are observed while using blended material measurement data in order to update different production locations in different benches. This provides great flexibility for future applications in terms of assisting the operational decision making in lignite production in the future. It is important to point out that this method can be applied to any bulk mining operation, without changing the core method. It should be noted that improvements are only achievable if a

- material tracking system, grade or quality control model and online-sensor measurement system are in place.
5. The updating framework is simplified and semi-automated for an easier application in a real mining environment. This simplified application method involves creating the prior realizations based on the company's short-term model. Improvement percentages, on average, were not significantly different when the case study results we compared with the results obtained from a case study where the prior realizations are generated with geostatistical simulations. This dissertation validates that the automation of the developed framework during real applications can be performed based on a short-term model without any additional process being required in order to prepare the prior model.
 6. The added value created by the application of the real-time resource model updating framework is evaluated. The expected economical benefits of additional information (due to the integration of the online-sensor measurement into the resource model) is compared to different cases where there is no additional information integrated into the process. Six different case studies are performed in order to investigate the VOI for the resource model updating concept with different prior models. These prior models are created based on different information sources in order to test different exploration strategies and other replacement options (such as using the short-term mining model as the prior model). Within the case studies, the calculated VOI continued to increase after iterations even when the prior models were getting less accurate. This indicates a great success of real-time resource model updating framework. It is expected that, this study will lead to approximately € 550,000 annual cost reduction or saving. Moreover, the using the presented research in the coal mining will provide environmental benefits such as less energy consumption and reduced CO₂ emissions.

9.2. RECOMMENDATIONS FOR FUTURE RESEARCH

The research described in this dissertation left a few open issues of interest for future research.

The first recommendation for future research would be to solve the drawback which is caused by localization strategies mentioned in Section 5.4. A future study can develop a case specific localization function in a way that it defines the block boundaries and acts according to those distances.

A second recommendation for future research would be to use the same methodology presented in this dissertation including more accurate measurement data. As mentioned in Section 2.4, it is already known that the sensor data are not very reliable. By using more accurate measurement data, such data acquired by laboratory analysis, the predictions of the quality of the future mining blocks should improve significantly.

A third recommendation for future research would be bringing the current research's technological readiness level from TRL 6 to TRL 7, TRL 8 and finally to TRL 9. This can be done initially by demonstrating a system prototype in an operational environment. This will be TRL 7. Next, a complete and qualified system is required to reach TRL 8. Once an actual system has been proven in operational environment, it can be referred to as TRL 9.

A fourth recommendation for future research would be adding more sensors to the operational environment. With this additional measurement information, the value of the current research can be increased since the additional sensors will improve the material tracking. An increase in the value of the current research is expected with the increased accuracy of the measurements. As a consequence of this, the annual cost reduction/savings can be increased.

A fifth recommendation for future research would be the application of the resource model updating framework into different mines. This dissertation presented different applications in coal mining. Future research could focus on applications in other commodities and ore body styles in order to increase the cost reductions/savings in the overall mining industry.

REFERENCES

1. *Data on Lignite Composition from Operational Datasets of Rwe Power Ag, Lignite Mine Garzweiler, Germany*, unpublished, Editor.
2. Benndorf, J., Yueksel, C., Shishvan, M.S., Rosenberg, H., Thielemann, T., Mittmann, R., Lohsträter, O., Lindig, M., Minnecker, C., and Donner, R., *Rtro-Coal: Real-Time Resource-Reconciliation and Optimization for Exploitation of Coal Deposits*. Minerals, 2015. **5**(3): p. 546-569.
3. Ghil, M., Cohn, S., Tavantzis, J., Bube, K., and Isaacson, E., *Applications of Estimation Theory to Numerical Weather Prediction*, in *Dynamic Meteorology: Data Assimilation Methods*. 1981, Springer. p. 139-224.
4. Bengtsson, L., Ghil, M., and Källén, E., *Dynamic Meteorology: Data Assimilation Methods*. Vol. 36. 1981: Springer New York.
5. Daley, R., *Atmospheric Data Analysis*. 1993: Cambridge university press.
6. Houtekamer, P.L. and Mitchell, H.L., *Data Assimilation Using an Ensemble Kalman Filter Technique*. Monthly Weather Review, 1998. **126**(3): p. 796-811.
7. Houtekamer, P.L. and Mitchell, H.L., *A Sequential Ensemble Kalman Filter for Atmospheric Data Assimilation*. Monthly Weather Review, 2001. **129**(1): p. 123-137.
8. Houtekamer, P.L., Mitchell, H.L., Pellerin, G., Buehner, M., Charron, M., Spacek, L., and Hansen, B., *Atmospheric Data Assimilation with an Ensemble Kalman Filter: Results with Real Observations*. Monthly Weather Review, 2005. **133**(3): p. 604-620.
9. Barbieri, R. and Schopf, P., *Oceanographic Applications of the Kalman Filter*. 1982, Greenbelt, Maryland 20771: Goddard Space Flight Center.
10. Miller, R.N., *Toward the Application of the Kalman Filter to Regional Open Ocean Modeling*. Journal of Physical Oceanography, 1986. **16**(1): p. 72-86.
11. Budgell, W.P., *Nonlinear Data Assimilation for Shallow Water Equations in Branched Channels*. Journal of Geophysical Research: Oceans, 1986. **91**(C9): p. 10633-10644.
12. Webb, D.J., *Assimilation of Data into Ocean Models*, in *Oceanic Circulation Models: Combining Data and Dynamics*, D.T. Anderson and J. Willebrand, Editors. 1989, Springer Netherlands. p. 233-256.
13. Heemink, A. and Kloosterhuis, H., *Data Assimilation for Non-Linear Tidal Models*. International journal for numerical methods in fluids, 1990. **11**(8): p. 1097-1112.

14. Ghil, M. and Malanotte-Rizzoli, P., *Data Assimilation in Meteorology and Oceanography*. Advances in geophysics, 1991. **33**: p. 141-266.
15. Verlaan, M. and Heemink, A., *Tidal Flow Forecasting Using Reduced Rank Square Root Filters*. Stochastic Hydrology and Hydraulics, 1997. **11**(5): p. 349-368.
16. Tuan Pham, D., Verron, J., and Christine Roubaud, M., *A Singular Evolutive Extended Kalman Filter for Data Assimilation in Oceanography*. Journal of Marine systems, 1998. **16**(3): p. 323-340.
17. Bertino, L., Evensen, G., and Wackernagel, H., *Combining Geostatistics and Kalman Filtering for Data Assimilation in an Estuarine System*. Inverse problems, 2002. **18**(1): p. 1.
18. Nævdal, G., Mannseth, T., and Vefring, E.H. *Near-Well Reservoir Monitoring through Ensemble Kalman Filter*. in *SPE/DOE Improved Oil Recovery Symposium*. 2002.
19. Brouwer, D., Nævdal, G., Jansen, J., Vefring, E., and Van Kruijsdijk, C. *Improved Reservoir Management through Optimal Control and Continuous Model Updating*. in *SPE Annual Technical Conference and Exhibition*. 2004. Society of Petroleum Engineers.
20. Nævdal, G., Johnsen, L.M., Aanonsen, S.I., and Vefring, E.H., *Reservoir Monitoring and Continuous Model Updating Using Ensemble Kalman Filter*. SPE journal, 2005. **10**(01): p. 66-74.
21. Sebacher, B., Hanea, R., and Heemink, A., *A Probabilistic Parametrization for Geological Uncertainty Estimation Using the Ensemble Kalman Filter (Enkf)*. Computational Geosciences, 2013. **17**(5): p. 813-832.
22. Benndorf, J., *Making Use of Online Production Data: Sequential Updating of Mineral Resource Models*. Mathematical Geosciences, 2015. **47**(5): p. 547-563.
23. Wambeke, T. and Benndorf, J., *A Simulation-Based Geostatistical Approach to Real-Time Reconciliation of the Grade Control Model*. Mathematical Geosciences, 2016: p. 1-37.
24. Benndorf, J., *Application of Efficient Methods of Conditional Simulation for Optimising Coal Blending Strategies in Large Continuous Open Pit Mining Operations*. International Journal of Coal Geology, 2013. **112**: p. 141-153.
25. Srivastava, R.M., *Geostatistics: A Toolkit for Data Analysis, Spatial Prediction and Risk Management in the Coal Industry*. International Journal of Coal Geology, 2013. **112**: p. 2-13.
26. Tercan, A.E. and Sohrabian, B., *Multivariate Geostatistical Simulation of Coal Quality Data by Independent Components*. International Journal of Coal Geology, 2013. **112**: p. 53-66.
27. Pardo-Igúzquiza, E., Dowd, P.A., Baltuille, J.M., and Chica-Olmo, M., *Geostatistical Modelling of a Coal Seam for Resource Risk Assessment*. International Journal of Coal Geology, 2013. **112**: p. 134-140.
28. Klostermann, J., *Die Wanderung Der Kontinente. Grundlagen Der Plattentektonik Und Die Junge Beanspruchung Der Niederrheinischen Bucht*

- Aus Heutiger Sicht. Natur und Landschaft am Niederrhein*, 1991. **10**: p. 61-98, Krefeld.
29. Hager, H., *Peat Accumulation and Syngenetic Clastic Sedimentation in the Tertiary of the Lower Rhine Basin, Fr Germany*. Mem Soc Geol France NS, 1986. **149**: p. 51-56.
 30. Schäfer, A., Utescher, T., Klett, M., and Valdivia-Manchego, M., *The Cenozoic Lower Rhine Basin–Rifting, Sedimentation, and Cyclic Stratigraphy*. International Journal of Earth Sciences, 2005. **94**(4): p. 621-639.
 31. Haq, B.U., Hardenbol, J., and Vail, P.R., *Chronology of Fluctuating Sea Levels since the Triassic*. Science, 1987. **235**(4793): p. 1156-1167.
 32. Buchardt, B., *Oxygen Isotope Palaeotemperatures from the Tertiary Period in the North Sea Area*. 1978.
 33. Zagwijn, W. and Hager, H., *Correlations of Continental and Marine Neogene Deposits in the South-Eastern Netherlands and the Lower Rhine District*. Mededelingen van de Werkgroep voor Tertiaire en Kwartaire Geologie, 1987. **24**(1-2): p. 59-78.
 34. Schneider, H. and Thiele, S., *Geohydrologie Des Erftgebietes: Ministerium Für Ernährung*. Landwirtschaft und Forsten, NRW, Düsseldorf, 1965.
 35. MIBRAG, *Geological Structure of the Deposit Profen*. 2017: (unpublished).
 36. Zimmer, R., *Workshop Onlinemessung, Kohlequalitätsmanagement: Eps Kolubara Mining Project „Energie Efficiency by Ecological Coal Quality Management“; Kolubara Mine*. 2014, MIBRAG Consulting International GmbH.
 37. Jansen, J.-D., Brouwer, D.R., Naevdal, G., and Van Kruijsdijk, C.P.J.W., *Closed-Loop Reservoir Management*. First Break, 2005. **23**(1).
 38. Jansen, J.-D., Bosgra, O.H., and Van den Hof, P.M., *Model-Based Control of Multiphase Flow in Subsurface Oil Reservoirs*. Journal of Process Control, 2008. **18**(9): p. 846-855.
 39. Benndorf, J. and Jansen, J.D., *Recent Developments in Closed-Loop Approaches for Real-Time Mining and Petroleum Extraction*. Mathematical Geosciences, 2017. **49**(3): p. 277-306.
 40. Bertino, L., Evensen, G., and Wackernagel, H., *Sequential Data Assimilation Techniques in Oceanography*. International Statistical Review, 2003. **71**(2): p. 223-241.
 41. Kalman, R.E., *A New Approach to Linear Filtering and Prediction Problems* Transactions of the ASME–Journal of Basic Engineering, 1960. **82 (Series D)**: p. 35-45.
 42. Kalman, R.E. and Bucy, R.S., *New Results in Linear Filtering and Prediction Theory*. Journal of basic engineering, 1961. **83**(1): p. 95-108.
 43. Evensen, G., *Sequential Data Assimilation with a Nonlinear Quasi-Geostrophic Model Using Monte Carlo Methods to Forecast Error Statistics*. Journal of Geophysical Research: Oceans (1978–2012), 1994. **99**(C5): p. 10143-10162.

44. Evensen, G., *Advanced Data Assimilation for Strongly Nonlinear Dynamics*. Monthly weather review, 1997. **125**(6): p. 1342-1354.
45. Evensen, G. *Application of Ensemble Integrations for Predictability Studies and Data Assimilation*. in Monte Carlo Simulations in Oceanography Proceedings' Aha Huliko'a Hawaiian Winter Workshop, University of Hawaii at Manoa. 1997. Citeseer.
46. Evensen, G. and Van Leeuwen, P.J., *Assimilation of Geosat Altimeter Data for the Agulhas Current Using the Ensemble Kalman Filter with a Quasigeostrophic Model*. Monthly Weather Review, 1996. **124**(1): p. 85-96.
47. Evensen, G. and Van Leeuwen, P.J., *An Ensemble Kalman Smoother for Nonlinear Dynamics*. Monthly Weather Review, 2000. **128**(6): p. 1852-1867.
48. Burgers, G., Jan van Leeuwen, P., and Evensen, G., *Analysis Scheme in the Ensemble Kalman Filter*. Monthly weather review, 1998. **126**(6): p. 1719-1724.
49. Bishop, C.H., Etherton, B.J., and Majumdar, S.J., *Adaptive Sampling with the Ensemble Transform Kalman Filter. Part I: Theoretical Aspects*. Monthly weather review, 2001. **129**(3): p. 420-436.
50. Whitaker, J.S. and Hamill, T.M., *Ensemble Data Assimilation without Perturbed Observations*. Monthly Weather Review, 2002. **130**(7): p. 1913-1924.
51. Maybeck, P.S., *Square Root Filtering*. Stochastic models, estimation and control, 1979. **1**: p. 368-409.
52. Stengel, R., *Optimal Control and Estimation*. 1994, Dover Publications: New York.
53. Cohn, S.E., *An Introduction to Estimation Theory*. JOURNAL-METEOROLOGICAL SOCIETY OF JAPAN SERIES 2, 1997. **75**: p. 147-178.
54. Chevalier, C., Emery, X., and Ginsbourger, D., *Fast Update of Conditional Simulation Ensembles*. Mathematical Geosciences, 2014: p. 1-19.
55. Chilès, J.P. and Delfiner, P., *Geostatistics: Modeling Spatial Uncertainty, Second Edition*. Wiley, New York, 2012: p. 705-714.
56. Chevalier, C., Ginsbourger, D., and Emery, X., *Corrected Kriging Update Formulae for Batch-Sequential Data Assimilation*, in *Mathematics of Planet Earth*. 2014, Springer. p. 119-122.
57. Emery, X., *The Kriging Update Equations and Their Application to the Selection of Neighboring Data*. Computational Geosciences, 2009. **13**(3): p. 269-280.
58. Sakov, P. and Bertino, L., *Relation between Two Common Localisation Methods for the Enkf*. Computational Geosciences, 2011. **15**(2): p. 225-237.
59. Wambeke, T. and Benndorf, J., *Data Assimilation of Sensor Measurements to Improve Production Forecasts in Resource Extraction*, in IAMG. 2015: Freiberg (Saxony) Germany.
60. Zhou, H., Gómez-Hernández, J.J., Hendricks Franssen, H.-J., and Li, L., *An Approach to Handling Non-Gaussianity of Parameters and State Variables in Ensemble Kalman Filtering*. Advances in Water Resources, 2011. **34**(7): p. 844-864.

61. Goovaerts, P., *Geostatistics for Natural Resources Evaluation*. Applied Geostatistics Series. 1997, New York Oxford: Oxford University Press.
62. Wambeke, T. and Benndorf, J., *A Geostatistical Approach to Real-Time Reconciliation of the Grade-Control Model*. Mathematical Geosciences, 2016.
63. Isaaks, E.H. and Srivastava, R.M., *An Introduction to Applied Geostatistics*. 1989.
64. Krige, D., *A Statistical Approach to Some Mine Valuation and Allied Problems on the Witwatersrand: By Dg Krige*. 1951, University of the Witwatersrand.
65. Krige, D., *Lognormal-De Wijsian Geostatistics for Ore Evaluation*. 1981: South African Institute of mining and metallurgy Johannesburg.
66. Liu, N., Betancourt, S., and Oliver, D.S. *Assessment of Uncertainty Assessment Methods*. in *SPE Annual Technical Conference and Exhibition*. 2001. Society of Petroleum Engineers.
67. Hegstad, B.K. and Henning, O., *Uncertainty in Production Forecasts Based on Well Observations, Seismic Data, and Production History*. *Spe Journal*, 2001. **6**(04): p. 409-424.
68. Barker, J.W., Cuypers, M., and Holden, L. *Quantifying Uncertainty in Production Forecasts: Another Look at the Pung-S3 Problem*. in *SPE Annual Technical Conference and Exhibition*. 2000. Society of Petroleum Engineers.
69. Liu, N. and Oliver, D.S., *Evaluation of Monte Carlo Methods for Assessing Uncertainty*. *SPE Journal*, 2003. **8**(02): p. 188-195.
70. Jeong, C., Mukerji, T., and Mariethoz, G. *Iterative Spatial Resampling Applied to Seismic Inverse Modeling for Lithofacies Prediction*. in *81st Annual International Meeting, SEG, Expanded Abstracts*. 2011.
71. Mitchell, H.L., Houtekamer, P.L., and Pellerin, G., *Ensemble Size, Balance, and Model-Error Representation in an Ensemble Kalman Filter**. *Monthly Weather Review*, 2002. **130**(11): p. 2791-2808.
72. Horn, R.A. and Johnson, C.R., *Matrix Analysis*. Cambridge, Cambridge, 1985.
73. Gaspari, G. and Cohn, S.E., *Construction of Correlation Functions in Two and Three Dimensions*. *Quarterly Journal of the Royal Meteorological Society*, 1999. **125**(554): p. 723-757.
74. Yin, J., Zhan, X., Zheng, Y., Hain, C.R., Liu, J., and Fang, L., *Optimal Ensemble Size of Ensemble Kalman Filter in Sequential Soil Moisture Data Assimilation*. *Geophysical Research Letters*, 2015. **42**(16): p. 6710-6715.
75. Devore, J.L., *Probability and Statistics for Engineering and the Sciences*. 2015: Cengage Learning.
76. Dekking, F.M., *A Modern Introduction to Probability and Statistics: Understanding Why and How*. 2005: Springer Science & Business Media.
77. Howard, R.A., *Information Value Theory*. *IEEE Transactions on systems science and cybernetics*, 1966. **2**(1): p. 22-26.
78. Raiffa, H., *Decision Analysis: Introductory Lectures on Choices under Undertainty*. 1968: Addison-Wesley.

79. Matheson, J.E., *Using Influence Diagrams to Value Information and Control*. Influence diagrams, belief nets and decision analysis, 1990: p. 25-63.
80. Peck, J. and Gray, J., *Mining in the 21st Century Using Information Technology*. CIM bulletin, 1999. **92**(1032): p. 56-59.
81. Barnes, R.J. *The Cost of Risk and the Value of Information in Mine Planning*. in *19th APCOM Symposium*. 1986.
82. Phillips, J., Newman, A.M., and Walls, M.R., *Utilizing a Value of Information Framework to Improve Ore Collection and Classification Procedures*. The Engineering Economist, 2009. **54**(1): p. 50-74.
83. Bratvold, R.B., Bickel, J.E., and Lohne, H.P., *Value of Information in the Oil and Gas Industry: Past, Present, and Future*. SPE Reservoir Evaluation & Engineering, 2009. **12**(04): p. 630-638.
84. Bhattacharjya, D., Eidsvik, J., and Mukerji, T., *The Value of Information in Spatial Decision Making*. Mathematical Geosciences, 2010. **42**(2): p. 141-163.
85. Barros, E., Hof, P., and Jansen, J., *Value of Information in Closed-Loop Reservoir Management*. Computational Geosciences, 2016. **20**(3): p. 737-749.
86. Grayson, C.J., *Decisions under Uncertainty: Drilling Decisions by Oil and Gas Operators*. 1960: Ayer.
87. Newendorp, P.D., *Decision Analysis for Petroleum Exploration*. 1975, Petroleum Publishing Co.,Tulsa, OK.
88. Stibolt, R. and Lehman, J. *The Value of a Seismic Option*. in *SPE Hydrocarbon Economics and Evaluation Symposium*. 1993. Society of Petroleum Engineers.
89. Houck, R.T., *Predicting the Economic Impact of Acquisition Artifacts and Noise*. The Leading Edge, 2004. **23**(10): p. 1024-1031.
90. Steagall, D.E., Gomes, J.A.T., De Oliveira, R.M., Ribeiro, N., Queiroz, R.Q., Carvalho, M.J., and Souza, C. *How to Estimate the Value of the Information (Voi) of a 4d Seismic Survey in One Offshore Giant Field*. in *SPE Annual Technical Conference and Exhibition*. 2005. Society of Petroleum Engineers.
91. Bickel, J.E., Gibson, R.L., McVay, D.A., Pickering, S., and Waggoner, J., *Quantifying 3d Land Seismic Reliability and Value*. SPE Reservoir Evaluation and Engineering, 2008. **11**(5).
92. Mollema, H., *Investigation into Simulation Based Optimization of a Continuous Mining Operation*, in *Department of Geoscience and Engineering*. 2015, Delft University of Technology.
93. EuropeanCommission, *Technology Readiness Levels (Trl)*, in *G. Technology readiness levels (TRL)*. 2014: Horizon 2020 Work Programme 2014-2015 General Annexes, Extract from Part 19 - Commission Decision C(2014)4995.

EPILOGUE & ACKNOWLEDGEMENTS

Four years ago when I started my life as a PhD, I wasn't sure if I could make it to the point where I am today. Looking back at these four years, there were times I suffered a lot, but there were also times that were awesome. While I am writing this, I can't believe that this dissertation is finished. During my PhD, I learned a lot, experienced being an expat, build a new life and even got a family. Most importantly, I have met amazing people that inspired, supported and encouraged me. Without your help, I would not have made it this far. Thank you.

I would first like to thank to my second promotor and daily supervisor Prof. dr. -ing. **Joerg** Benndorf, who allowed this journey to happen in the first place. Thank you for giving me the chance to be part of this project and supporting me in all of the work we have conducted together. Many of the work I have done throughout my doctoral studies would not be the way they are if you did not push me to look deeper into subjects and supervise me the way you did.

In addition, I would like to thank my promotor Prof. Dr. Ir. **Jan Dirk** Jansen for his valuable comments in our periodical progress meetings and also reviewing my work. It has been a pleasure to work under his supervision.

I would also like to thank to Dr. **Mike** Buxton for his support throughout my doctoral studies. He became my copromotor in my last year however his continued support throughout my entire doctoral studies significantly increased my motivation and success. I enjoyed all of the discussions we had (both scientific and non-scientific ones).

I also would like express my gratitude to my dearest colleagues. Together we formed a band of brothers, which helped me to fully enjoy my doctoral studies. Without you, our office would be very boring. **Masoud**, we started our doctoral adventure at the same day, in the same project. You were one of those people who helped me to settle down in Delft, including helping me to buy a decent bike when I had no idea. Thank you for supporting me when I needed it. **Tom**, I enjoyed the discussions we had on our research and I learned a lot from you. Thank you for everything. **Adriana**, we were passing from the similar roads every day in terms of being part of a Dutch family. It was nice to have someone in the office to share and gossip. **Marinus**, I am going to miss the times when you were the boss of our office, you were the coolest boss. **Feven**, I am very happy that you joined our team, I enjoyed a lot our girly talks. **Angel**, we had tons of fun together both in Valencia and Perth (you were a great host in Valencia). I enjoyed a lot our discussions. **Elif**, it all went very fast with you, once you were here and then gone. When I was doing my bachelor you were my teacher, now my friend. I am very happy to know you, thank you for all the motivation you gave to me. **Jack**, thank you very much for translating parts of my thesis into Dutch.

I would like to state my sincere thanks to my best friends in Ankara. **Setenay**, you never missed to see me every time I come back to Ankara. You were my ex-colleague but also the greatest support when I started to work, when I was writing my master's thesis and when I was moving to the Netherlands. Thank you for believing in me. **Funda**, even though we were both very busy with our academical lives, we never got apart. We started to talk as if we saw each other yesterday. Thank you for visiting me in my first real home in Delft and being my friend. **Ozan**, as Funda did, you made me very happy by visiting my Delft home not only once but twice. You are a friend whom I can always count on, thank you. **Deniz**, you have always been supporting me last 13 years. Thank you for always being there for me.

My favorite Italians, **Fabio** and **Gabriele**, we shared so many memories together and almost all of those memories were involving amazingly delicious Italian food (eventually resulting me gaining couple of kilos). No regrets, it was totally worth it. Thank you for your huge support especially at the times I thought I cannot finish this PhD. Ting, I am happy to meet you in the beginning of my Delft adventure, we had great memories. **Elly**, thank you for being there for me at the times where I freaked out when I thought something is wrong with Wasabi, you are the strongest girl that I've ever met. My sweet girls, **Giulia** and **Faidra**, you were there for me almost from the beginning of this journey. Thank you for being inspirational, all your support when I needed and all the fun we shared. **Aris, Stef, Ezgi, Giannis, Dimitris, Floor, Alessandro** and **Martino**; thanks for all the night outs, dinners, parties and other countless moments we had together which made my PhD years way more beautiful. **Kristina**, I think the most important thing that I gained from that Dutch course was your friendship. Thank you for the amazing memories and see you in another life where we drink bubbles every day!

And, the Turkish gang; you have become family to me. Thanks to you, I felt less homesick. Thank you for all the memories we shared. **Tilbe**, even though we knew each other since we were 8 years old, we become best friends here, in Delft. I was so lucky that you were already in Delft when I moved. We shared many gossips, parties, weekend-getaways in the last four years. You are a great friend! **Burak**, you are my oldest friend in Delft. I am so happy to have met you. I can't imagine Delft especially without you two guys. **Ekin**, the ultimate Bouwpub and Klooster buddy. What a pity that I could never help you to find an "ekmek". **Onursal**, you are like an older brother to me, thank you for all your support (especially for the dissertation writing and looking for a job process) and introducing Haarlem to us. **Argun**, my talented artistic friend. Thank you very much for your friendship, and also designing the cover of my dissertation. You always introduced me to some eccentric cool stuff. **Emre**, thank you for all the discussions we had, I'm sure that you'll have great adventures in Harvard. **Cansel**, thanks for all the fun memories and girly talks. **Musti**, you are a funny friend and I admire that you can sleep everywhere in every condition. **Alper**, may we have

more and more bbq parties. And the “yenge”s of “Guliz Abi”, **Rosemary** and **Leontine**, thank you for all the fun we shared together, you are the best “yenge”s.

I must express my very profound gratitude to all members of my family. My Dutch family, **Minie**, **Henk** and **Henk Jr.**, thank you very much for your warm welcome to your family. Since the day I met you, you always showed me warmth, love and endless support. My Turkish, blood family; thank you for believing in me and making my Turkey holidays lots of fun. My dearest sister, **Aysin**; you are my silly little sister, my best friend and my fashion director. I feel so lucky to have you, I still remember how happy I was when you were born. Regardless of the distance, we are always together. My beloved **parents**; I am grateful for all of your unconditional and endless support, inspiration and encouragement throughout my life. Thank you for giving me a chance to prove and improve myself.

My cute furry little friend; **Wasabi**. Before I met you, I could never imagine a life with a pet. You brought lots of joy and happiness to my life. Your love was a great motivation for me during my doctoral studies.

And finally, last but not least, I thank to my loving fiancé **Bas**. If I didn't get this PhD position, we could never find each other. You were always there at times I thought that it is impossible to continue, you helped me to keep things in perspective. Thank you for your unfailing love, support, understanding and encouragement throughout this experience. You were the one who was there for me during the article/thesis writing hell to help me quickly proofread and give suggestions. You contributed to this dissertation more than you could think of. I am so grateful to have you. You and Wasabi are the sunshine of my life.

*Cansın Yüksel
Delft, November 2017*

CURRICULUM VITAE



Cansin Yüksel was born on the 26th of November 1990, in Ankara, Turkey. She studied mining engineering in Hacettepe University, Turkey and graduated in 2011 with the third highest grade in her department. During her bachelor studies, in 2010, she spent 6 months in Hungary as an Erasmus student at Miskolc University. After graduating from her bachelor studies, she worked for Suda Maden Inc. (a member of AMG-Advanced Metallurgical Group) during her master studies, as a member of the exploration and mining team of antimony. She obtained her MSc degree in mining engineering at Hacettepe University in 2013. She started her doctoral research at the Geoscience & Engineering Department of Delft University of Technology on November 2013, within the Resource Engineering Section under the guidance of Prof. dr. -ing. J. Benndorf. The promoter of her doctorate was Prof. dr. ir. J. D. Jansen, the head of the Geoscience & Engineering Department of Delft University of Technology. During her doctorate, on 1st of October 2016, Prof. Dr. Joerg Benndorf was promoted at the University of Mining and Technology in Freiberg, Germany, after which Cansin continued her research under the guidance of Dr. M.W.N. Buxton. Prof. dr. -ing. J. Benndorf continued to supervise Cansin in her research as her second promoter.

LIST OF PUBLICATIONS

PEER-REVIEWED PUBLICATIONS

Benndorf, J., **Yüksel, C.**, Shishvan, M. S., Rosenberg, H., Thielemann, T., Mittmann, R., Lohsträter, O., Lindig, M., Minnecker, C., Donner, R., & Naworyta, W. (2015). RTRO–Coal: Real-Time Resource-Reconciliation and Optimization for Exploitation of Coal Deposits. *Minerals*,5(3), 546-569.

Yüksel, C., Thielemann, T., Wambeke, T., & Benndorf, J. (2016). Real-Time Resource Model Updating for Improved Coal Quality Control Using Online Data. *International Journal of Coal Geology*. doi: <http://dx.doi.org/10.1016/j.coal.2016.05.014>.

Yüksel, C., Benndorf, J. (2017) Performance analysis of continuous resource model updating in lignite production *Geostatistics Valencia 2016* (pp. 431-446): Springer.

Ozcelik, Y., Hasanpour, R., **Yüksel, C.** (2016). Study the most important ground parameters affecting tunneling in squeezing conditions, presented at 6th International Conference on Computer Applications in the Minerals Industry (CAMI 2016), Istanbul 2016.

Yüksel, C., Benndorf, J., Lindig, M., Lohsträter, O. (2017) Updating the coal quality parameters in multiple production benches based on combined material measurement: A full case study. *International Journal of Coal Science & Technology*, 2017: p. 1-13.

Yüksel, C., Minnecker, C., Shishvan, M.S., Benndorf, J., & Buxton, M. (2017). Value of Information Introduced by a Resource Model Updating Framework. *Mathematical Geosciences*. (submitted)

PRESENTATIONS

Yüksel, C., Benndorf, J., Application of the Ensemble Kalman Filter for Improved Mineral Resource Recovery. 10th International EnKF Workshop, Flåm, Norway, June 2015.

Yüksel, C., Benndorf, J., Application of the Ensemble Kalman Filter for Improved Mineral Resource Recovery. Ecole des Mines, Fontainebleau/France, September 2015.

Yüksel, C., Benndorf, J., Performance Analysis of Continuous Resource Model Updating in Lignite Production. GEOSTATS, Valencia, Spain, September 2016.

Yüksel, C., Benndorf, J., Added Value of Using Real-Time Resource Reconciliation in Coal Mining. 18. Geokinematischer Tag, Freiberg, Germany, May 2017.

Yüksel, C., Benndorf, J., Value Of Information Introduced By Resource Model Updating Framework. IAMG, Perth, Australia, September 2017.